An Electrochemical Study of the

llisation and Dissolution

of Sparingly Soluble Salts.

A Thesis by

Dorothy M. S. Little, B.Sc. Supervisor, Dr. G. H. Nancollas.

presented for the degree of Doctor of Philosophy

to

The University of Glasgow. October, 1964.

CONTENTS.

SUMMARY.

The crystallisation and dissolution of lead sulphate and barium sulphate have been studied by following the change in conductivity which occurs when supersaturated or subsaturated solutions of these salts are inoculated with seed crystals. The dissolution into water of barium sulphate crystals, labelled with ^{35}Sulphur has also been studied by a radiochemical technique.

In Part 1 of this thesis, experiments on the crystallisation of lead sulphate and barium sulphate are described. The growth of [illegible]ntions has been found to follow a second order rate law, which is preceded, in the case of lead sulphate, by an initial growth surge, of order greater than two. This surge has been interpreted in terms of two-dimensional nucleation on the surface of the added seed crystals. The crystallisation of lead sulphate from supersaturated solutions containing non-equivalent ionic concentrations of lead and sulphate has also been studied.

Sodium dodecylsulphate, sodium pyrophosphate, sodium trimetaphosphate and sodium tetrametaphosphate have all been found to retard the rate of growth, and if present in sufficiently high concentrations, to stop it entirely. It was observed that the duration and apparent kinetic order of the initial growth surge increased with increasing concentration of impurity, and this was more pronounced when the conductivity water used had been prepared by an ion-exchange method

rather than by distillation. The additive is assumed to be preferential adsorbed at active sites on the crystal surface, and thus fewer sites are available for normal second order growth. Fresh sites have therefore to be created by surface nucleation. It would seem that some organic matter is leached off the ion-exchange resin, and that this also occupies some of the available growth sites, thus enhancing the need for two-dimensional nucleation.

The growth of barium sulphate has been studied at various temperatures ranging from 15° - 45°C., and a value for the energy of activati for growth was obtained; E = 8 K.Cals. / mole.

s experiments on the dissolution of lead sulphate and barium sulphate. The dissolution of both salts into subsaturated solution, and of barium sulphate into water, has been found to follow a second order rate law, after a small initial surge of order greater than two. Anionic adsorbates have been found to retard the rate of solution of lead sulphate, although the concentration required to stop it almost entirely was considerably greater than for growth.

Barium sulphate dissolution into water has been investigated conductimetrically and radiochemically at various temperatures between 15° and 45°C., and the energy of activation for dissolution is approximately 12 K.Cals. / mole.

Kinetic Studies of the Precipitation and Dissolution of Sparingly Soluble Electrolytes.

Interest in crystallisation dates from the 8th Century, when recrystallisation was found to be useful as a method of purification. In 1691, Robert Boyle noted the modification of crystal habit by the rate of deposition from solution, while in the 19th Century, Sweigger (1) realised that a certain minimum size of seed crystal was necessary in order to initiate crystallisation.

Modern interest in the subject, however, dates from 1897, when Ostwald (2) determined that the upper limit for the effective size of a nucleating crystal of sodium chlorate was 10^{-10} grams. Modern theories of growth still incorporate many of Ostwald's ideas, thus he was the first to recognise that there are two clearly defined regions of supersaturation, the metastable and the labile. In the former region, no nucleation will take place unless it is induced by mechanical shock, or addition of seed crystals; as the supersaturation

is increased, however, a metastable limit is reached, beyond which immediate nucleation takes place. Work in this labile region is difficult to reproduce, since such factors as dust, age and history of the solutions, contact with the walls of the containing vessel (3) have all been shown to induce spontaneous nucleation.

Originally it was believed that growth and dissolution should be reciprocal processes, but this was disproved by Marc (4,5) who found the rate of dissolution to be very much faster than that of crystallisation, and this was supported by the results of Lehmann and Schmandt (6). From a study of the growth of seed crystals from a supersaturated solution, using a conductimetric technique, Marc was led to propose that at low values of supersaturation crystallisation was a second order reaction. He interpreted the kinetics in terms of a very thin adsorbed layer, probably of molecular dimensions, which existed at the crystal surface.

More recently Davies and Jones (7) have reached a similar conclusion from their study of silver chlorides. Bircumshaw and Riddiford (8) proposed that the steps at the crystal - solution interface were five-fold:-

1- Transport of solute to the interface.

2- Adsorption of solute at the interface.

3- Chemical reaction at the interface.

4- Desorption of products from the interface.

5- Transport of solute from the interface to the bulk of the solution.

Either growth or dissolution would take place, depending on the relative rates of the steps.

Davies and Jones (7) have combined steps 2,3 and 4 to give an overall interface control step, and proposed that in crystallization 2 is faster than 4, while the reverse holds for dissolution. This idea has been supported by Turnbull (9), Doremus (10) and O'Rourke and Johnson (11). Turnbull has studied the precipitation of barium sulphate, using a conductimetric technique. He found that in the earliest stages of precipitation the rate of growth of the crystals was independent of their size, and limited by a reaction at the crystal - solution interface; after the crystals reached a certain size, however, diffusion became the controlling mechanism. Davies derived growth equations for an interface controlled process, and found good agreement with the experimental results reported for silver chromate, strontium sulphate and barium sulphate. O'Rourke and Johnson, in a study of barium sulphate precipitation, arrived at a similar conclusion.

On the other hand, Collins and Leineweber (12), who also investigated barium sulphate precipitation, concluded that diffusion was the rate-controlling process, and interpreted their results in terms of a theory of two-dimensional surface nucleation on low index planes, proposed by Becker and Doring (13).

Gibbs (14) suggested that a perfect crystal should grow by repeated two-dimensional nucleation of new layers, with the peripheral

of each nucleus providing a growth step at which molecules could be incorporated into the crystal. Thus, energetically, there should be a critical supersaturation below which the crystal should not grow. Volmer and Schultze (15), who found a number of systems in which no such critical supersaturation existed, suggested that there was a mobile self-absorbed layer in thermodynamic equilibrium with the crystal surface. Frequent collisions would be expected between the constituent particles in this layer, and from these the germ of a two-dimensional crystal could be formed, which would attach itself to the lattice plane below.

Frank (16), however, suggested that the surfaces of real crystals are rarely perfect, nearly always containing dislocations. The presence of a dislocation which terminates in the crystal surface ensures that there are always exposed molecular terraces on which growth can take place; assimilation of the solute occurs at kinks in the growth steps. Hence, the need for two-dimensional nucleation does not arise at low supersaturations. Indeed, Burton, Cabrera and Frank (17) have postulated that a supersaturation greater than 50% is necessary before surface nucleation will take place; below this value screw dislocations should be the only source of growth steps. However, when diffusion in the medium is of importance, surface nucleation would be expected to occur at the corners of the crystal, resulting in dendritic branching (18). In many cases the growth of

crystals is slower than predicted by this theory, and Burton, Cabrera and Frank have suggested two possible reasons:

1) That there are too many dislocations too close together, preventing a critical nucleus from passing between the spirals, or

2) That there are not enough dislocations in the crystal. The authors favour the latter alternative, although Cabrera and Vermilyea (19) believe that one dislocation should be sufficient to grow a large crystal.

Albon (20) considered that in the initial stages of growth from a nucleus of critical size the crystals are probably dislocation-free, since this would enhance their stability, but that contact between the crystals would result in the formation of dislocations. Frank (18), on the other hand, attributed the majority of dislocations to impurities in the crystals, and evidence for this has been provided by Newkirk (21,22) from the growth of cadmium iodide.

Much experimental evidence has been produced in support of Frank's dislocation theory of growth, thus Sears (23) has observed potassium chloride and mercury whiskers to grow by dislocation spirals. Newkirk (21) has found a similar phenomenon with cadmium iodide, while Reynolds and Greene (25) have shown the growth of cadmium sulphide crystals from the vapour to proceed by a dislocation mechanism.

On the other hand, O'Rourke and Johnson (11) and Nielsen believe that the growth of barium sulphate proceeds by a two-dimensional surface nucleation mechanism, resulting in a fourth order rate law, whereas, in studies of near-perfect crystals Sears (24, 27, 28) has found both the Frank mechanism and growth by two-dimensional nucleation to be operative on different planes of a single crystal.

Since precipitation is so important in quantitative inorganic analysis, most of the work has been done on spontaneous crystallisation from the labile region of supersaturation. Such precipitations have often been found to exhibit an induction period, during which nucleus formation was assumed to be proceeding. Most theoretical analyses of spontaneous crystallisation have regarded the build-up of a critical nucleus as a steady-state process, consisting of stepwise incorporation of ions into ion-embryos. Christiansen (29) has shown that delays in nucleation may be anticipated on the basis of the relaxation time required for attainment of the steady-state concentrations of the embryos, but evaluation of this relaxation time is prohibitively difficult. Collins (30) however, has developed a solution with which the relaxation time can be determined from experimental values of surface tension, supersaturation and molecular encounter frequency.

Von Weimarn (31) suggested that the rate of precipitation

and the number of particles was proportional to the degree of supersaturation at the time of precipitation. Christiansen and Nielsen (32) have developed a similar idea, and have shown that the time of crystallisation varied inversely as some significant power of the initial concentration,

$$k = c_o^p T,$$

where c_o is the initial concentration of the supersaturated solution, T is the induction period, and k and p are constants, p being the number of ions required to form the critical nucleus. This theory predicts a constant nucleus size, with little dependence of the nucleation rate on the supersaturation; the critical nucleus is therefore relatively small. Indeed, values (32) of 8, 9 and 6 for p have been obtained for barium sulphate, calcium fluoride and silver chloride, respectively. Klein, Gordon and Walnut (33), using a similar relationship, found a nucleus of five ions to be indicated for silver chloride.

These views are in direct contrast with the theory of Volmer, and Becker and Doring, in which it is assumed that the supersaturation is built up slowly and homogeneously until a critical supersaturation is reached. This would result in a fairly large nucleus. Support for this theory has been given by Duke and Brown (34) who concluded that a nucleus of sufficient size to be stable in contact with a supersaturated solution should contain

several tens of ions, and by La Mer and Dinegar (35), who calculated that the radius of the critical nucleus for barium sulphate was 0.01μ.

If spontaneous crystallisation occurs by homogeneous nucleation and growth, the question then arises as to whether nucleation has ceased before growth sets in, or whether these processes take place concurrently. Collins and Leineweber (12), Turnbull (9), and Doremus (10) all favour consecutive processes, with nucleation taking place in an initial burst, and followed by growth thereafter. Christiansen and Nielsen, and O'Rourke and Johnson, however, believe that nucleation and crystallisation occur simultaneously, and Johnson and O'Rourke (36), who studied barium sulphate, derived equations for the two processes. They represented the initial part of the precipitation by a relation accounting for simultaneous nucleation and growth, and a good fit with experimental data was obtained for the first six minutes of the reaction. For the remainder of the precipitation they assumed the nucleation rate to be negligible, and developed a rate equation involving only growth on a fixed number of particles. Once again they obtained good agreement with the experimental results.

Many of these workers, however, have considered that the precipitation was not taking place purely by a homogeneous process. In experiments where the supersaturated solution is prepared by direct mixing of reagents, it is sometimes difficult to avoid

local concentration excesses, which would favour nucleation. La Mer and Dinegar (35), in an attempt to overcome this objection, studied the precipitation of barium sulphate, and produced sulphate ions in situ by the reaction

$$S_2O_8^{2-} + 2S_2O_3^{2-} \rightarrow 2SO_4^{2-} + S_4O_6^{2-} ,$$

and obtained constant values for the critical supersaturation. Collins and Leineweber, however, using a similar technique, concluded that even in this case the nucleation was heterogeneous, since they found the value of the critical supersaturation to be strongly dependent on the purity of the reagents, and other workers have supported these ideas. Nielsen (37) found that steaming out of the reaction vessel prior to use reduced the number of nuclei formed by a factor of ten, and Fischer even goes as far as to predict that pure homogeneous nucleation cannot be achieved.

Thus there are many factors which affect the validity of studies of spontaneous crystallisation, and which make reproducibility almost impossible. It is obviously more informative to study crystallisation under conditions which ensure that only growth, or only nucleation , is taking place. This can be done very easily by the method exploited by C. W. Davies and his co-workers, who prepared supersaturated solutions of silver chloride which remained stable until seed crystals were added (7, 38 - 40). All

growth then took place on these crystals (41), and the rate of crystallisation was measured conductimetrically. This technique has been successfully extended to silver chromate (42), magnesium oxalate (43), and silver iodate (44).

The dissolution of many electrolytes has been shown to follow a first order rate law. This has been interpreted in terms of diffusion of solute away from the hydrated crystal surface. Diffusion control has been observed for most systems, but some exceptions have been recorded, at temperatures other than 25°C.(45).

This thesis is in two parts, the first describing a study of the kinetics of crystallisation of lead sulphate and barium sulphate. Measurements have been made in the presence of added impurities, to test the adequacy of the existing theories when there is adsorption on the surface of the crystals. Barium sulphate growth has been studied at various temperatures, from 15° - 45°C.

The second part of the thesis is concerned with a study of the dissolution of lead sulphate into subsaturated solution at 25°C., and also in the presence of adsorbates. The dissolution of barium sulphate into water at temperatures ranging from 15° - 45°C. has also been investigated, both conductimetrically and by a radiotracer method. Dissolution into subsaturated solution at 25°C. has been followed.

Apparatus and Experimental Technique.

The crystal growth of lead sulphate and barium sulphate from supersaturated solutions has been followed. Supersaturated solutions of lead sulphate were prepared by mixing sodium sulphate and lead nitrate solutions of known concentrations. Similarly, for barium sulphate, supersaturated solutions were prepared from sodium sulphate and barium chloride. The rate of crystallisation after inoculation with seed crystals was followed by measuring the decrease in conductivity with time.

Dissolution of lead sulphate into subsaturated solution, and of barium sulphate into water and subsaturated solutions, have been studied in the same manner. In addition, dissolution of barium sulphate into water has been studied by a radiochemical method, using ^{35}Sulphur as tracer.

Measurement of Resistance.

An a-c screened Wheatstone network of the type described by Jones and Joseph (46) and Shedlovsky (47) was used for the conductivity measurements (fig. 1).

R_1 was the conductivity cell, R_2 a Sullivan and Griffiths non-reactive resistance box, reading from 0.1 to 10,000 ohms. The ratio arms R_3 and R_4 were provided by a Sullivan high frequency 100 ohm decade potentiometer, subdivided into four decades

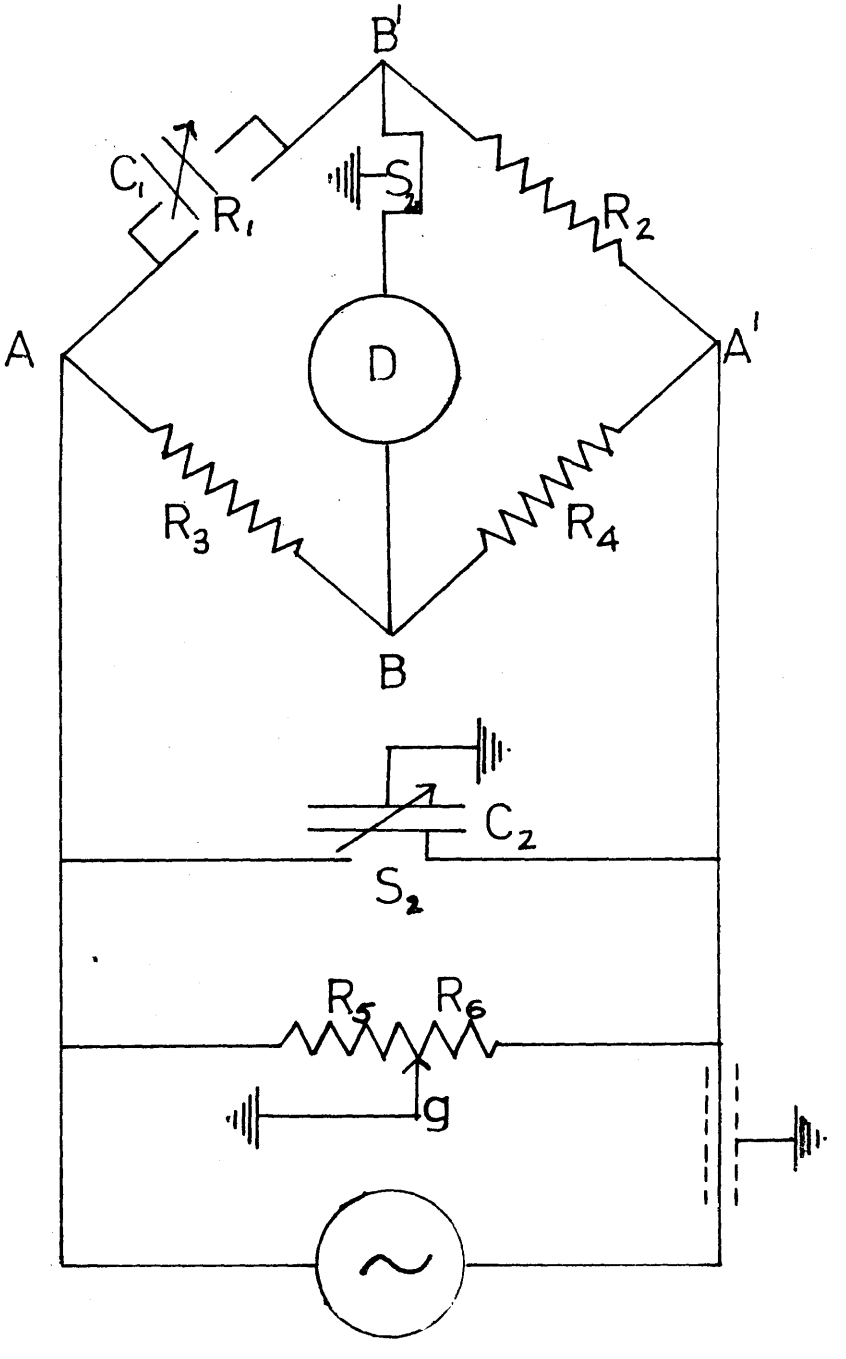

Figure 1.

from 0.01 to 100 ohms. To enable readings to be made to 0.001 ohms, the bridge was made more sensitive by the addition of a 1.2 ohm Pye precision slide wire in series with the decade potentiometer.

Since the cell itself behaves as a condenser, a variable Sullivan stable decade mica condenser, C_1, reading from 0 to 1μF. was connected across R_1 or R_2 to balance out any capacity effects between the electrodes, and between the electrodes and the cell wall. In practice, the condenser was always connected across R_1.

The output from the bridge was amplified by a high gain mains operated amplifier (Elesco Electronics Limited). A mains operated variable frequency oscillator (Advance model H - 1) was used as a source of frequency. A frequency of 1000 cycles per second was normally used, this being the optimum for aural detection. Earthed and screened leads connected the oscillator to a balanced and screened Sullivan transformer. This transformer was designed to screen the supply source from the bridge without affecting the balance of the latter to earth. The transformer was connected to the bridge by screened, earthed leads.

A modified Wagner Earth of the type described by Jones and Joseph (46) was employed to ensure that the telephone ear-piece was maintained at ground potential, so that there was no leakage of current between the telephone coils and the operator. The Wagner Earth (fig. 1) is represented by the resistances R_5, R_6,

variable condenser C_2 and sliding contact g. Once the bridge was balanced in the usual way, the detector, D, was connected to ground by switch S_1, R_5 and R_6 were then adjusted through the contact g, so that $R_5/ R_6 = R_3/ R_4$, thus ensuring that B was at earth potential. The bridge was again balanced and the process was repeated until no change in the sound minimum was observed between successive measurements.

The cell was brought into circuit by two copper leads stretching from the platinum - mercury contacts of the electrodes to mercury cups supported in the thermostat. The copper leads were of equal length to compensate for their resistance, as were screened leads from the mercury cups to the resistance box R_2. The mercury cups were kept in the thermostat to ensure that they were at the same temperature as the cell.

When water and solutions of high resistance were being measured, a 10,000 ohm non-reactive standard resistance was connected in parallel with the cell.

Thermostat and Temperature Control.

All conductivity experiments were carried out in a constant temperature room, maintained at 25°C.; this prevented condensation on the cell cap. The cell was placed in a large earthed and heat insulated metal tank, filled with transformer oil, to reduce capacity errors (46). Tho oil was stirred by an effective rotary paddle stirrer, to ensure an even temperature was maintained throughout the tank. The temperature of the bath at 25°C. was controlled to ± 0.005°C. by a mercury - toluene spiral regulator, fitted with a Sunvic proportionating head. Heat was supplied by a 60 watt bulb, and a continuous stream of cooling water passed through copper coils immersed in the bath.

Experiments at 15°, 35° and 45°C. were carried out using a water filled thermostat, which was fitted with a booster heater and a refridgerating unit to assist in temperature control. The conductivity cell was held in a small box, which contained transformer oil, to eliminate the capacity effects discussed previously. Temperature control was maintained to ± 0.01°C. at 15°, 35°, and 45°C. Measurement of all temperatures was made with Beckmann thermometers which had been standardised against a calibrated platinum resistance thermometer (48).

During experiments at 35° and 45°C. the temperature of the air in the vicinity of the top of the cell was raised by means of

two 60 watt red bulbs, to prevent condensation on the cell cap.

Seed suspensions for use at 25°C. were aged in the constant temperature room. Those for use at other temperatures were maintained at the required temperature for a few days prior to use.

Preparation of Conductivity Water.

The early part of the work was done using deionised water, which was prepared by passing distilled water over a mixed-bed resin (49). Two resins were used:

1) Amberlite IR 120 (H) acid resin and Amberlite IRA 400 basic resin, mixed in a proportion of 1 : 2 by volume. With such a column an intimate mixture was essential, so that H^+ ions liberated from the resin by exchange of cations were immediately neutralised by OH^- ions liberated from the basic resin by anions.

2) Permutit "Biodeminrolit" which is supplied ready for use as both a cation and an anion exchanger.

Water obtained in this way was stored in a pyrex flask, fitted with a soda-lime guard tube to exclude carbon dioxide. The specific conductivity of this water varied from 0.08 to 0.3×10^{-6} reciprocal ohms.

In later experiments a gas fired Bourdillon still with a tin fractionating column was used for preparing conductivity water, to

ensure that it was free from contamination by organic impurity. The supply of pure air was obtained by passing compressed air through tubes filled with glass beads; two of the tubes contained a 30% potassium hydroxide solution, and the last contained water. The specific conductivity of this water was 0.2 to 0.6 x 10^{-6} reciprocal ohms.

Latterly, water from an electrically heated all-glass still, constructed on the model of the Bourdillon still was used. This gave water with a specific conductivity of 0.3 to 0.6 x 10^{-6} reciprocal ohms.

The Conductivity Cell.

The conductivity cell was of the type described by Hartley and Barrett (50), and was constructed from pyrex glass. The body was supplied by Quickfit, and had a B.55 ground glass joint at the neck. The cap carried the electrodes, an aperture through which the stirrer passed, another for addition of solutions, and a horizontal side arm fitted with a tap, through which carbon dioxide free nitrogen was admitted (Plate 1).

The electrodes were of greyed platinum, perforated to ensure stirring of the solution between the plates, which were held firmly at a fixed distance by four small pyrex glass rivets. The electrodes

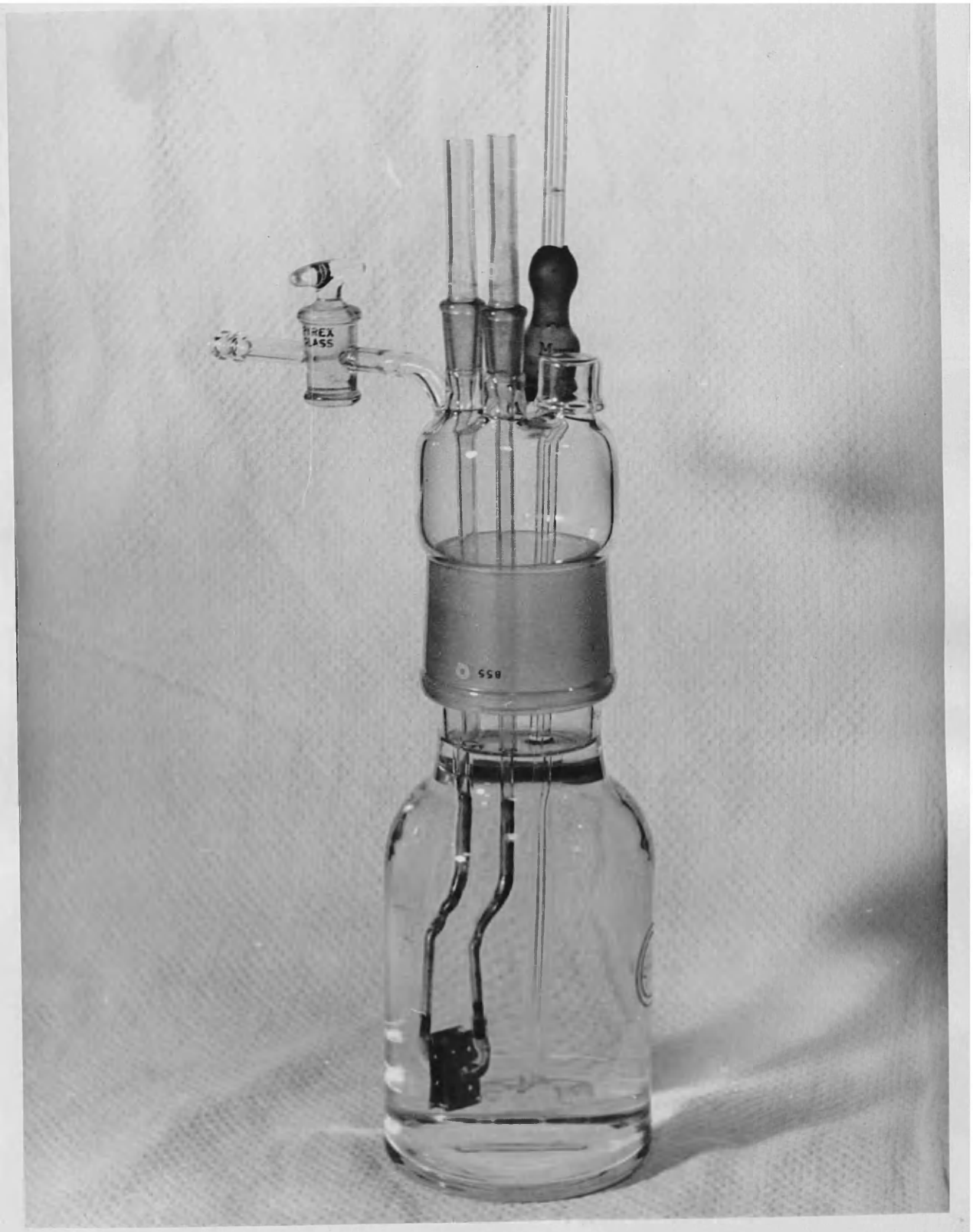

Plate 1.

were carried by platinum wires which were fused into the glass supports, but since it is not possible to make a perfect platinum - glass seal, a little powdered Araldite thermosetting epoxy resin was set in the bottom of each support. This was left overnight at 60°C. to fuse, and then allowed to cool slowly, making a permanent seal. The electrodes were situated near the wall of the cell, and their supports were fixed to the cap by two B.10 Quickfit joints, and sealed into position with Araldite. Alignment of a mark on cell and cap ensured that the electrodes were placed in the same position relative to the outer container for each experiment.

Stirring was supplied by a Vibromix motor (Shandon Scientific Company), the actual stirrer being a circular glass disk, perforated with conical holes and fused to a glass rod. The maximum amplitude of the oscillations was 0.03 inches, and the rate of stirring could be varied widely. With this type of stirrer it was possible to ensure that the disc was in the same place relative to the electrodes in every experiment.

The cell was kept free of carbon dioxide by the passage of a continuous stream of nitrogen, which was introduced through the side arm. A dust cap sealed the aperture through which additions of solutions were made, and dust was prevented from entering through the stirrer aperture by a rubber teat.

Preparation of Stock and Cell Solutions.

Pyrex glass apparatus was used in the preparation and storing of all solutions. Pipettes were of Grade A standard. Flasks were cleaned with chromic acid and steamed out prior to use; they were filled with distilled water when not in use.

Solids were weighed in pyrex sample tubes on a Stanton Model S.M.1 balance, using platinum plated weights. Solutions were made up by weight from conductivity water, using a Sartorius balance of 2 Kg. capacity, which was sensitive to 0.005g. The weights for both balances had been calibrated by the method of Kohlrausch (51), and all weights were vacuum corrected.

Analar salts were used throughout, and potassium chloride used in cell constant determinations was recrystallised three times from conductivity water. Stock solutions were prepared by weight from conductivity water. Dilute solutions were freshly made up for each experiment from these stock solutions, the concentration of the former being such that 10 ml. added from a calibrated pipette to about 300 g. of conductivity water in the cell would give a cell solution of the required concentration. The dilute solutions were prepared by weight from the stock solutions in exactly the same way.

A typical experiment involved washing the cell thoroughly with distilled and conductivity water, filling it with conductivity water,

and weighing. It was then placed in the thermostat, and carbon dioxide was removed by passing nitrogen, which had been presaturated with water at 25°C., into the cell. When temperature and carbon dioxide equilibrium had been reached, the dilute solutions were added, the second one drop by drop over a period of 5 - 10 minutes, to prevent the formation of high local concentrations which would favour spontaneous nucleation. After each addition the cell was allowed to come to equilibrium again. The conductivity would then remain steady for 24 - 48 hours, but in practice, seed crystals were usually added after one hour.

Carbon dioxide was removed from the seed suspension before addition to the cell by passing a rapid stream of nitrogen over it for 30 - 60 minutes. The seed crystals were added to the cell from a rapid delivery pipette. Zero time for the reaction was taken as the time when half of the seed suspension had reached the cell contents. The change in conductivity was determined at minute intervals at the start of the experiment, then at 15 minute and latterly at 30 minute intervals. Many runs were followed for 24 hours or more.

Determination of the Concentration of the Added Seed Suspensions.

The concentration of each preparation of seed crystals was determined by filtration of a 5 ml. sample through a number 4 sinter, drying and weighing. Generally, the average of three such estimations

was used.

In later work, when very high concentrations of seed suspension were being used, it was difficult to add a reproducible amount of solid to each experiment. The concentration of seed crystals added in each run was then determined by filtration of the final cell solution, in the manner described above.

Determination of Cell Constant.

The cell constant was determined by the method of Frazer and Hartley (52). Thrice recrystallised potassium chloride was used in the preparation of the stock solutions. A small quantity of this pure material was heated in a platinum crucible to a dull red heat for about 10 minutes, and allowed to cool in a desiccator. About 1g. was then weighed out in a pyrex sample tube and the resulting stock solution was approximately decinormal.

The cell was weighed, and then about 250g. conductivity water were added. It was then allowed to come to carbon dioxide and temperature equilibrium; this was usually attained in 2 - 3 hours, and resistance readings would then remain constant for 24 hours or more.

Once the conductivity had remained steady for about one hour, additions of the stock solution of potassium chloride were made to

the cell, using a weight burette. Equilibrium was usually reached again after about 20 - 30 minutes, when the resistance was measured. The resistance box R_2 was adjusted until the balance position was close to the centre of the ratio arms R_3 and R_4. Values of both R_3 and R_4 were obtained, and the value of R_2 was then changed by five ohms, and two further readings made on the ratio arms. The average conductivity value was calculated from both pairs of ratio arms readings, and then corrected for the water resistance.

Further additions from the weight burette were made until the concentration of potassium chloride in the cell was about 0.001M. The cell was removed, and after its outer surface had been cleaned and dried it was weighed again.

The cell constant was calculated by comparing each measured value with the conductivity derived by Shedlovsky (53), at the same concentration, using the interpolation formula

$$\Lambda = 149.92 - 93.85\ c^{\frac{1}{2}} + 50c$$

where Λ is the equivalent conductivity of potassium chloride of normality c (54). The value of the cell constant for each cell used was obtained from at least twelve determinations (three series).

Cell A had a cell constant of 0.0700 ± 0.1%

Cell B had a cell constant of 0.07124 ± 0.1%

Cell D had a cell constant of 0.06949 ± 0.1%

Cell E had a cell constant of 0.07312 ± 0.1%.

The conductivity technique described above was used in the first two parts of this work. The radiochemical technique used is described in detail in part 2b.

PART 1. Crystallisation of Sparingly Soluble Salts in Aqueous Solutions.

1a. Lead Sulphate.

1b. Barium Sulphate.

INTRODUCTION.

An equation of the type

$$-\frac{dm}{dt} = k\,s\,(m - m_o)^n \quad . \; . \; . \; . \; . \; . \; (1)$$

where k is the rate constant, s is a function of surface area, m is the instantaneous ionic concentration, m_o is the solubility value, and n the order of the reaction, has been generally accepted as representing the crystallisation process, but opinions have differed about the value of n. Values of 2, 3, 4 and even 8 (32) have been reported, and each explained by a different mechanism of crystal growth. Values of n greater than 2, however, have generally been obtained from studies of nucleation rather than growth.

In a study of the growth of silver chloride seed crystals, Davies and Jones (7) found a value of 2 for n, and interpreted the kinetics in terms of an adsorbed monolayer of ions at the crystal surface. They made the following two assumptions:

(1) A crystal in contact with an aqueous solution always tends to be covered with a monolayer of hydrated ions, and secondary adsorption on this monolayer is negligible.

(2) Crystallisation occurs through simultaneous dehydration of pairs of anions and cations.

When the surface reaches equilibrium the rate of adsorption

of ions from the solution must be sufficient to maintain the monolayer intact, and it is assumed that every ion striking the surface from a saturated solution enters this mobile adsorbed layer. Then the rate of adsorption of cations = $k_1 s[A_o^{m+}]$, and of anions = $k_1 s[B_o^{n-}]$, where the subscript zero indicates the solubility value of each ion species. In an unsaturated solution, ions leave the surface faster than they are replaced, while in a supersaturated solution, all ions reaching the surface do not enter the monolayer, and those which do not, $([A^{m+}] - [A_o^{m+}])$ for cations, and $([B^{n-}] - [B_o^{n-}])$ for anions, are available for deposition. These ions either suffer elastic collisions at the surface of the monolayer, or, should a cation and an anion arrive simultaneously at a growth site, the underlying ion pair can become dehydrated and incorporated into the crystal lattice. For a symmetrical electrolyte such as silver chloride or lead sulphate, m = n, and the rate equation would become

$$-\frac{dm}{dt} = k([A^{m+}] - [A_o^{m+}])([B^{n-}] - [B_o^{n-}])$$

$$= k(m - m_o)^2 \quad \ldots\ldots\ldots (2)$$

Walton (54) has arrived at a similar rate equation from a more theoretical viewpoint, by considering the adsorption of ions upon sols of the same material as following the Gibbs Adsorption Isotherm,

$$\Gamma_{A^+} = k_1 \ln [A^+] + \text{constant}_1 \quad \ldots\ldots (3)$$

where Γ_{A^+} represents the total concentration of adsorbed cations. A similar expression holds for anions,

$$\Gamma_{A^+} = k_2 \ln [B^-] + \text{constant}_2 \quad . \quad . \quad . \quad . \quad . \quad . \quad (4)$$

The rate of surface reaction per unit area may be expressed as

$$J = - k (A^+ + B^-) \quad . \quad . \quad . \quad . \quad . \quad . \quad . \quad . \quad . \quad (5)$$

By substitution from (3) and (4), (5) reduces to

$$J \simeq \frac{k k_1 k_2}{c_0^2} (c - c_0)^2$$

in the special case where the ionic concentrations are equivalent, and $c \longrightarrow c_0$. Similar expressions can be derived for non-equivalent ionic concentrations, and non-symmetrical electrolytes.

Doremus (10) has suggested two possible mechanisms for the transfer of dehydrated ions from the adsorbed layer to the growth sites. In Model A he proposed that the adsorbed ions combined in the surface layer to form neutral "molecules", which then diffused along the crystal surface until they reached a suitable growth site. To explain certain experimental results, in which a third order rate law was found to apply, he postulated, by analogy with gas phase reactions, that an additional adsorbed ion takes part in the surface combination process. In Model B, the adsorbed ions are considered to collide directly with a kink in the growth step, resulting in alternative incorporation of cations and anions in the crystal lattice. This model gives rise to a second order r

equation for a symmetrical electrolyte.

Doremus showed that results obtained from spontaneous crystallisation experiments on barium sulphate by Turnbull (9), and by Johnson and O'Rourke (36), and on silver chromate by Van Hook (56) could be explained satisfactorily by Model A. On the other hand, data obtained by Howard and Nancollas (42), for the crystallisation of silver chromate on added seed crystals, fitted Model B, as did results for silver chloride (38) and barium sulphate (57). Doremus interpreted this disparity in terms of the widely different supersaturations used in the two sets of experiments.

For Model A, and a symmetrical electrolyte, the rate of precipitation should be proportional to the third power of the solute concentration, whereas for a 1:2 electrolyte such as silver chromate, the rate should vary with the fourth power of the solute concentration. With Model B, however, and a symmetrical electrolyte, the rate of precipitation should depend on the second power of concentration, while the rate should be proportional to the third power for a 1:2 electrolyte. Thus, at high supersaturations, conditions should favour Model A, while at lower concentrations, Model B should apply.

The supersaturations used in the spontaneous crystallisation experiments (9, 36, 56) are much higher than those used in seeded growth (38, 42, 57) and Doremus considered this to explain the apparently conflicting results obtained with silver chromate and

barium sulphate.

In the above theories of growth, it was assumed that the adsorbed monolayer contained equal numbers of positive and negative ions, but in general it will not be so. If one ion is adsorbed more strongly to the precipitate than the other, due to differences in the adsorption energies, the surface will assume an electrical charge, resulting in an electrical double layer being set up around the particle. However, for concentration ratios equal or near to the stoichiometric one this selective adsorption will be negligible.

When the ionic concentrations are non-equivalent, a different situation arises. When seed crystals are added to a solution in which $[A^{m+}] / [B^{n-}] = r$, where $r > 1$, more A^{m+} ions will be adsorbed and a potential difference, ψ, will be set up between the adsorbed layer and the solution. In such a situation, the crystal growth will be controlled by the concentration of the deficient ion B^{n-} only, since the surface concentration of excess ions remains effectively constant. The equilibrium value of ψ is such that cations and anions enter the adsorbed layer in equivalent amounts.

The availability of cations at the surface is then given by

$$k_1 \, s \, [A^{m+}] \exp. (-\psi / RT)$$

and that of anions by

$$k_2 \, s \, [B^{n-}] \exp. (\psi / RT).$$

These are equal when m = n, hence

$$\exp. (\psi / RT) = [A^{m+}]^{\frac{1}{2}} / [B^{n-}]^{\frac{1}{2}} = r^{\frac{1}{2}}.$$

Since the number of ions of each type entering the monolayer is m_o, the rate of crystallisation is given by

$$-\frac{dm}{dt} = k\,s\,([A^{m+}]r^{-\frac{1}{2}} - m_o)([B^{n-}]r^{\frac{1}{2}} - m_o)$$

$$= k\,s\,([A^{m+}]^{\frac{1}{2}}[B^{n-}]^{\frac{1}{2}} - m_o)^2$$

which reduces, when $[A^{m+}] = [B^{n-}]$, to equation (1), with n = 2.

Crystallisation of symmetrical electrolytes could therefore be expected to follow a second order rate law, even when the ionic concentrations are not equivalent. This has been shown to be the case for silver chloride (7), barium sulphate, (56), and magnesium oxalate (43).

Another method of altering the surface of the seed crystals is the addition of impurity molecules which are likely to adsorbed by the crystals. Davies and Nancollas (39) have studied crystal growth in the presence of a variety of such additives, and found that while they all had a considerable effect on the rate of growth, the mechanism was unchanged.

Part Ia of this thesis describes a conductimetric study of the crystallisation of lead sulphate from supersaturated solutions of equivalent and non-equivalent ionic concentrations. Experiments were also made in the presence of surface active agents.

Results obtained at equivalent ionic concentrations were in agreement with the theory described above. Second order growth was observed for most of the reaction, with the exception of an initial

very fast growth surge, which has been interpreted in terms of enhanced two-dimensional nucleation on the surface of the added seed crystals. Growth in the presence of adsorbates was also found to follow a second order rate law, but deviations from this were observed when the concentration of additive was high. Crystallisation at non-equivalent ionic concentrations did not follow the proposed mechanism, and no satisfactory explanation of the results has been made so far.

Part 1b is concerned with the crystallisation of barium sulphate at various temperatures. The rate of reaction was found to be temperature dependent, and followed second order kinetics. Heats of crystallisation have been evaluated.

PART 1a. Lead Sulphate.

Of the three common sparingly soluble sulphates, that of barium has been most studied, because of its importance in quantitative analysis. Much of the work on lead sulphate has been concerned with its precipitation and aging, and there is little to be found in the literature concerning the growth process itself.

The present study was undertaken with the object of determining the similarities, if any, between the crystallisation behaviour of this salt and barium sulphate. In particular it would be interesting

to see if the growth of lead sulphate was characterised by an initial, very fast growth surge similar to that found by Nancollas and Purdie (57) for the barium salt.

Hahnert (58) described the great differences in the shapes of lead sulphate crystals produced by varying the mixing time of the reagents, and by the presence of added impurities. He observed that the most perfect rhombohedra were formed from dilute solutions, and that as the reagent concentrations were increased, imperfect crystals, which he described as "somatoide" appeared.

Kolthoff and his co-workers (59, 60) made similar observations, and noted that as the concentrations of reagents were increased, the size of the precipitate particles passed through a maximum. They also reported (61) that a considerable supersaturation could be maintained before spontaneous crystallisation took place, and determined the critical concentration product to be 200 times greater than the activity product of a saturated solution of the salt.

In an earlier study, Kolthoff and Rosenblum (60, 62) studied the rate of aging of lead sulphate precipitates, and found it to be independent of stirring speed. Since the speed of agitation would be important in Ostwald ripening, they concluded that this was not taking place, and suggested that the aging occurred by recrystallisation in a liquid layer round the particles. Kolthoff and Rosenblum (60) also showed that neither sodium sulphate nor lead nitrate was

specifically adsorbed on the surface of the crystals. On the other hand, dyes such as wool violet (64), were very strongly adsorbed, to the extent of one dye ion per 1.5 lead ions on the surface in neutral solution. If the concentration of wool violet was sufficiently high, no crystallisation of lead sulphate took place.

It has been long known that small amounts of impurities may appreciably alter the growth behaviour of crystals (65), and many workers (23, 66 - 68) have observed a considerable reduction in the rate of growth in the presence of adsorbates. Small concentrations of orthophosphate, triphosphate, and pyrophosphate ions have been found to decrease the rate of precipitation of strontium sulphate, and, if present in sufficiently high concentrations, to inhibit precipitation entirely (66, 67). Inhibition of nucleation has also been described by Rigterink and France (69), Reitemeier and Buehrer (70), and others (71, 72). Habit modification has also been observed in many systems (72 - 75), due to slowing of growth by selective adsorption of impurities on particular faces, while the remaining faces continued to grow at the normal rate.

Sears (76) has suggested that small molecules are most likely to be adsorbed at kinks in growth steps, and that monostep coverage (77) would be necessary to cause an appreciable reduction in the rate of step motion. He proposed (78) that the adsorbed impurities must prevent assimilation of further growth molecules

into the lattice. If this were not the case, the impurity would be built into the crystal, and the growth rate would not be much retarded. Further advance of a step, once poisoned, can only occur by nucleation of a new step of substrate atoms at the poisoned step. Adsorption of a poison at a growth step should reduce the step energy, and hence the critical energy for two-dimensional nucleation, and an increase in the rate of surface nucleation should result.

For large molecules, however, Cabrera and Vermilyea (19) considered that the effect is not usually specific, since these would be adsorbed at any point on the crystal because of the dispersion forces. In such a situation, therefore, the size of the molecule would be one of the most important factors governing its effectiveness as a growth inhibitor.

Sears (78) has shown that a concentration of 2×10^{-6} mole fractions of ferric fluoride was sufficient to hinder step motion in lithium fluoride, and that a similar concentration caused an appreciable increase of two-dimensional nucleation on perfect lithium fluoride surfaces. Similarly (23), potassium chloride crystals, in the presence of two parts per million by weight of lead chloride, were observed to thicken without impingement on one another, a phenomenon which must also be due to two-dimensional surface nucleation, since the presence of lead chloride would lower the step energy. Nucleation of etch pits in presence of impurity is

considered to be due to the same effect.

It would be interesting to determine if any similar phenomena could be detected in the study of lead sulphate crystallisation in the presence of impurities.

Experimental.

Preparation of Solutions.

Analar reagents were used throughout, unless otherwise stated. Stock solutions of lead nitrate and sodium sulphate were prepared by weight, the concentration usually being about 10^{-2} molar. Dilute solutions were made up for each run, and 10 ml. of these solutions were added to the known weight of water in the cell, as described previously.

This method of preparation of the supersaturated solution resulted in a high concentration of the supporting electrolyte, sodium nitrate, being present. Attempts were made to prepare lead sulphate supersaturated solutions without such a supporting electrolyte, using ion-exchange techniques. Amberlite IR 120 (H) resin was prepared by passing through a 2N. hydrochloric acid solution, and washing free from chloride ions with distilled water. A Molar solution of lead nitrate was passed slowly through the column, which

was washed again, until the effluent was free of lead ions.

A solution of sodium sulphate of the required concentrati[illegible] was then passed through, at a rate of about one drop every 20 [illegible], and the effluent was delivered directly into the cell, and wei[illegible]. The conductivity of this solution was higher than the calculated value, and tests with a flame photometer showed some sodium ion[illegible] still to be present. The affinity of the resin for lead ions [illegible] greater than that for sodium ions, and a complete exchange of [illegible] for sodium was never achieved.

Attempts were then made using an anion exchange resin, Pe[illegible] De-acidite FF (SRA 69). The resin was prepared in the chlorid[illegible] and converted to sulphate with 2 Molar sodium sulphate solutio[illegible]. The column was washed thoroughly before use. A lead nitrate s[illegible] of the required concentration was then passed through, but the exchange of nitrate for sulphate was even less complete than t[illegible] of sodium for lead, and lead sulphate was seen to have precipi[illegible] on the column.

Preparation of Adsorbate solutions.

1. Sodium Dodecylsulphate.

$CH_3 (CH_2)_{10} CH_2OSO_3^- \quad Na^+$ Molecular Weight = [illegible]

A pure sample, kindly given by Imperial Chemical Industries, L[illegible] was used without further purification. Solutions of various concentrations were made up by weight.

2. Sodium Pyrophosphate.

$Na_2 P_2 O_7 10H_2O$. Molecular Weight. = 446.11

Analar sodium pyrophosphate was used without further purification, and solutions made up as before.

3. Sodium Tetrametaphosphate.

$(Na PO_3)_4 4 H_2O$. Molecular Weight = 480

A pure sample, kindly given by Dr. C. B. Monk, was used without further purification.

4. Sodium Trimetaphosphate.

$(Na PO_3)_3 6 H_2O$ Molecular Weight = 414

A pure sample, kindly given by Messrs. Albright and Wilson Ltd., was used without further purification.

5. Cetyl Trimethyl Ammonium Bromide.

$CH_3 (CH_2)_{14} CH_2 N(CH_3)_3^+ Br^-$ Molecular Weight = 346.56

A pure sample, kindly given by Imperial Chemical Industries, Ltd., was used without further purification.

Preparation of Seed Suspensions.

Since lead sulphate has a low temperature coefficient of solubility, preparation of seed crystals by recrystallisation was not feasible, and precipitation techniques were used. Various methods

were tried, and the most successful was found to be dropwise addition of 100 ml. portions of 0.1 Molar lead nitrate and 0.1 Molar sulphuric acid to 200 ml. of water with constant vibratory stirring, which was continued for 24 hours. The seeds thus formed were usually well-characterised rhombs, of average size 40 μ, but occasionally batches of crystals which showed highly developed faces were found (Plate 2,B(3)). These were generally needle-shaped, but some had "waists", or were the obtuse-angled cross shape, as has also been observed by Kolthoff and Van't Riet (59).

Attempts to obtain reproducible methods for the production of the various kinds of crystals have been largely unsuccessful; careful control of the conditions of precipitation, stirring, drop-rate, concentration and temperature has not yielded any method by which the desired type of crystal shape can be obtained, except that the more dilute solutions were usually found to give better rhombs.

When a suitable batch of crystals, of uniform shape and size was obtained, the crystals were washed thoroughly with distilled water, then with conductivity water, and stored in pyrex stock bottles. They were set aside at 25°C. to age, for 2 - 4 weeks before use. Details of the suspensions are given in Table 1.

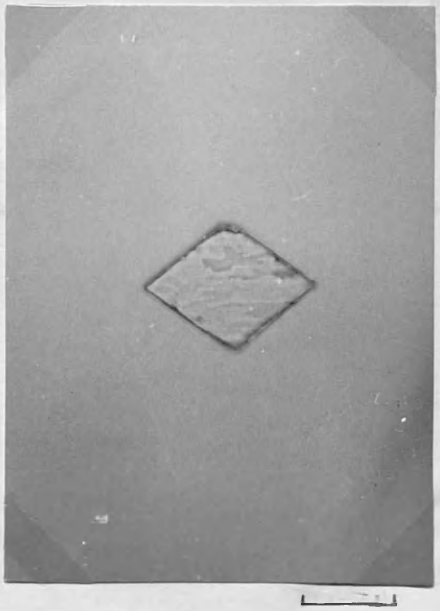

A

20μ

B

20μ

C

20μ

D

20μ

Plate 2.

TABLE. 1.

Seed	Shape	Conc. (mg/ml.)	Plate 2
A	needle	60	B, C, D
B	needle	65	B, C, D
D	rhombic	100	A
E	rhombic	8	A
G	rhombic	100	A

Determination Of Solubility.

The solubility of lead sulphate seed crystals was determined by letting crystallisation and dissolution experiments proceed to equilibrium. Values obtained from both methods agreed to within 1% of each other. The solubility of lead sulphate was found to be 1.466×10^{-4} moles / l. at 25°C., which is intermediate between 1.490×10^{-4} moles / l. (80) and 1.40 moles / l. at 22 - 23°C. (63).

The thermodynamic solubility product, K, given by

$$K = [Pb^{2+}][SO_4^{2-}] f_2^2 ,$$

has the value 1.7174×10^{-8}, where f_2 was obtained from the Davies equation (81),

$$- \log f_\pm = z_1 z_2 A \left(\frac{\sqrt{I}}{1 + \sqrt{I}} - 0.2I \right) ,$$

with A = 0.5092.

The solubility value was corrected for ionic strength at the various concentrations of supersaturated and subsaturated solutions used.

Determination of Concentration of Crystals Added to the Cell.

Since the concentration of seed crystals added to the cell was very high - in the region of 300 mg / ml. - reproducibility was not good, and so the weight of seeds added to each experiment was determined by filtration of the cell solution through a Number 4 sinter after the run had been completed.

Experiments in the Presence of Adsorbates.

The required amount of adsorbate solution was added to the supersaturated solution in the cell, before inoculation with seed crystals. Once the cell solution had again reached temperature and carbon dioxide equilibrium, and the conductivity had remained steady for one hour, seed crystals were added, and the change in conductivity followed in the usual way.

RESULTS.

The experiments described in this section were carried out in order to determine the rate of crystallisation of lead sulphate at 25°C., and to find the effect of inorganic impurities on the growth. Some experiments were also made with non - equivalent concentrations of lead and sulphate ions.

The supersaturated solutions were stable until the addition of seed crystals, and since these had been aged for 2 - 4 weeks prior to use, it was not possible for fresh nuclei to be formed; all growth therefore took place on the crystals supplied (41).

Ionic Mobilities and Equivalent Conductivity.

The ionic mobility of sulphate was taken as 80.0 (82), and that of lead as 69.40 (83) at 25°C.

The equivalent conductivity can be obtained from the Onsager equation if the conductivity at infinite dilution and the concentration of the solution are known. For lead sulphate, the equivalent conductivity is given by (84)

$$\Lambda^\circ_{PbSO_4} = \Lambda^\circ - (1.8216\,\Lambda^\circ + 239.44)\sqrt{2m_i} \quad . \quad . \quad . \quad . \quad . \quad (1)$$

the concentration m_i being expressed in g. mole. / l., and Λ° = 149.40.

The equivalent conductivity can be evaluated in another way from measured conductivity values and the cell constant,

$$\Lambda = \frac{1000 \times 1/R \times \text{cell constant}}{2 \times m} \quad . \quad . \quad . \quad . \quad (2)$$

where R is the resistance of the solution corrected for the resistance of water. Calculation of experimental values using equation (2) gave results which agreed to within 0.5% of the theoretical value for all cell solutions. Hence an independent check on the accuracy of preparation of the cell solutions could be made.

The activity of the solution was taken as the concentration, so that over the very small concentration changes involved the value of Λ was considered constant, and taken as 140.56 at the concentration 1.774×10^{-4} moles / l. The change in concentration in solutions of equivalent ionic concentration was evaluated from the expression

$$\Delta m = \Delta l/R \times F$$

where F is given by

$$\frac{1000 \times \text{cell constant}}{2 \times \Lambda}$$

Crystallisation at Equivalent Ionic Concentrations.

Trial experiments were carried out to determine the initial concentration which would give a reasonable rate of growth, and a supersaturation of 80% was found to be suitable. Typical smooth plots of the reciprocal of resistance against time are shown in Fig. 6, Tables 4, 7 and 8. The initial rate of crystallisation was obtained by making a short extrapolation of this growth curve to

zero time. Differences between the instantaneous values of 1/R and this initial value of 1/R were used to calculate the amount of lead sulphate precipitated at any time. Plots of the integrated form of the second order rate equation

$$-\frac{dm}{dt} = k\,s\,(m - m_o)^2$$

were found to be good straight lines with the exception of an initial very fast growth surge, the order of which was obviously not two. A typical plot is shown in Fig. 2, using data given in Table 3.

The effect of increasing the concentration of seed crystals, and of reducing the initial supersaturation was tested, and the results are summarised in Table 2. The result of increasing the seed concentration can be seen from Runs 9, 11 and 13, (Table 4), and rate plots are shown in Fig. 3. Runs 17, 18 and 28 (Table 5) and Runs 31 and 32 (Table 6) show the effect of a reduction in supersaturation, and the corresponding second order plots are shown in Figs. 4 and 5.

Results with Different Types of Seed Crystals.

The seed crystals used in the experiments described so far were regular rhombs, of average size 40 μ (Plate 2A). Some batches of crystals, however, were predominately needle-shaped, although a number had pronounced "waists" (Plate 2B, C, D). These crystals were

TABLE. 2.

Crystallisation of Lead Sulphate.

Experiment Number	Seed Suspension	Seed conc. (mg/ml)	$m_i \times 10^4$ moles/l.	Duration of initial part (mins.)	% reaction followed.
9	E	8	1.7740	5	34
11	E	30	1.7740	3	34
13	E	96	1.7740	0	42
17	D	100	1.7740	15	31
18	D	100	1.7740	15	43
28	D	100	1.6780	9	30
31	G	100	1.7740	15	30
32	G	100	1.6250	5	22
14	A	90	1.7702	30	77
15	A	90	1.7740	30	58
19	B	100	1.7740	30	85

TABLE. 3.

Crystallisation of Lead Sulphate.

Time	10^3 / R ohms^{-1}	10^4 m moles/l.	10^4 ($m-m_o$) moles/l.	$10^{-4}\sqrt{(m-m_o)}$ l./mole	I* l./mole.
Run 8.					
0 min.	1.26250	1.7740	0.2574	0.3885	
1.5	1.25785	1.7628	0.2462	0.4062	1.77
6	1.24719	1.7323	0.2157	0.4636	7.53
15	1.23914	1.7143	0.1977	0.5058	11.7[illegible]
30	1.23414	1.6990	0.1824	0.5482	15.9[illegible]
1 hr.	1.22816	1.6838	0.1672	0.5981	20.9[illegible]
2	1.22074	1.6649	0.1483	0.6743	28.5[illegible]
3.5	1.21337	1.6461	0.1295	0.7722	38.3[illegible]
4.5	1.20848	1.6342	0.1176	0.8503	46.[illegible]

Cell B. F = 0.2548

$$I^* = \left\{(m - m_o)^{-1} - (m_i - m_o)^{-1}\right\} \times 10^{-2}$$

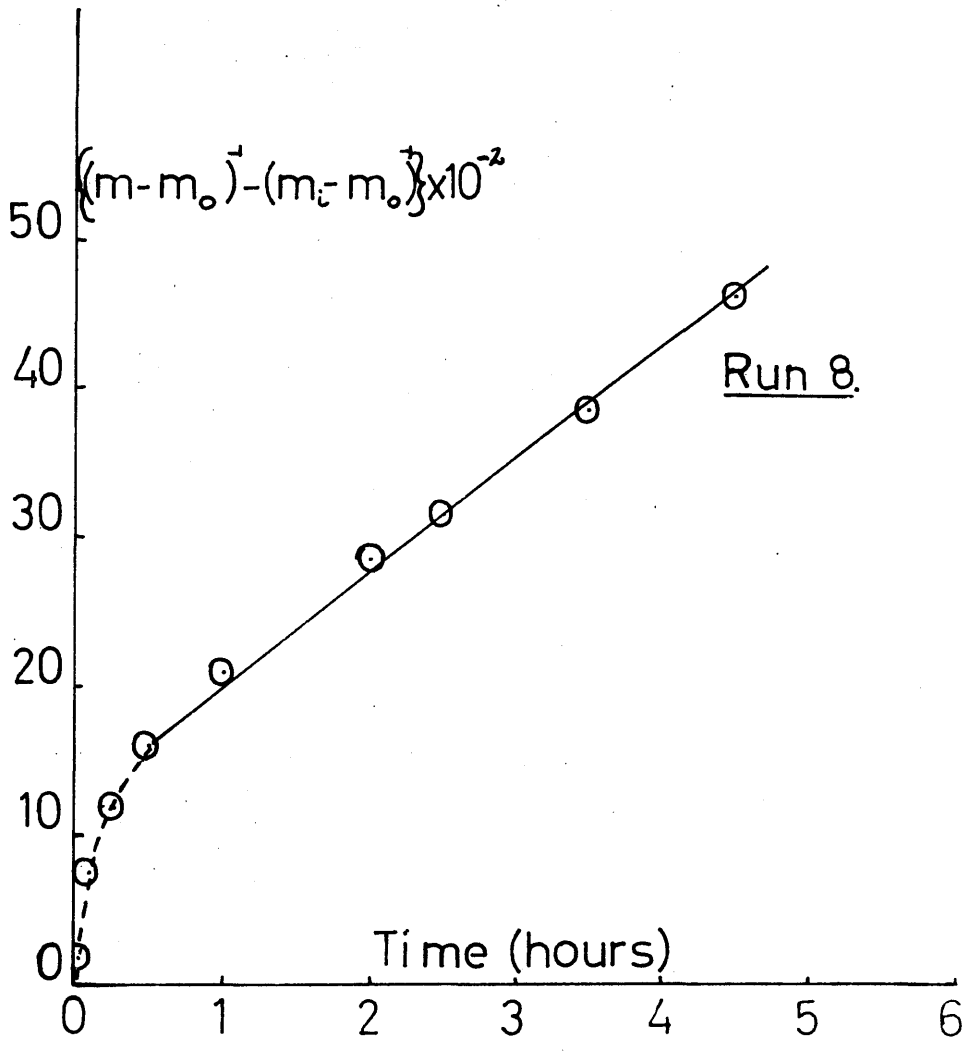

Figure 2.

TABLE. 4. Crystallisation of Lead Sulphate.

Time	10^3 / R ohms^{-1}	10^4 m moles/l.	10^4 (m-m_o) moles/l.	10^{-4}/(m-m_o) l./mole.	Σ l./mole.
Run 9.					
0 min	1.26030	1.7740	0.2574	0.3885	-
3	1.25834	1.7690	0.2524	0.3962	0.77
15	1.25683	1.7652	0.2486	0.4023	1.38
30	1.25530	1.7613	0.2447	0.4087	2.02
2 hrs.	1.24770	1.7419	0.2253	0.4439	5.54
3.5	1.24215	1.7278	0.2112	0.4735	8.50
7.5	1.23164	1.7010	0.1844	0.5423	15.38
8.25	1.22965	1.6959	0.1793	0.5577	16.92
Run 11.					
0 min.	1.25855	1.7740	0.2574	0.3885	-
3	1.25734	1.7709	0.2543	0.3922	0.37
10	1.25632	1.7683	0.2517	0.3973	0.88
15	1.25581	1.7670	0.2504	0.3994	1.09
30	1.25479	1.7644	0.2478	0.4036	1.51
1 hr.	1.25175	1.7567	0.2401	0.4165	2.80
1.5	1.24921	1.7502	0.2336	0.4281	3.96
2.5	1.24417	1.7374	0.2208	0.4529	6.44
3.5	1.23914	1.7246	0.2080	0.4009	11.56

TABLE. 4. (cont.)

Time	10^3 / R ohms^{-1}	10^4 m moles/l.	10^4 (m-m_o) moles/l.	10^{-4}/(m-m_o) l./mole.	[illegible] l./mole.
Run 13.					
0 min.	1.25161	1.7740	0.2574	0.3885	
3	1.25073	1.7723	0.2557	0.3911	[illegible]
7	1.24972	1.7692	0.2526	0.3959	[illegible]
15	1.24795	1.7647	0.2481	0.4031	[illegible]
30	1.24467	1.7563	0.2397	0.4172	[illegible]
1 hr.	1.23914	1.7422	0.2256	0.4433	[illegible]
1.5	1.23464	1.7315	0.2149	0.4652	[illegible]
2	1.23065	1.7206	0.2040	0.4902	[illegible]
3.25	1.22173	1.6979	0.1813	0.5516	[illegible]

Cell B. F = 0.2548.

$$I^* = \left\{(m - m_o)^{-1} - (m_i - m_o)^{-1}\right\} \times 10^{-2}$$

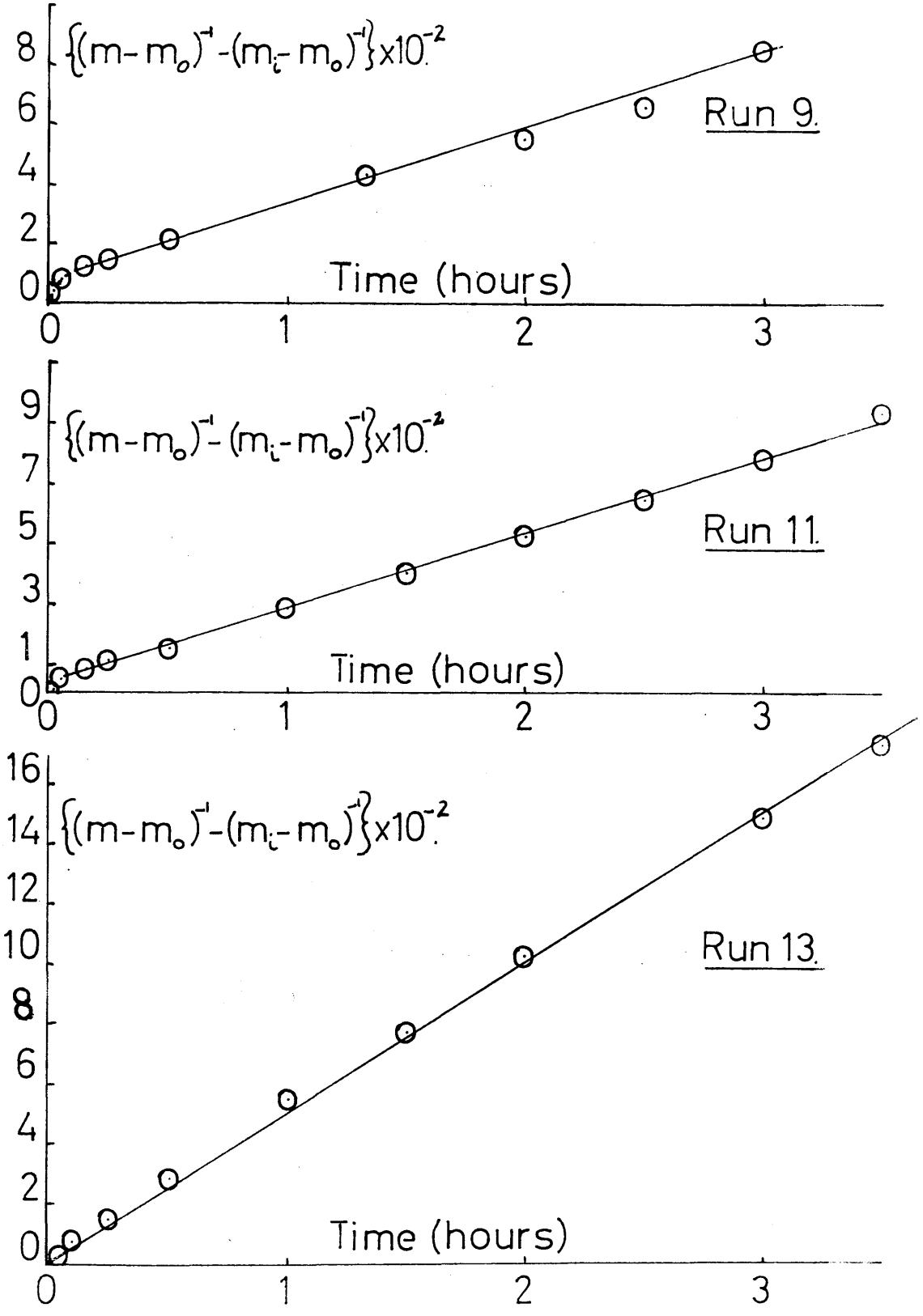
{(m-m_o)^-1 - (m_i-m_o)^-1} x10^-2
Run 9.
Time (hours)
0
2
4
6
8
1
2
3
{(m-m_o)^-1 - (m_i-m_o)^-1} x10^-2
Run 11.
Time (hours)
0
1
3
5
7
9
{(m-m_o)^-1 - (m_i-m_o)^-1} x10^-2
Run 13.
Time (hours)
0
2
4
6
8
10
12
14
16

Figure 3.

TABLE. 5. Crystallisation of Lead Sulphate.

Time	10^3 / R ohms^{-1}	10^4 m moles/l.	10^4 ($m-m_o$) moles/l.	$10^{-4}/(m-m_o)$ l./mole	I* l./mole.
Run 17.	Cell B.		F = 0.2548.		
0 min.	1.26275	1.7740	0.2574	0.3885	-
3	1.25702	1.7594	0.2428	0.4119	2.34
7	1.25627	1.7575	0.2409	0.4151	2.66
15	1.25474	1.7536	0.2370	0.4219	3.34
30	1.25291	1.7489	0.2323	0.4305	4.20
1 hr.	1.24966	1.7406	0.2240	0.4464	5.79
2.5	1.24189	1.7208	0.2042	0.4897	10.12
4	1.23532	1.7041	0.1875	0.5333	14.48
Run 18.	Cell B.		F = 0.2548.		
0 min	1.27270	1.7740	0.2574	0.3885	-
3	1.26747	1.7607	0.2441	0.4097	2.12
9	1.26619	1.7574	0.2408	0.4153	2.68
15	1.26491	1.7521	0.2355	0.4246	3.61
30	1.26276	1.7487	0.2321	0.4308	4.23
1.25 hr.	1.25717	1.7345	0.2179	0.4589	7.04
2	1.25312	1.7241	0.2075	0.4819	9.34
3	1.24882	1.7132	0.1966	0.5086	12.01
4.75	1.23976	1.6901	0.1735	0.5764	18.79

TABLE. 5. (cont.)

Time	10^3 / R ohms^{-1}	10^4 m moles/l.	10^4 (m-m_o) moles/l.	10^{-4}/(m-m_o) l./mole.	I* l./mole.
Run 28.					
0 min.	1.23260	1.6780	0.1669	0.5992	-
3	1.22884	1.6687	0.1576	0.6345	3.53
9	1.22775	1.6659	0.1548	0.6460	4.68
15	1.22680	1.6636	0.1525	0.6557	5.65
30	1.22502	1.6592	0.1481	0.6752	7.60
1 hr.	1.22915	1.6516	0.1405	0.7117	11.25
1.5	1.21924	1.6449	0.1338	0.7474	14.82
2	1.21687	1.6390	0.1279	0.7819	18.27
3	1.21295	1.6292	0.1181	0.8467	24.75

Cell D. F = 0.2481.

$$I^* = \left\{(m - m_o)^{-1} - (m_i - m_o)^{-1}\right\} \times 10^{-2}$$

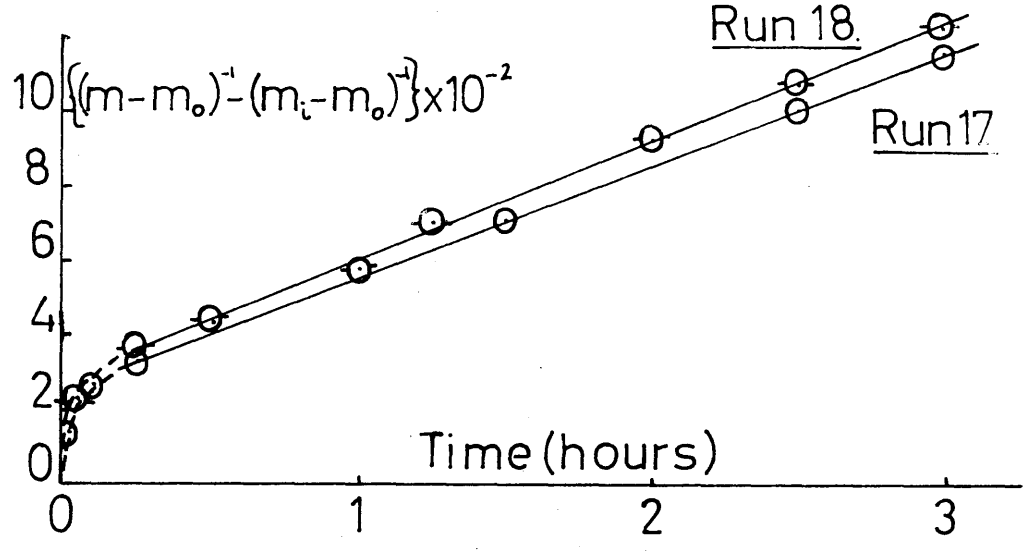
Run 18.
Run 17
$\{(m-m_o)^{-1}-(m_i-m_o)^{-1}\}\times10^{-2}$
Time (hours)
0
1
2
3
0
2
4
6
8
10

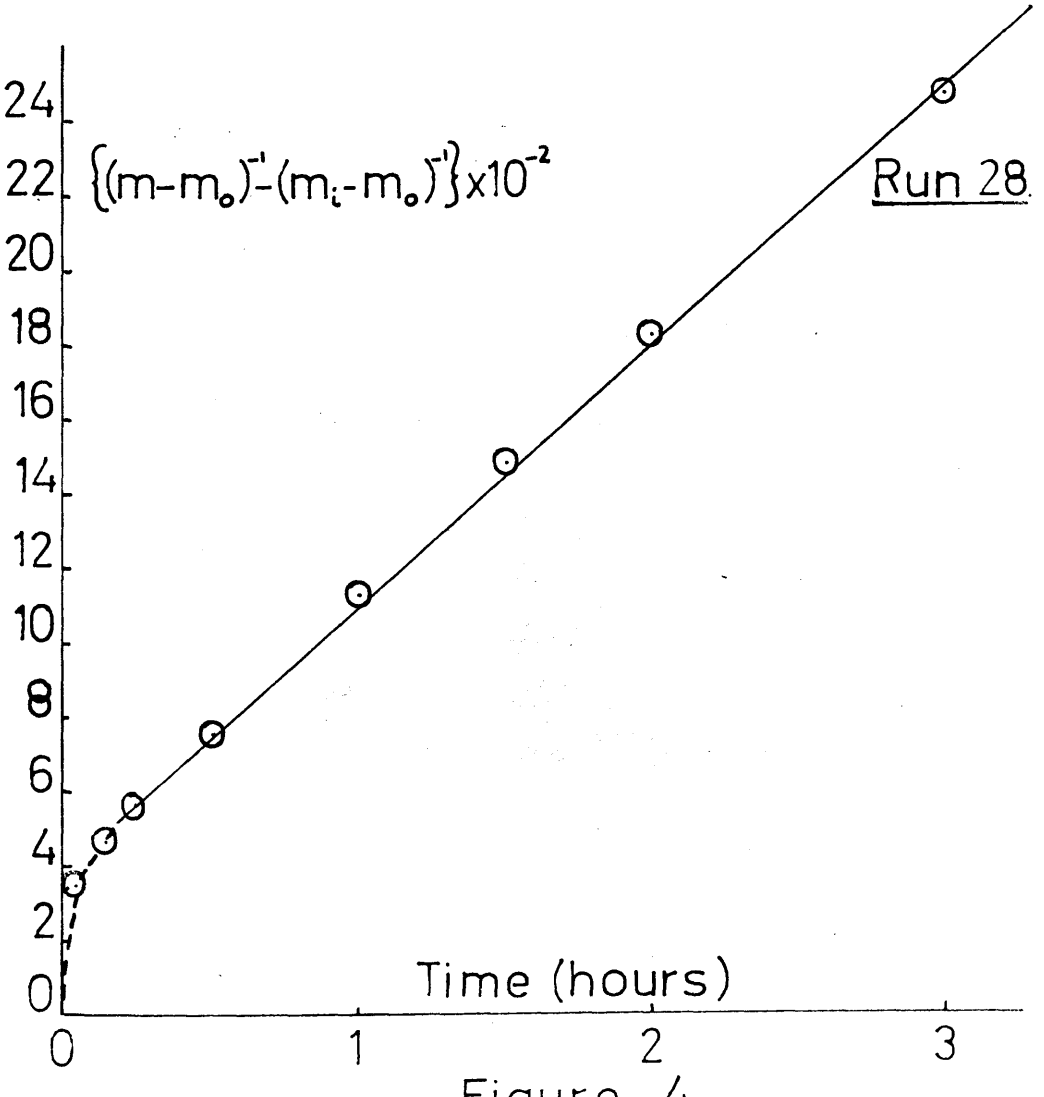
Run 28
$\{(m-m_o)^{-1}-(m_i-m_o)^{-1}\}\times10^{-2}$
Time (hours)
0
1
2
3
0
2
4
6
8
10
12
14
16
18
20
22
24

Figure 4.

TABLE. 6. Crystallisation of Lead Sulphate.

Time	10^3 / R ohms^{-1}.	10^4 m moles/l.	10^4 (m-m_o) moles/l.	10^{-4}/(m-m_o) l./mole.	I* l./mole.
Run 31.					
0 min.	1.21870	1.7740	0.2574	0.3885	-
1	1.21771	1.7714	0.2548	0.3925	0.40
3	1.21545	1.7655	0.2489	0.4018	1.33
9	1.21104	1.7546	0.2380	0.4202	3.17
15	1.20864	1.7477	0.2311	0.4327	4.42
30	1.20431	1.7364	0.2198	0.4550	6.65
1.5 hr.	1.19246	1.7054	0.1888	0.5297	14.12
1.75	1.18957	1.6978	0.1812	0.5519	16.34
Run 32.					
0 min.	1.12775	1.6250	0.1174	0.8518	-
3	1.12680	1.6225	0.1149	0.8703	1.85
9	1.12572	1.6197	0.1121	0.8921	4.03
15	1.12495	1.6177	0.1101	0.9083	5.65
30	1.12379	1.6147	0.1071	0.9337	8.19
1 hr.	1.12049	1.6061	0.0985	1.0152	16.34
2.75	1.11318	1.5870	0.0794	1.2954	44.36

Cell E. F = 0.2614.

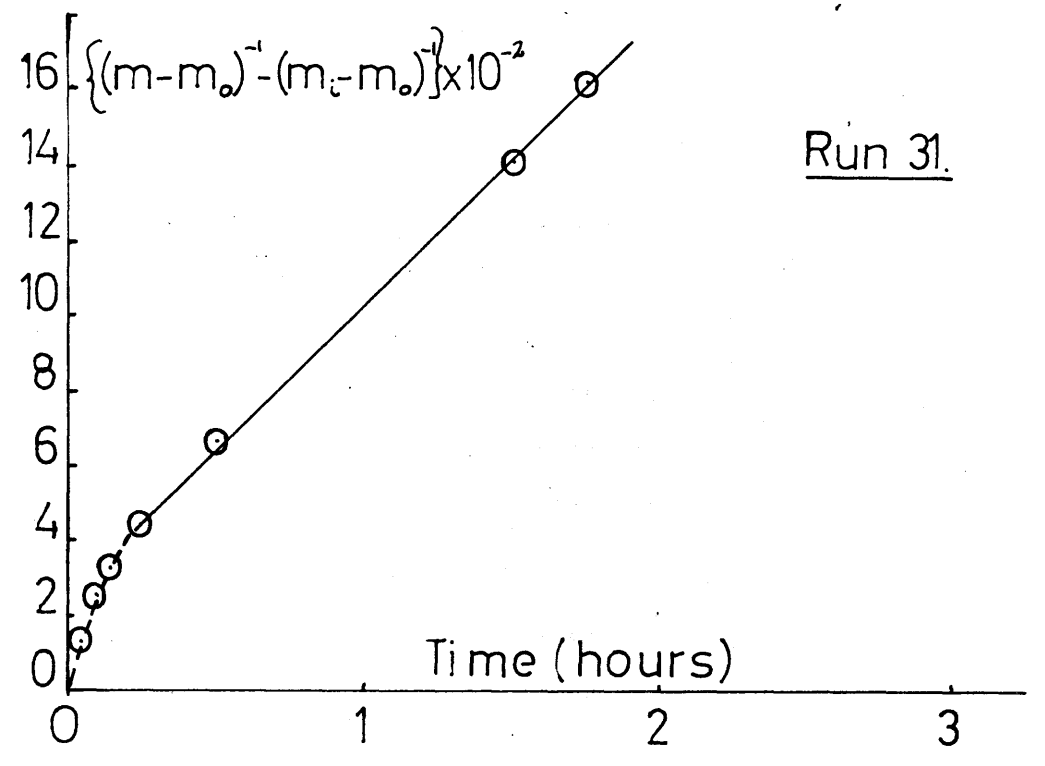
$\{(m-m_o)^{-1}-(m_i-m_o)^{-1}\}\times10^{-2}$
16
14
12
10
8
6
4
2
0
Run 31.
Time (hours)
0
1
2
3

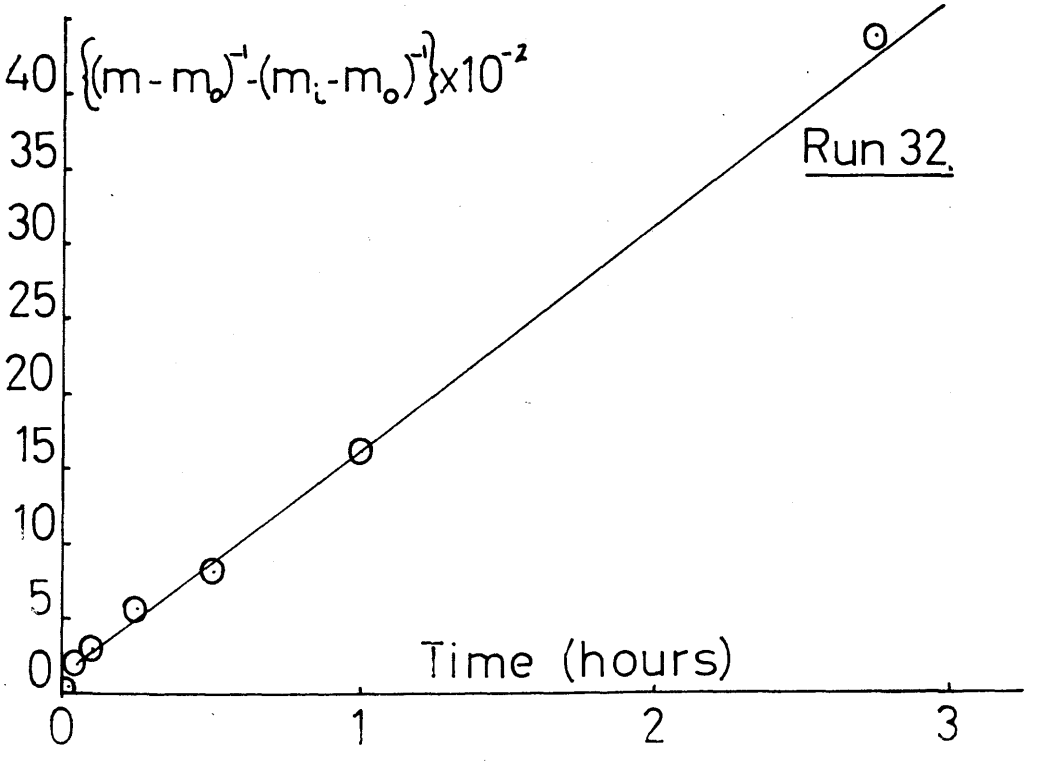
$\{(m-m_o)^{-1}-(m_i-m_o)^{-1}\}\times10^{-2}$
40
35
30
25
20
15
10
5
0
Run 32.
Time (hours)
0
1
2
3

Figure 5.

TABLE. 7. Crystallisation of Lead Sulphate.

Time	10^3 / R ohms^{-1}	10^4 m moles/l.	10^4 (m-m_o) moles/l.	10^{-4}/(m-m_o) l./mole.	I* l./mole.
Run 14.					
0 min.	1.26950	1.7702	0.2536	0.3943	-
1.5	1.24882	1.7172	0.2006	0.4985	11.00
6	1.24126	1.6982	0.1816	0.5507	16.22
15	1.23680	1.6869	0.1703	0.5872	19.87
30	1.23201	1.6747	0.1581	0.6325	24.40
2 hrs.	1.21399	1.6288	0.1122	0.8913	50.28
3	1.20617	1.6088	0.0922	1.0846	69.61
4.5	1.19735	1.5864	0.0698	1.4327	104.42
Run 15.					
0 min.	1.26510	1.7740	0.2574	0.3885	-
1.5	1.23700	1.7024	0.1858	0.5382	14.97
6	1.23077	1.6865	0.1699	0.5886	20.01
15	1.22670	1.6762	0.1596	0.6266	23.81
30	1.22333	1.6676	0.1510	0.6623	27.38
1 hr.	1.21840	1.6550	0.1384	0.7225	33.40
2.5	1.20734	1.6268	0.1102	0.9074	51.89
4.5	1.19765	1.6021	0.0855	1.1696	78.11

Cell B. F = 0.2548. $I^* = \left\{(m - m_o)^{-1} - (m_1 - m_o)^{-1}\right\} \times 10^{-2}$

TABLE. 8. Crystallisation of Lead Sulphate.

Time	10^3 / R ohms^{-1}	10^4 m moles/l.	10^4 (m-m_o) moles/l.	$10^{-4}/(m-m_o)$ l./mole.	I* l./mole.
Run 19.					
0 min.	1.26510	1.7740	0.2574	0.3885	-
1.5	1.24076	1.7120	0.1954	0.5118	[illegible]
6	1.23196	1.6896	0.1730	0.5780	[illegible]
15	1.22709	1.6771	0.1605	0.6231	[illegible]
30	1.22249	1.6654	0.1488	0.6720	[illegible]
1 hr.	1.21639	1.6499	0.1333	0.7502	[illegible]
3	1.19745	1.6016	0.0850	1.1765	[illegible]
5	1.18751	1.5763	0.0597	1.6750	[illegible]
6.5	1.18273	1.5641	0.0475	2.1053	[illegible]

Cell B. F = 0.2458.

$$I^* = \left\{(m - m_o)^{-1} - (m_i - m_o)^{-1}\right\} \times 10^{-2}$$

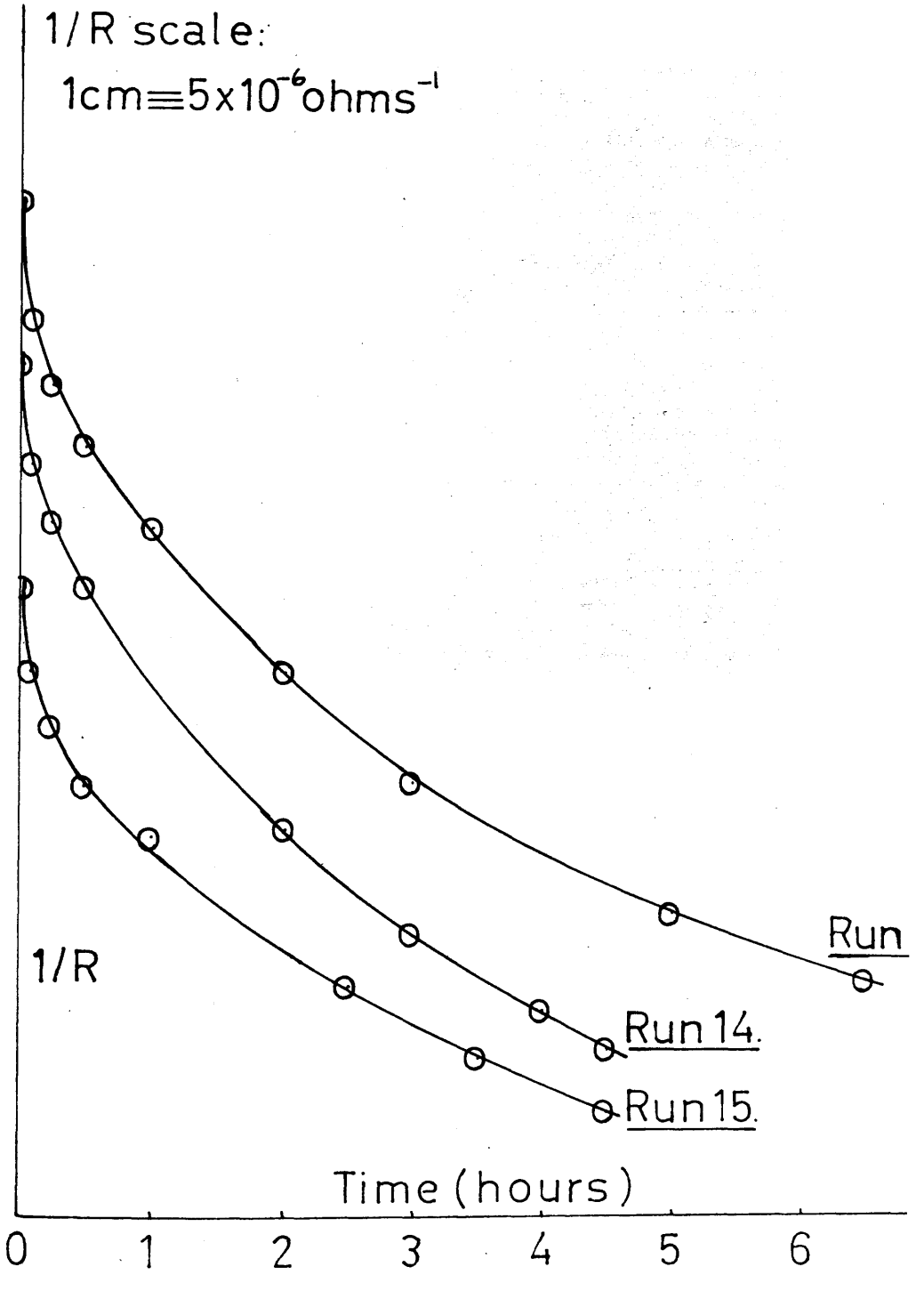
1/R scale:
1cm≡5x10⁻⁶ohms⁻¹
1/R
Run
Run 14.
Run 15.
Time (hours)
0
1
2
3
4
5
6

Figure 6.

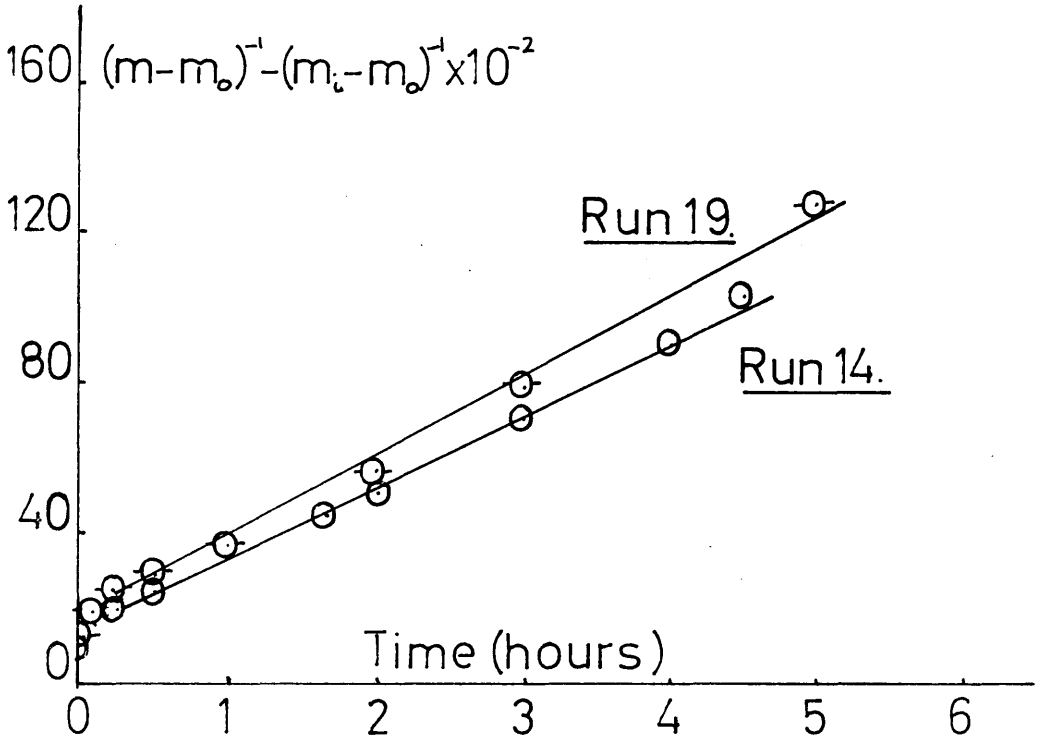
160
120
80
40
0
$(m-m_o)^{-1}-(m_i-m_o)^{-1}\times10^{-2}$
Run 19.
Run 14.
Time (hours)
0
1
2
3
4
5
6

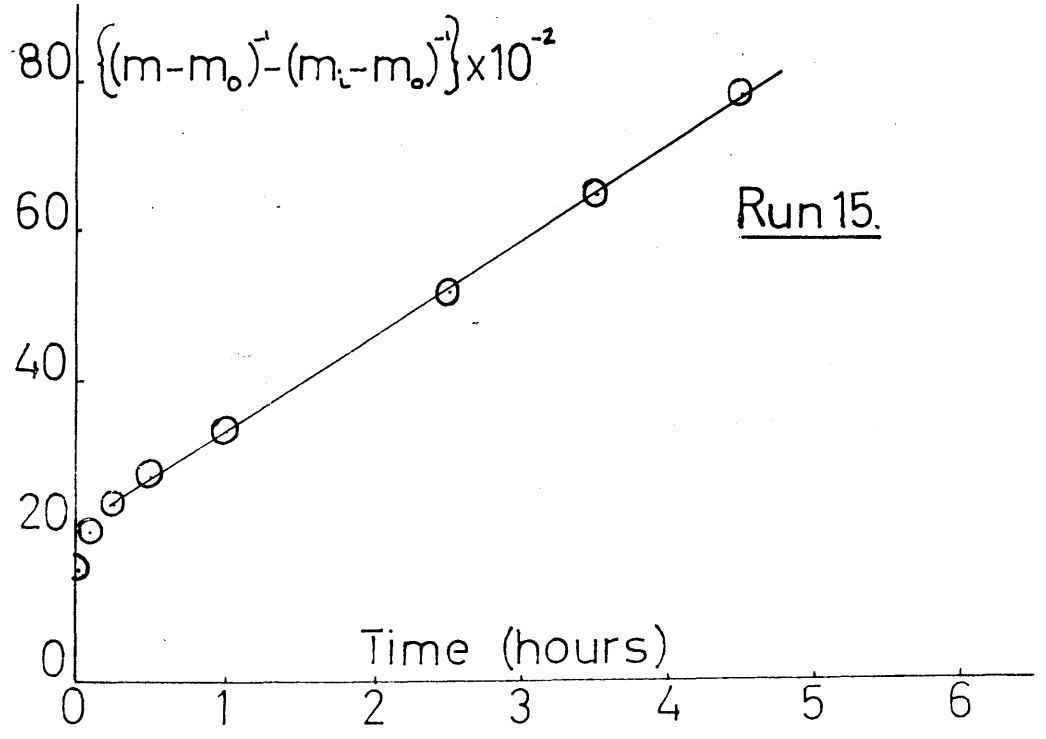
80
60
40
20
0
$\{(m-m_o)^{-1}-(m_i-m_o)^{-1}\}\times10^{-2}$
Run 15.
Time (hours)
0
1
2
3
4
5
6

Figure 7

generally larger than the rhombs, of average size 70μ. When these crystals were used in crystallisation experiments, the initial growth surge was much more pronounced than with the rhombic type. This effect was demonstrated by seed suspensions A and B, and the results are shown in Tables 7 and 8, and Figs. 6 and7. Due to the very steep initial slope of the plots of the reciprocal of resistance against time, it was difficult to obtain an accurate value of $1/R_i$ for Runs 14, 15 and 19 (Fig. 6).

Crystallisation in the Presence of Adsorbates.

The adsorbates studied in the present work were sodium dodecylsulphate, sodium pyrophosphate, sodium trimetaphosphate, sodium tetrametaphosphate and cetyl trimethyl ammonium bromide. In all cases the adsorbate solution was added to the supersaturated solution, and allowed to reach carbon dioxide and temperature equilibrium before inoculation with seed crystals.

Anionic Additives.

The results are summarised in Tables 10 and 15, and typical smooth curves obtained on plotting 1/R against time are shown in Figs. 8 - 11, Tables 11 - 14. The rate of growth of lead sulphate decreased with increasing concentration of impurity, until finally a concentration was reached at which growth stopped completely.

A very low concentration of sodium tetrametaphosphate (10^{-8}M.) markedly retarded the rate of growth, with sodium trimetaphosphate, sodium pyrophosphate, and sodium dodecyl sulphate being increasingly less effective, in that order. A comparison of the concentrations of these ions necessary just to retard the growth rate, and to stop growth almost entirely is made in Table 9.

TABLE. 9.

Additive.	Conc. slowing growth (moles/l.)	Conc. almost stopping growth (moles/l.)
Dodecylsulphate	3.8×10^{-5}	8.3×10^{-4}
Pyrophosphate	3.6×10^{-6}	2.0×10^{-5}
Trimetaphosphate	9.5×10^{-8}	1.5×10^{-6}
Tetrametaphosphate	6.7×10^{-8}	7.7×10^{-7}

The crystallisation process can be represented by the expression

$$-\frac{dm}{dt} = k\, s\, (m - m_o)^n$$

where n is the order of the reaction, and can be evaluated from a plot of $\log \frac{dm}{dt}$ against $\log (m-m_o)$. For lead sulphate, this graph was composed of two intersecting straight lines, of gradient n_1 and n_2, (Fig. 13) where n_1 represents the initial growth surge and n_2

represents the major part of the growth. In experiments in the presence of impurity, the duration of the fast part and the value of n_1 were both shown to increase with increasing concentration of the foreign substance (Tables 10 and 15).

In experiments carried out with solutions prepared from deionised water, a very low concentration of adsorbate was found to affect n_2 also. Instead of the main part of the growth following a second order rate law, it was found that n_2 also increased with increasing concentration of additive (Table 10).

When water prepared in a Bourdillon still was used, a much higher concentration of impurity could be added before any deviation from second order growth was observed in the main part of the reaction (Table 15).

A. DEIONISED WATER.

1. Sodium Dodecylsulphate.

Concentrations of this adsorbate used ranged from 3.76×10^{-5} M. which caused a noticeable slowing of the growth rate of lead sulphate, to 8.29×10^{-4} M., at which no growth took place at all. The results are summarised in Table 10, and 1/R against time plots are shown in Fig. 8 (Table 11). Since log-log plots indicated the value of n_2 to be greater than 2, it was not possible to draw second order rate plots. Even at the highest concentration studied, the critical micelle concentration, 7.7×10^{-3} moles /l. (85) was not exceeded.

2. Sodium Pyrophosphate.

Slightly lower concentrations of this additive affected the crystallisation of lead sulphate; 3.41×10^{-6} moles/l. decreased the rate of growth, and 2.0×10^{-5} moles/l. was sufficient to stop growth entirely. The results are shown in Table 12, and plots of 1/R against time are presented in Fig. 9.

3. Sodium Trimetaphosphate.

This additive had a greater effect on the growth of lead sulphate than the two adsorbates discussed previously. A concentration of 9.45×10^{-8} moles/l. slowed the growth, while at a concentration of 1.49×10^{-6} moles/l., crystallisation was stopped almost entirely. The results are summarised in Table 10, and time plots of 1/R are shown in Fig. 10 (Table 13).

4. Sodium Tetrametaphosphate.

This additive proved to be the most effective in retarding the growth of lead sulphate. A concentration of 7.0×10^{-8} moles/l. was sufficient to have a marked effect on the rate of crystallisation, while at 7.69×10^{-7} moles/l., growth was extremely slow. A summary of the results is made in Table 10, and 1/R against time plots are shown in Fig. 11 (Table 14).

From Table 10 it can be seen that each adsorbate studied had

TABLE. 10. Deionised Water.

Crystallisation of Lead Sulphate in the Presence of Adsorbates.

Experiment Number	Adsorbate conc. moles/l.	Seed Conc. (mg/ml.)	n_1	n_2	Duration of Initial Surge (mins)
Dodecylsulphate.	Seed H.				
43	-	-	18	2	12
44	3.76×10^{-5}	-	21	3	15
50	5.66×10^{-4}	-	(100	36	60)
51	6.56×10^{-4}	-	(430	53	90)
48	8.29×10^{-4}	-	No growth.		
Pyrophosphate.	Seed J.				
68	-	-	16	2	9
61	3.41×10^{-6}	4.8	35	6	15
60	8.50×10^{-6}	3.1	55	3	20
54	1.08×10^{-5}	5.6	(73	8	30)
55	2.15×10^{-5}	6.8	(100	10	45)
Trimetaphosphate.	Seed L.				
75	-	3.0	7	2	15
87	9.45×10^{-8}	4.9	10	5	15
85	1.12×10^{-6}	8.9	23	4	30
86	1.49×10^{-6}	5.8	(54	14	30)
Tetrametaphosphate.	Seed J.				
68	-	-	16	2	9
78	7.12×10^{-8}	2.9	14	4	30
65	2.76×10^{-7}	4.6	(40	19	60)
64	7.69×10^{-7}	4.5	(80	20	75)

Table. II.

Crystallisation of Lead Sulphate in Presence of Dodecylsulphate.

Time	$(1/R) \times 10^3$ ohms^{-1}	$m \times 10^4$ moles/l.	$(m-m_o) \times 10^4$ moles/l.
Run 43. [DDS] = zero.			
0 min.	1.21600	1.7740	0.2574
1.5	1.20962	1.7573	0.2407
6	1.20499	1.7452	0.2286
15	1.20013	1.7325	0.2159
30	1.19409	1.7167	0.2001
1 hr.	1.18378	1.6897	0.1731
2	1.17168	1.6581	0.1415
3.25	1.16177	1.6322	0.1156
Run 44. [DDS] = 3.76×10^{-5} moles/l.			
0 min.	1.23900	1.7740	0.2574
1.5	1.22909	1.7171	0.2005
6	1.22462	1.7054	0.1888
15	1.22156	1.6974	0.1808
30	1.21726	1.6875	0.1709
1 hr.	1.21211	1.6727	0.1561
2.25	1.20285	1.6485	0.1319
3	1.19897	1.6384	0.1218

Time	$(1/R) \times 10^3$ ohms^{-1}	$m \times 10^4$ moles/l.	$(m-m_o) \times 10^4$ moles/l.
Run 50. [DDS] = 5.66×10^{-4} moles/l.			
0 min.	1.77470	1.7740	0.2574
3	1.74292	1.7693	0.2527
6	1.74239	1.7680	0.2514
15	1.74111	1.7646	0.2480
30	1.73968	1.7609	0.2443
1 hr.	1.73818	1.7569	0.2403
3	1.73578	1.7507	0.2341
5.5	1.73399	1.7460	0.2294
22	1.72921	1.7335	0.2169
Run 51. [DDS] = 6.56×10^{-4} moles/l.			
0 min.	1.81825	1.7740	0.2574
3	1.81771	1.7726	0.2560
12	1.81763	1.7724	0.2558
30	1.81715	1.7711	0.2545
1 hr.	1.81683	1.7703	0.2537
2	1.81620	1.7686	0.2520
3.5	1.81580	1.7676	0.2510
6	1.81580	1.7676	0.2510

Run 48. [DDS] = 8.29×10^{-4} moles/l. No Growth.

Cell E. F = 0.2615.

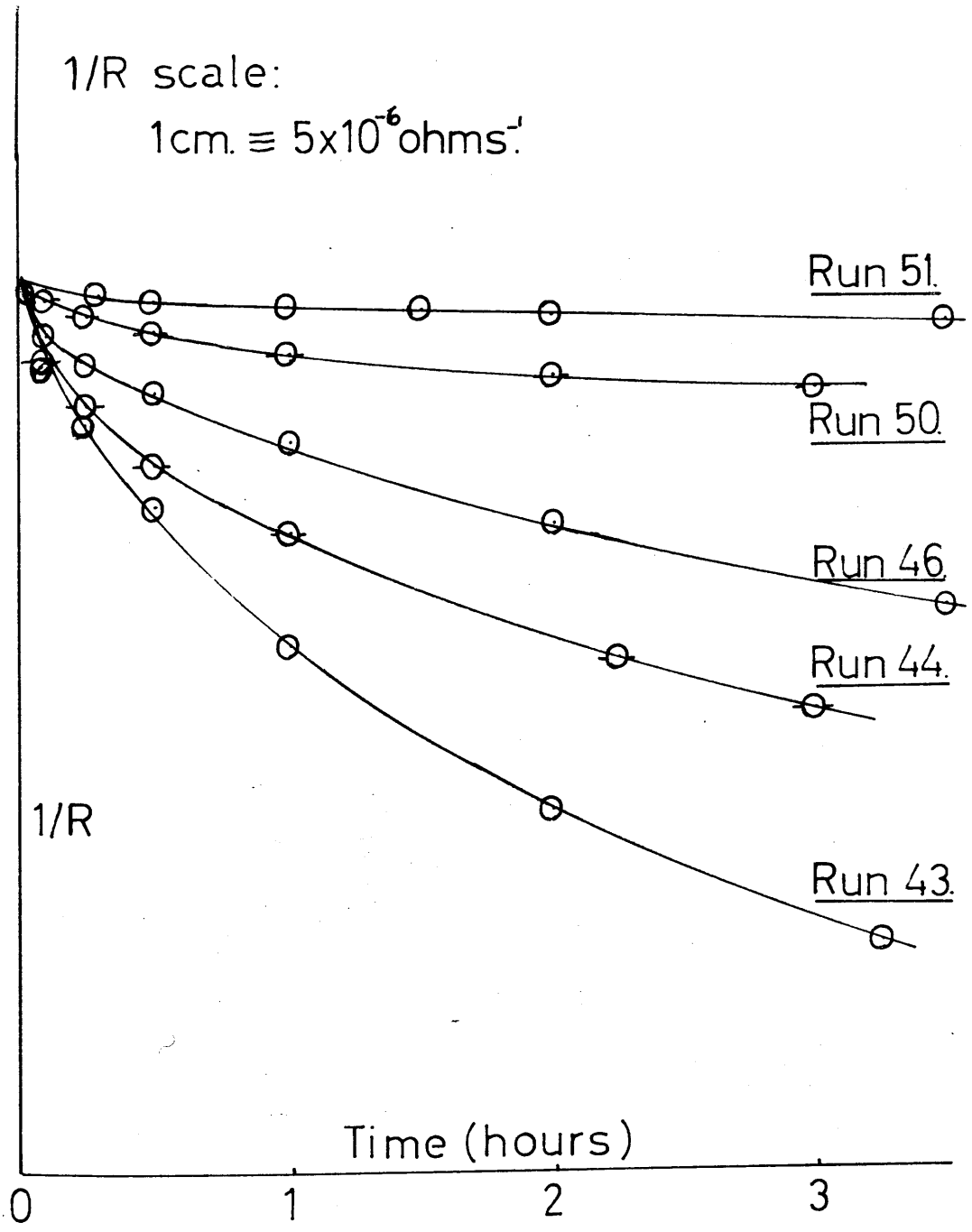
1/R scale:
1cm. ≡ 5x10⁻⁶ ohms⁻¹
Run 51.
Run 50.
Run 46.
Run 44.
Run 43.
1/R
Time (hours)
0
1
2
3

Figure 8.

TABLE. 12.

Crystallisation of Lead Sulphate in Presence of Pyrophosphate.

Time	10^3 / R ohms^{-1}	10^4 m moles/l.	10^4 (m-m_o) moles/l.	10^{-4} /(m-m_o) l./mole.	I* l./mole
Run 68. $[P_2O_7^{4-}]$ = zero.					
0 min.	1.23180	1.7740	0.2574	0.3885	-
0.5	1.22809	1.7643	0.2477	0.4037	1.52
3	1.22215	1.7488	0.2322	0.4307	4.22
9	1.21810	1.7382	0.2216	0.4513	6.28
15	1.21506	1.7302	0.2136	0.4682	7.97
30	1.20952	1.7157	0.1991	0.5023	11.38
1 hr.	1.20062	1.6925	0.1759	0.5685	18.00
2	1.18953	1.6635	0.1469	0.6807	29.22
4	1.17476	1.6248	0.1082	0.9242	53.57
5.5	1.16956	1.6112	0.0946	1.0571	66.86
23	1.15692	1.5782	0.0616	1.6234	123.49

$$I^* = \left\{(m - m_o)^{-1} - (m_i - m_o)^{-1}\right\} \times 10^{-2}$$

Cell E. F = 0.2615.

TABLE. 12. (cont.)

Time	$(1/R) \times 10^3$ ohms^{-1}	$m \times 10^4$ moles/l.	$(m-m_o) \times 10^4$ moles/l.
Run 61. $[P_2O_7^{4-}] = 3.41 \times 10^{-6}$ moles/l.			
0 min.	1.22695	1.7740	0.2574
1.5	1.22081	1.7579	0.2413
6	1.21751	1.7493	0.2327
15	1.21506	1.7429	0.2263
30	1.21202	1.7350	0.2184
1 hr.	1.20781	1.7239	0.2073
2	1.20183	1.7083	0.1917
2.75	1.19863	1.6999	0.1833
Run 60. $[P_2O_7^{4-}] = 8.50 \times 10^{-6}$ moles/l.			
0 min.	1.23225	1.7740	0.2574
1.5	1.22859	1.7644	0.2478
6	1.22750	1.7616	0.2450
9	1.22680	1.7597	0.2431
30	1.22259	1.7490	0.2324
1 hr.	1.21850	1.7380	0.2214
2	1.21515	1.7281	0.2115
2.5	1.21226	1.7217	0.2051
3	1.21030	1.7166	0.2000

TABLE. 12. (cont.)

Time	$(1/R) \times 10^3$ ohms^{-1}	$m \times 10^4$ moles/l.	$(m-m_o) \times 10^4$ moles/l.
Run 54. $[P_2O_7^{4-}] = 1.08 \times 10^{-5}$ moles/l.			
0 min.	1.22250	1.7740	0.2574
1.5	1.21993	1.7673	0.2507
6	1.21865	1.7633	0.2467
15	1.21737	1.7606	0.2440
30	1.21604	1.7571	0.2405
1 hr.	1.21427	1.7525	0.2359
2	1.21197	1.7465	0.2299
3	1.21025	1.7420	0.2254
Run 55. $[P_2O_7^{4-}] = 2.15 \times 10^{-5}$ moles/l.			
0 min.	1.22223	1.7740	0.2574
2	1.22205	1.7735	0.2569
6	1.22180	1.7729	0.2563
15	1.22141	1.7719	0.2553
30	1.22091	1.7705	0.2539
1 hr.	1.22032	1.7690	0.2524
2	1.22022	1.7687	0.2521
2.5	1.22012	1.7685	0.2519

Cell E. F = 0.2615.

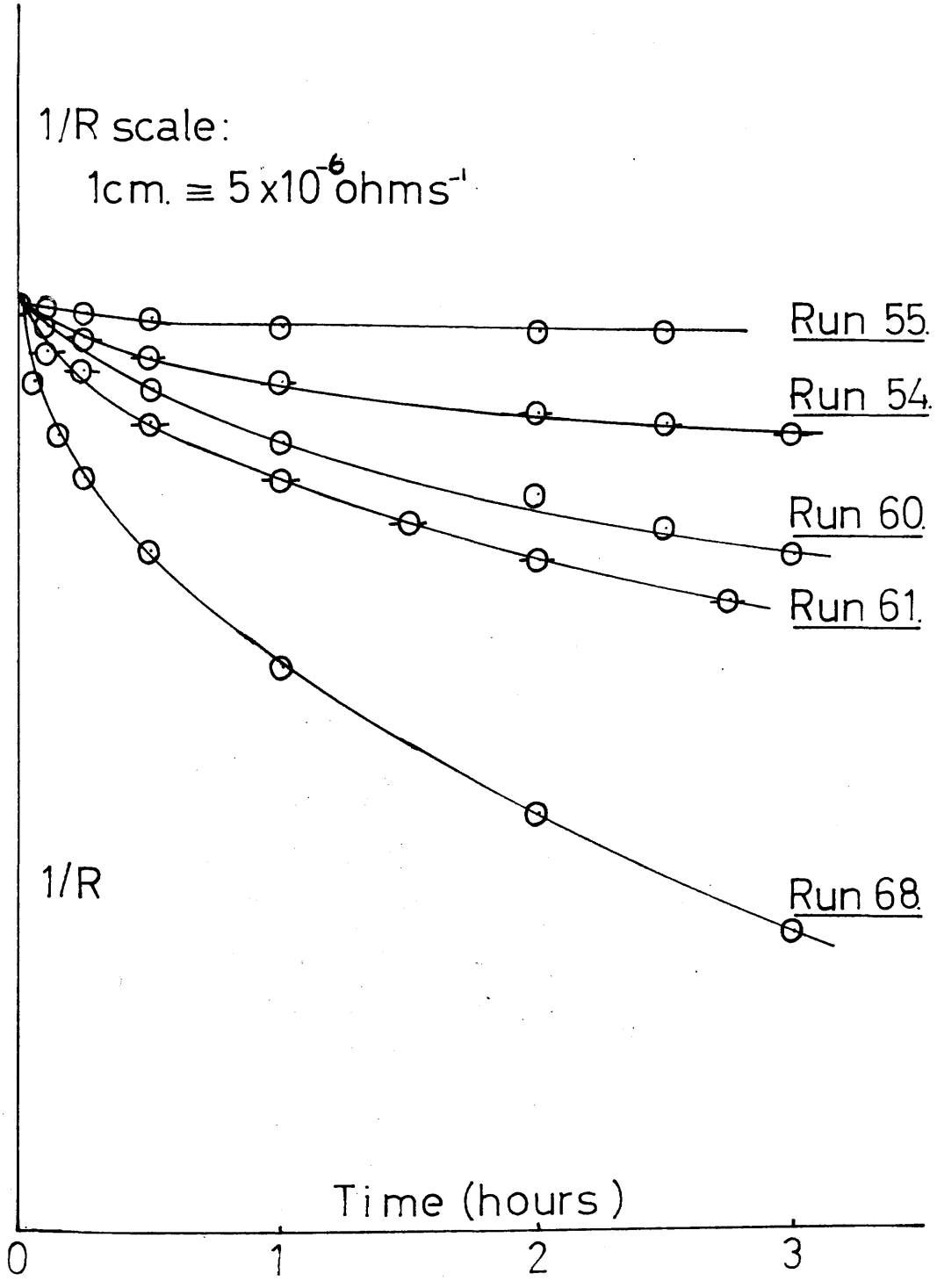
1/R scale:
1cm. ≡ 5 x10⁻⁶ ohms⁻¹
Run 55.
Run 54.
Run 60.
Run 61.
Run 68.
1/R
Time (hours)
0
1
2
3

Figure 9.

TABLE. 13.

Crystallisation of Lead Sulphate in Presence of Trimetaphosphate.

Time	10^3 / R ohms^{-1}	10^4 m moles/l.	10^4 (m-m_o) moles/l.	10^{-4} /(m-m_o) l./mole	I* l./mole.
Run 75.	[TriMP] = zero.				
0 min.	1.22800	1.7740	0.2574	0.3885	-
1.5	1.21943	1.7516	0.2350	0.4255	3.70
6	1.21545	1.7412	0.2246	0.4452	5.67
15	1.21025	1.7276	0.2110	0.4739	8.54
30	1.20466	1.7130	0.1964	0.5092	12.07
1.75 hr	1.18689	1.6665	0.1499	0.6671	27.86
4	1.17239	1.6286	0.1120	0.8929	50.44
8	1.16112	1.5991	0.0825	1.2121	82.36
12	1.15692	1.5881	0.0715	1.3986	101.01
22	1.15088	1.5723	0.0557	1.7953	140.68
Run 87.	[TriMP] = 9.45 x 10^{-8} moles/l.				
0 min.	1.23620	1.7740	0.2574	-	-
1.5	1.23427	1.7690	0.2524	-	-
6	1.23252	1.7644	0.2478	-	-
15	1.22936	1.7561	0.2395	-	-
30	1.22556	1.7462	0.2296	-	-
1.5 hr	1.21545	1.7197	0.2031	-	-
3	1.21001	1.7055	0.1889	-	-

$$I^* = \left\{ (m - m_o)^{-1} - (m_i - m_o)^{-1} \right\} \times 10^{-2}$$

TABLE. 13. (cont.)

Time	$(1/R) \times 10^3$ $ohms^{-1}$	$m \times 10^4$ moles/l.	$(m-m_0) \times 10^4$ moles/l
Run 85. [Tri MP] = 1.12×10^{-6} moles/l.			
0 min.	1.23935	1.7740	0.2574
1.5	1.23787	1.7701	0.2535
6	1.23597	1.7667	0.2501
15	1.23497	1.7625	0.2459
30	1.23277	1.7568	0.2402
1.5 hrs.	1.22924	1.7476	0.2310
3	1.22254	1.7300	0.2134
5	1.21820	1.7187	0.2021
8.25	1.21079	1.6993	0.1827
9.75	1.20850	1.6933	0.1767
Run 86. [Tri MP] = 1.49×10^{-6} moles/l.			
0 min.	1.24100	1.7740	0.2574
1.5	1.24038	1.7724	0.2558
6	1.23938	1.7698	0.2532
15	1.23827	1.7669	0.2503
30	1.23702	1.7636	0.2470
1.75 hrs.	1.23372	1.7550	0.2384
3	1.23078	1.7473	0.2307
5	1.22983	1.7448	0.2282

Cell E. F = 0.2615.

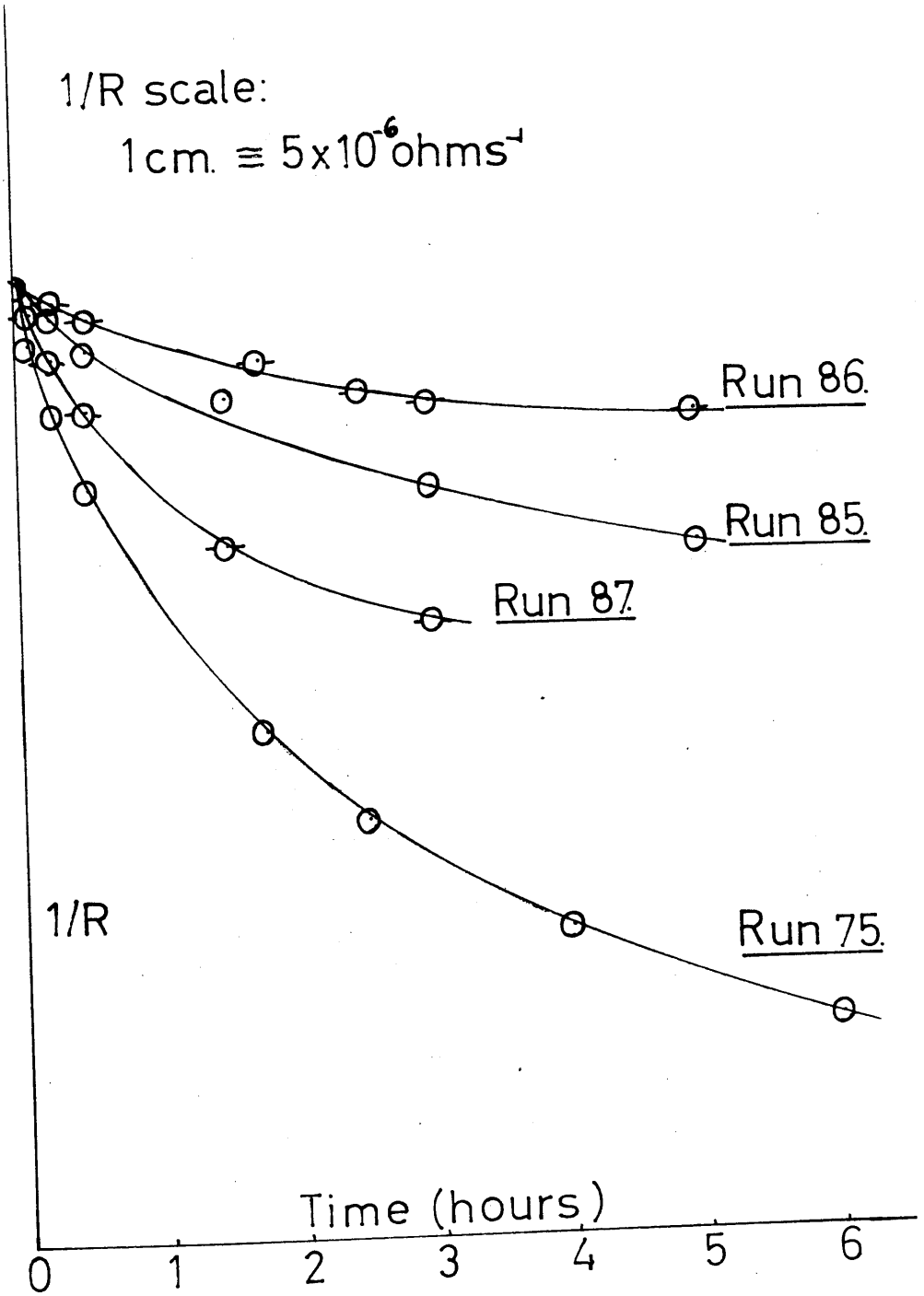
1/R scale:
1cm. ≡ 5x10⁻⁶ ohms⁻¹
Run 86.
Run 85.
Run 87.
Run 75.
1/R
Time (hours)
0
1
2
3
4
5
6

Figure 10.

TABLE. 14.

Crystallisation of Lead Sulphate in Presence of Tetrametaphosphate.

Time	$(1/R) \times 10^3$ ohms^{-1}	$m \times 10^4$ moles/l.	$(m-m_o) \times 10^4$ moles/l.
Run 78. [TMP] = 7.12×10^{-8} moles/l.			
0 min.	1.22760	1.7740	0.2574
1.5	1.22017	1.7546	0.2380
6	1.21579	1.7431	0.2265
15	1.21280	1.7353	0.2187
30	1.20991	1.7278	0.2112
1 hr.	1.20552	1.7163	0.1997
2	1.19931	1.7000	0.1834
4	1.19164	1.6800	0.1634
9	1.18083	1.6517	0.1351
22.25	1.16824	1.6190	0.1024
Run 65. [TMP] = 2.76×10^{-7} moles/l.			
0 min.	1.23270	1.7740	0.2574
1.5	1.22556	1.7553	0.2387
6	1.22284	1.7482	0.2316
15	1.22156	1.7449	0.2283
30	1.22096	1.7433	0.2267
1 hr.	1.21564	1.7294	0.2128
2	1.21324	1.7231	0.2065
2.9	1.20781	1.7089	0.1923

TABLE, 14. (cont.)

Time	$(1/R) \times 10^3$ ohms^{-1}	$m \times 10^4$ moles/l.	$(m-m_o) \times 10^4$ moles/l.
Run 64. [TMP] = 7.67×10^{-7} moles/l.			
0 min.	1.22820	1.7740	0.2574
1.5	1.22541	1.7667	0.2501
6	1.22363	1.7620	0.2454
15	1.22136	1.7561	0.2395
30	1.21934	1.7508	0.2342
1 hr.	1.21717	1.7452	0.2286
2	1.21515	1.7399	0.2233
4	1.21275	1.7336	0.2170
6	1.21113	1.7294	0.2128
8.25	1.21000	1.7264	0.2098
20.25	1.20504	1.7134	0.1968

Cell E. F = 0.2615.

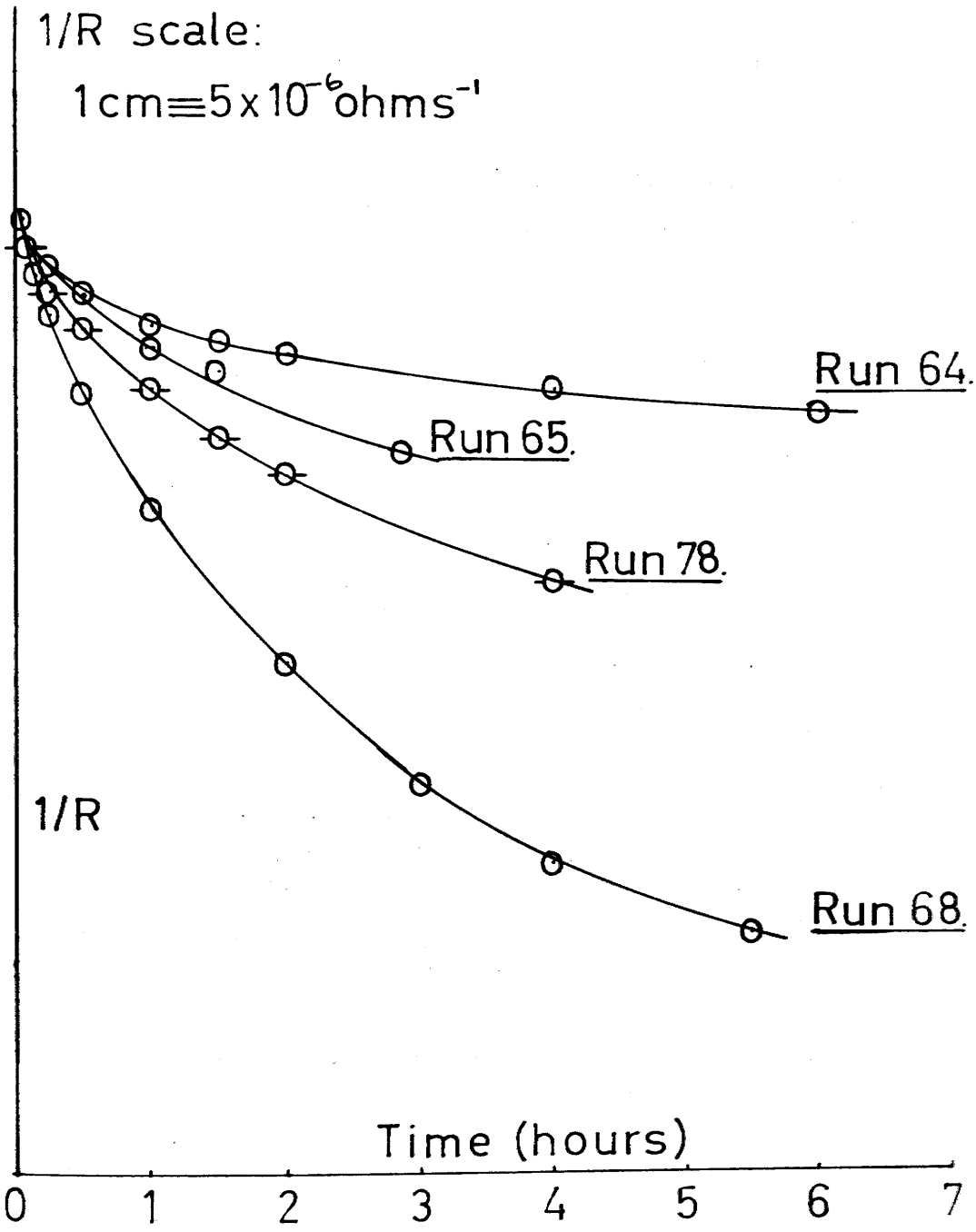
1/R scale:
1cm≡5x10⁻⁶ohms⁻¹
Run 64.
Run 65.
Run 78.
Run 68.
1/R
Time (hours)
0
1
2
3
4
5
6
7

Figure 11.

the effect of causing an increase in the values of n_1 and n_2, and in the duration of the initial growth surge. In experiments with very high concentrations of adsorbate, little significance can be attached to the large values found for n_1 and n_2, since the growth was extremely slow, and accurate gradients difficult to obtain.

Since impurities present in water prepared by ion-exchange have a definite effect on the crystallisation process, all subsequent experiments were made using water prepared in a Bourdillon still.

B. WATER PURIFIED BY DISTILLATION.

Experiments were carried out with three of the anionic adsorbates, sodium dodecylsulphate, sodium pyrophosphate, and sodium tetrametaphosphate, for which all the solutions and seed crystals were prepared with distilled water. The results are summarised in Table 15, and time plots of 1/R are shown in Figs. 12 and 14. In the presence of a low concentration of each of the additives, lead sulphate crystallisation followed a second order rate equation, although the rate of growth was retarded. Second order plots are shown in Fig. 15 (Tables 17 - 19).

The presence of the impurity caused an increase in the duration of the initial growth surge, and in the value of n_1. Run 106, with a tetrametaphosphate concentration of 6.66×10^{-8} moles/l., which had no initial fast part was the only exception to this (Table 19).

As was found previously with deionised water, the value of n_1, and the duration of the growth surge increased with increasing concentration of impurity (Table 15). With sodium dodecylsulphate and sodium tetrametaphosphate, a concentration was reached at which the kinetics of the second part of the growth followed an order greater than two. This will be discussed later.

Cationic Additive.

Cetyl trimethyl ammonium bromide was the cationic additive studied, and only distilled water was used in these experiments. Concentrations ranging from 9.75×10^{-7} moles /l. to 1.08×10^{-4} moles/l. had little effect on the rate of crystallisation. If anything, this adsorbate tended to increase the growth rate slightly. The results are summarised in Table 20 below, and time plots of 1/R are shown in Fig. 16 (Table 21). In Run 116, a slightly larger amount of seed crystals was added, which may account for the small acceleration.

At both concentrations, an initial growth surge was observed, and the value of n_1 increased with adsorbate concentration. At the lower cetyl trimethyl ammonium bromide concentration, n_2 was two, but at the higher concentration, n_2 had risen to three, ionic strength corrections having been made.

The solubility of lead bromide is 0.0264 moles/l. (80), and the solubility product is 1.394×10^{-3} moles^3/l^3. The value of

TABLE. 15.

Crystallisation of Lead Sulphate in Presence of Adsorbates.

Distilled Water.

Experiment Number	[Adsorbate] moles/l.	Seed conc. mg/ml.	n_1	n_2	Duration of Init. Surge. (mins.)
100	-	2.83	-	2	-
Dodecylsulphate.					
107	3.39×10^{-5}	2.98	8	2	45
111	2.19×10^{-4}	3.28	13	6	105
Pyrophosphate.					
108	2.86×10^{-6}	4.38	29	2	60
110	9.41×10^{-6}	1.34	14	2	75
Tetrametaphosphate.					
106	6.66×10^{-8}	2.70	-	2	-
104	1.23×10^{-7}	3.80	7	2	60
103	1.64×10^{-6}	1.60	(50	28	15)

TABLE. 16.

Crystallisation of Lead Sulphate.

Distilled Water.

Time	10^3 / R ohms^{-1}	10^4 m moles/l.	10^4 (m-m_o) moles/l.	10^{-4} /(m-m_o) l./mole.	I* l./mole.
Run 100.					
0 min.	1.23395	1.7740	0.2574	0.3885	-
1.5	1.23272	1.7708	0.2542	0.3934	0.49
6	1.23038	1.7647	0.2481	0.4031	1.48
15	1.22725	1.7565	0.2399	0.4168	2.83
30	1.22462	1.7496	0.2330	0.4292	4.07
1 hr.	1.22096	1.7400	0.2234	0.4476	5.91
2	1.21407	1.7220	0.2054	0.4869	9.84
4	1.20489	1.6980	0.1814	0.5513	16.28
6	1.19800	1.6800	0.1634	0.6120	22.35
10	1.18670	1.6504	0.1338	0.7474	35.89
23	1.16980	1.6062	0.0896	1.1161	72.76

Cell E. F = 0.2615.

$$I^* = \left\{(m - m_o)^{-1} - (m_i - m_o)^{-1}\right\} \times 10^{-2}$$

TABLE. 17 Lead Sulphate Crystallisation in Presence of Dodecylsulphate.

Distilled Water.

Time	10^3 / R $ohms^{-1}$	10^4 m moles/l.	10^4 $(m-m_o)$ moles/l.	10^{-4} /$(m-m_o)$ l./mole.	I* l./mole.
Run 107.	[DDS] = 3.39 x 10^{-5} moles/l.			Cell E.	
0 min.	1.31580	1.7740	0.2574	0.3885	-
6	1.29777	1.7268	0.2102	0.4757	8.72
15	1.29318	1.7148	0.1982	0.5045	11.60
30	1.29003	1.7066	0.1900	0.5263	13.78
1 hr.	1.28532	1.6943	0.1777	0.5627	17.42
3	1.27222	1.6600	0.1434	0.6974	30.89
6	1.26035	1.6290	0.1124	0.8897	50.12
10.5	1.24961	1.6009	0.0843	1.1862	79.77
14	1.24400	1.5862	0.0695	1.4388	105.03
24.25	1.23372	1.5593	0.0427	2.3419	195.34
Run 111.	[DDS] = 2.19 x 10^{-4} moles/l.			Cell E.	
0 min.	1.30950	1.8435	0.3269	-	-
9	1.30063	1.8203	0.3037	-	-
15	1.29994	1.8185	0.3019	-	-
30	1.29830	1.8142	0.2976	-	-
1 hr.	1.29624	1.8088	0.2922	-	-
2.5	1.29192	1.7975	0.2809	-	-
5	1.28615	1.7828	0.2662	-	-
9.75	1.27766	1.7602	0.2436	-	-
24.25	1.26127	1.7174	0.2008	-	-

TABLE 15. Lead Sulphate Crystallisation in Presence of Pyrophosphate.

Distilled Water.

Time	$10^3 / R$ ohms^{-1}	10^4 m moles/l.	10^4 (m-m_o) moles/l.	$10^{-4} /$(m-m_o) l./mole.	* l./mole.
Run 108.	$[P_2O_7^{4-}] = 2.86 \times 10^{-6}$ moles/l.			**Cell E.**	
0 min.	1.25045	1.7740	0.2574	0.3885	-
6	1.24335	1.7554	0.2388	0.4188	3.03
15	1.24234	1.7528	0.2362	0.4234	3.49
30	1.24124	1.7499	0.2333	0.4286	4.01
1 hr.	1.23958	1.7456	0.2290	0.4367	4.82
3	1.23522	1.7342	0.2176	0.4596	7.11
5	1.23138	1.7241	0.2075	0.4819	9.34
8	1.22680	1.7121	0.1955	0.5115	12.30
12	1.22121	1.6975	0.1809	0.5528	16.43
27	1.20796	1.6629	0.1463	0.6835	29.50
Run 110.	$[P_2O_7^{4-}] = 9.41 \times 10^{-6}$ moles/l.			**Cell E.**	
0 min.	1.20775	1.7740	0.2574	0.3885	-
6	1.20611	1.7697	0.2531	0.3951	0.66
15	1.20557	1.7683	0.2517	0.3973	0.88
30	1.20518	1.7673	0.2507	0.3989	1.04
1.5 hr.	1.20434	1.7651	0.2485	0.4024	1.39
3	1.20377	1.7636	0.2470	0.4049	1.64
5.5	1.20207	1.7591	0.2425	0.4124	2.39
9	1.20052	1.7551	0.2385	0.4193	3.08
25.25	1.19602	1.7433	0.2267	0.4411	[illegible]

TABLE. 19. Lead Sulphate Crystallisation in Presence of Tetrametaphosphate

Distilled Water.

Time	$10^3 / R$ ohms^{-1}	10^4 m moles/l.	10^4 ($m-m_o$) moles/l.	$10^{-4} / (m-m_o)$ l./mole.	I* l./mole.
Run 104.	[TMP] = 1.23 x 10^{-7} moles/l.				
0 min.	1.25865	1.7740	0.2574	0.3885	-
6	1.25098	1.7539	0.2373	0.4214	3.29
15	1.24992	1.7512	0.2346	0.4263	3.78
30	1.24809	1.7464	0.2298	0.4352	4.67
1 hr.	1.24511	1.7386	0.2220	0.4505	6.20
2.5	1.23837	1.7210	0.2044	0.4892	10.07
5.5	1.22785	1.6935	0.1769	0.5653	17.68
11	1.21427	1.6579	0.1413	0.7077	31.92
24	1.19617	1.6106	0.0940	1.0638	67.53
Run 106.	[TMP] = 6.66 x 10^{-8} moles/l.				
0 min.	1.24080	1.7740	0.2574	0.3885	-
6	1.23482	1.7584	0.2418	0.4136	2.51
15	1.23362	1.7552	0.2386	0.4191	3.06
30	1.23202	1.7512	0.2346	0.4263	3.78
1 hr.	1.22973	1.7450	0.2284	0.4378	4.93
2	1.22462	1.7317	0.2151	0.4649	7.64
4	1.21692	1.7115	0.1949	0.5131	12.46
8	1.20547	1.6816	0.1650	0.6061	21.76
14.25	1.19193	1.6462	0.1296	0.7716	38.31
25	1.17822	1.6103	0.0937	1.0672	167.87

TABLE. 19. (cont.)

Time	$(1/R) \times 10^3$ $ohms^{-1}$	$m \times 10^4$ moles/l.	$(m-m_o) \times 10^4$ moles/l.
Run 103. [TMP] = 1.64×10^{-6} moles/l.			
0 min.	1.25600	1.7740	0.2574
1.5	1.25428	1.7695	0.2529
6	1.25250	1.7648	0.2482
15	1.25199	1.7635	0.2469
30	1.25139	1.7619	0.2453
1 hr.	1.25037	1.7593	0.2427
2	1.24921	1.7562	0.2396
4	1.24759	1.7520	0.2354
6	1.24678	1.7499	0.2333
9	1.24486	1.7449	0.2283
23.25	1.24365	1.7419	0.2251

Cell E. F = 0.2615.

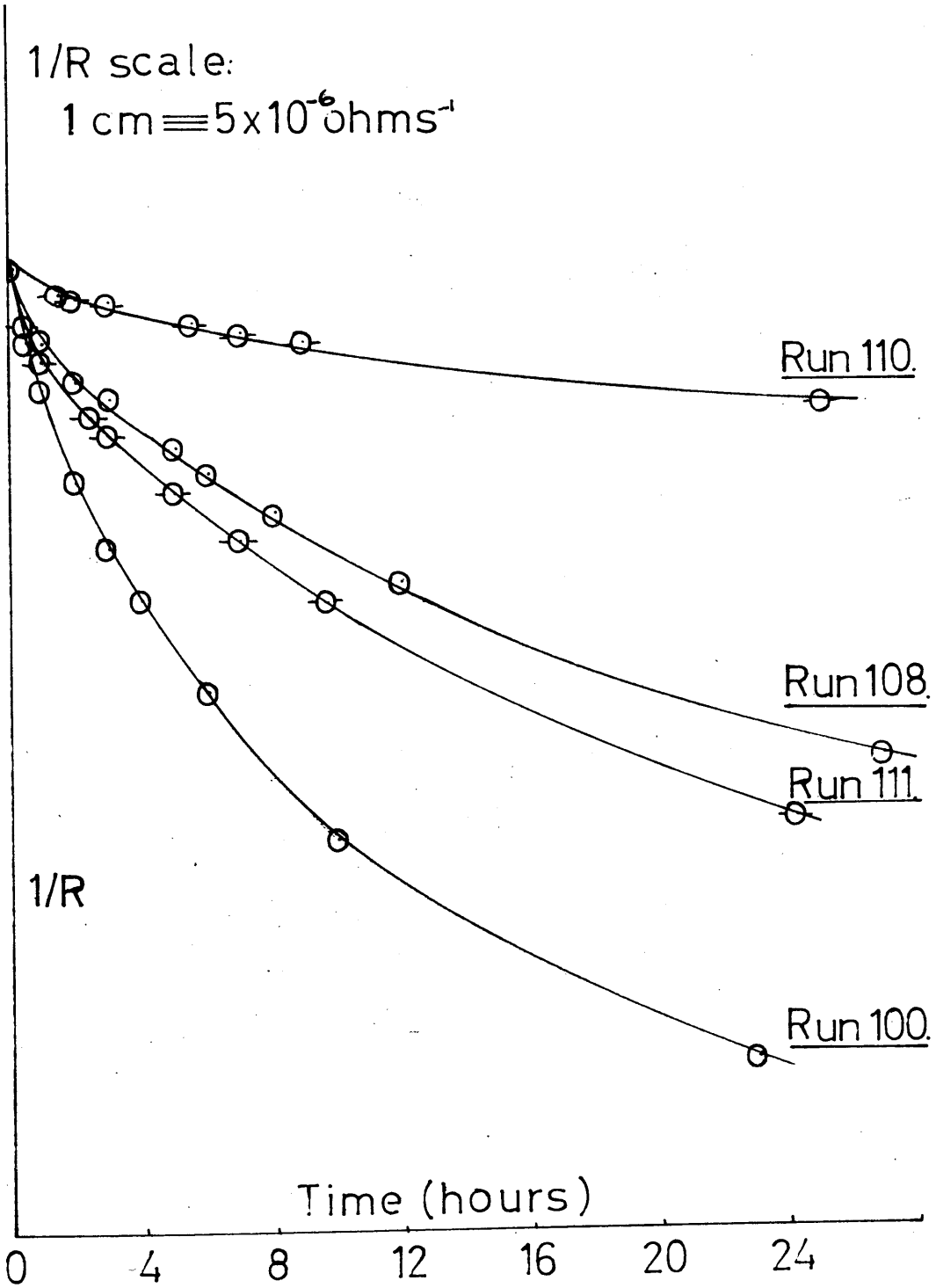
1/R scale:
1 cm ≡ 5x10⁻⁶ ohms⁻¹
Run 110.
Run 108.
Run 111.
Run 100.
1/R
Time (hours)
0
4
8
12
16
20
24

Figure 12.

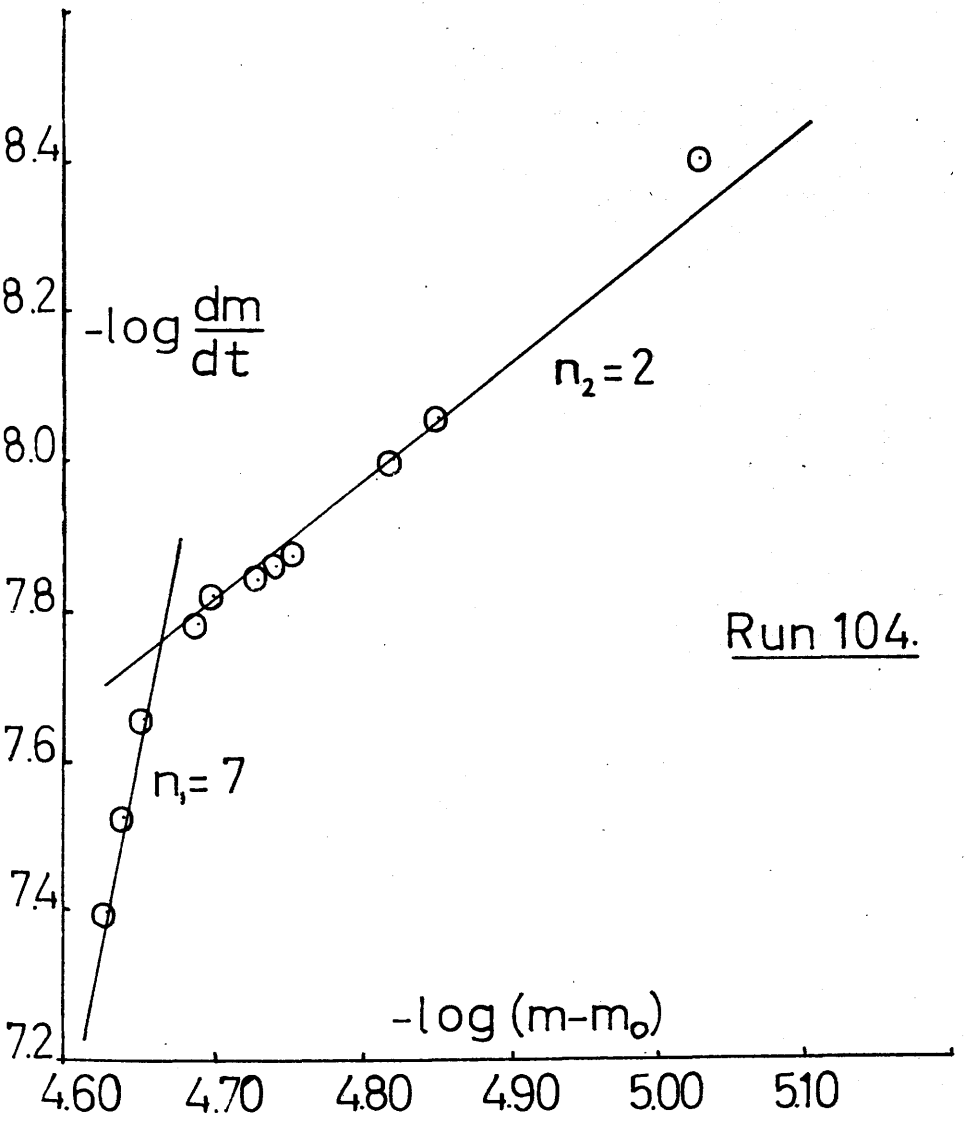
8.4
8.2
8.0
7.8
7.6
7.4
7.2
-log dm/dt
n₂ = 2
n₁ = 7
Run 104.
-log (m-m₀)
4.60
4.70
4.80
4.90
5.00
5.10

Figure 13.

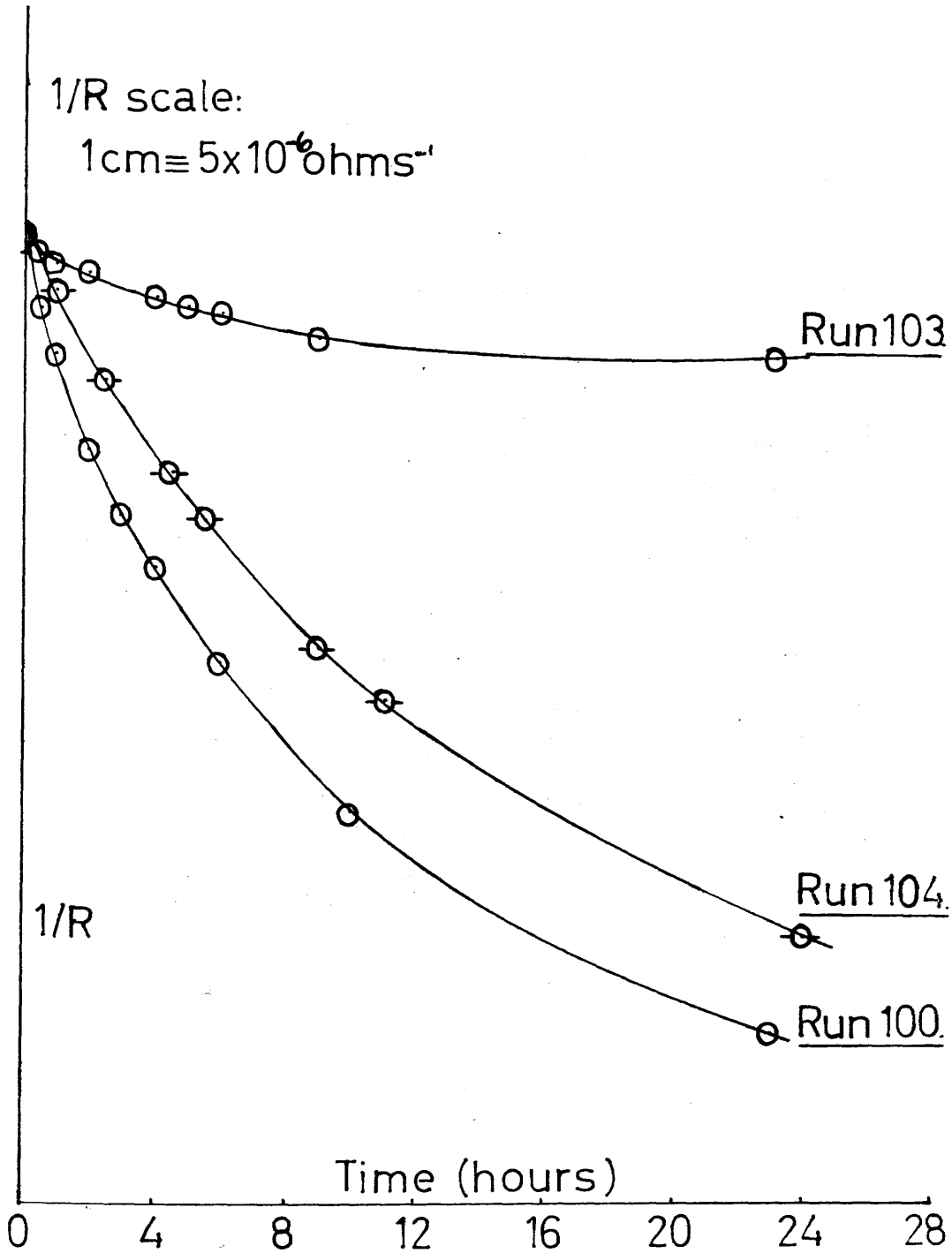
1/R scale:
1cm≡5x10⁻⁶ohms⁻¹
Run103
Run104.
Run100.
1/R
Time (hours)
0
4
8
12
16
20
24
28

Figure 14.

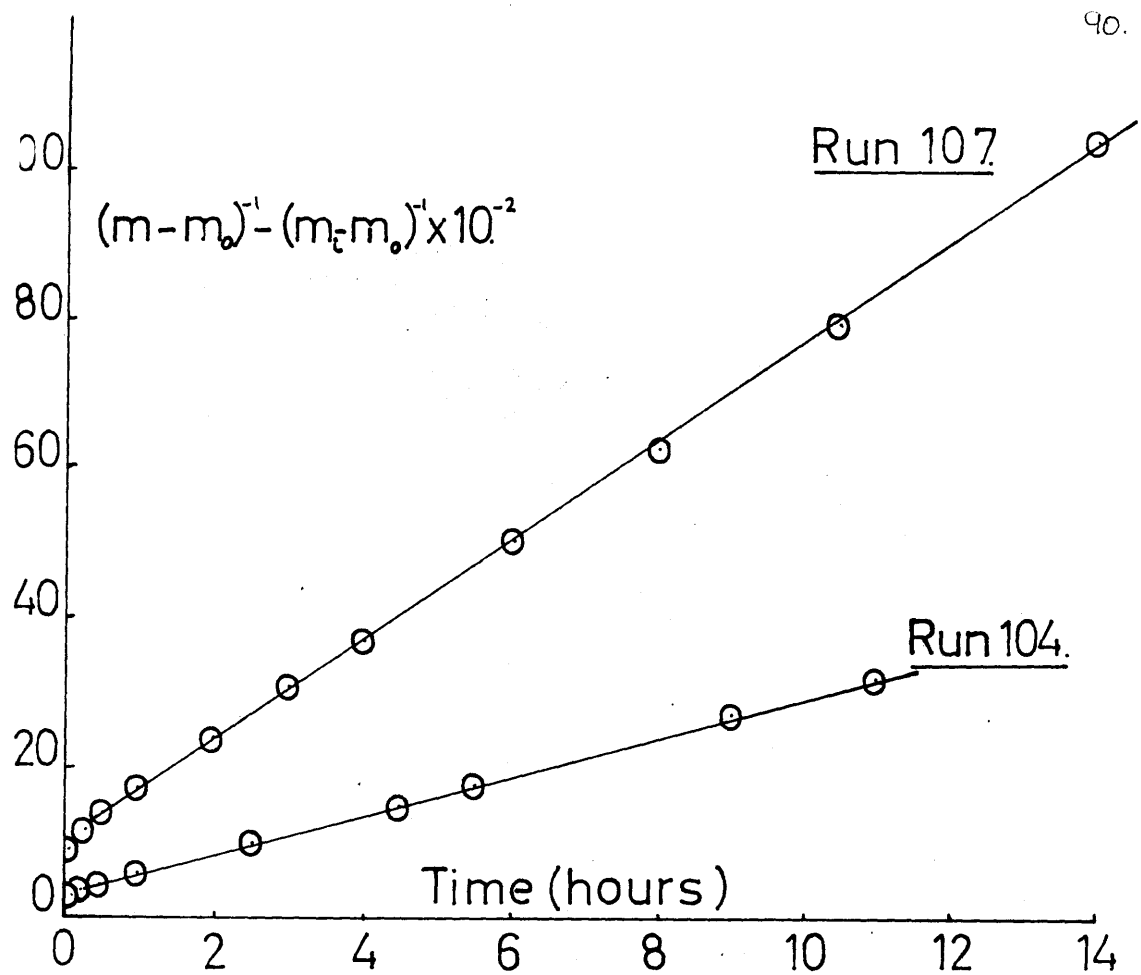
Run 107
$(m-m_o)^{-1}-(m_t-m_o)^{-1}\times10^{-2}$
Run 104.
Time (hours)
0
20
40
60
80
0
2
4
6
8
10
12
14

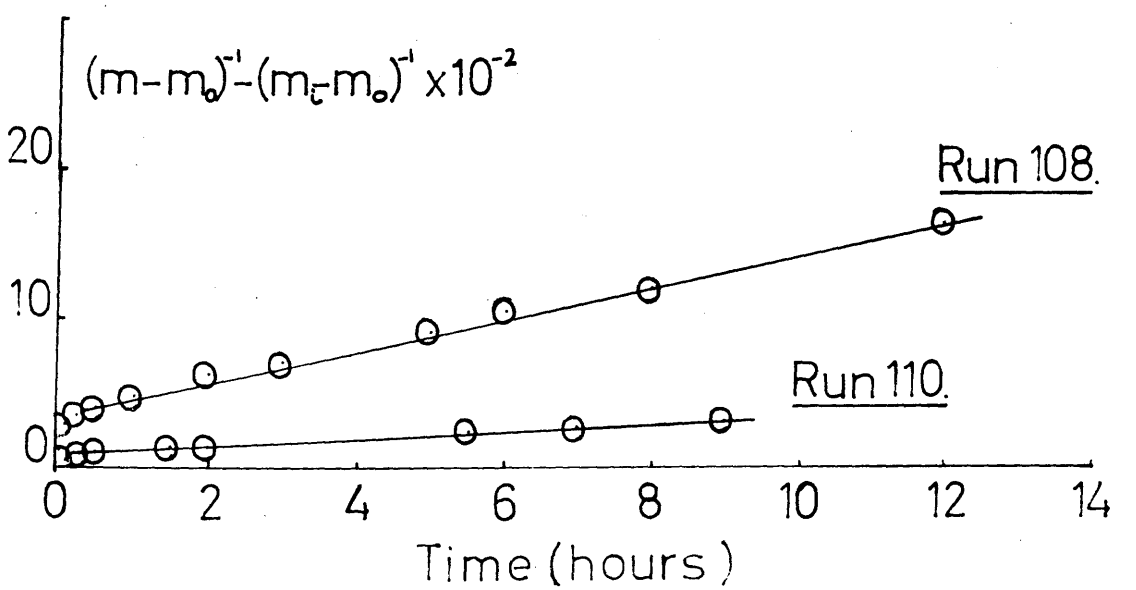
$(m-m_o)^{-1}-(m_t-m_o)^{-1}\times10^{-2}$
Run 108.
Run 110.
Time (hours)
0
10
20
0
2
4
6
8
10
12
14

Figure 15.

$[Pb^{2+}][Br^{-}]^2$ in these experiments was 2.07×10^{-12} moles^3/l^3., so crystallisation of this salt cannot be the explanation of the third order kinetics found.

Since cetyl trimethyl ammonium bromide had such a samll effect on the rate of growth of lead sulphate, no other cationic additives were studied.

TABLE. 20.

Crystallisation of Lead Sulphate in Presence of Cetyl Trimethyl Ammonium Bromide.

Experiment Number	Adsorbate conc. moles/l.	Seed conc. (mg/ml.)	n_1	n_2	Duration of Init. surge. (mins.)
100	-	2.83	-	2	-
116	9.75×10^{-7}	3.60	6	2	15
119	1.08×10^{-4}	2.28	12	3	15

Cell E. F = 0.2615.

Crystallisation at Non-Equivalent Ionic Concentrations.

The experiments at non-equivalent ionic concentrations are recorded in Table 22. Smooth curves of 1/R against time are shown in Figs. 17 and 18, and the reaction was usually followed for 12 - 24 hours, corresponding to about 60% of the total growth.

The results were interpreted in terms of the amount, Δ , of lead sulphate to be precipitated before equilibrium was reached. The instantaneous concentrations are given by the relationships

$$[Pb^{2+}_e] = [Pb^{2+}] - \Delta \qquad \text{and} \quad [SO^{2-}_{4\,e}] = [SO^{2-}_4] - \Delta \ ,$$

where $[Pb^{2+}_e]$ and $[SO^{2-}_{4\,e}]$ are the equilibrium ionic concentrations which satisfy the solubility product relationship

$$[Pb^{2+}_e][SO^{2-}_{4e}] = K_s = 1.7164 \times 10^{-8} \text{ moles}^2/l^2.$$

at 25°C. Therefore,

$$([Pb^{2+}_e] - \Delta)([So^{2-}_{4\,e}] - \Delta) = K_s \ .$$

The initial value of Δ can be found since the initial values of $[Pb^{2+}]$ and $[SO^{2-}_4]$ are known experimentally, and the change in Δ can be calculated from the measured change in resistance.

The rate of crystallisation may be written

$$-\frac{dm}{dt} = k\, s\, (\Delta)^n,$$

where n is normally 2.

When this method of analysis was applied to the lead sulphate results, n values as high as ten for $Pb / SO_4 = 1 / 4$ and $4 / 1$ were obtained. In all cases the growth was slower than at equivalent ionic

concentrations, but since the n values were different, except at the 4/1 and 1/4 ratios, only these are strictly comparable.

An excess of lead ions caused a greater retardation of the growth rate than an excess of sulphate ions.

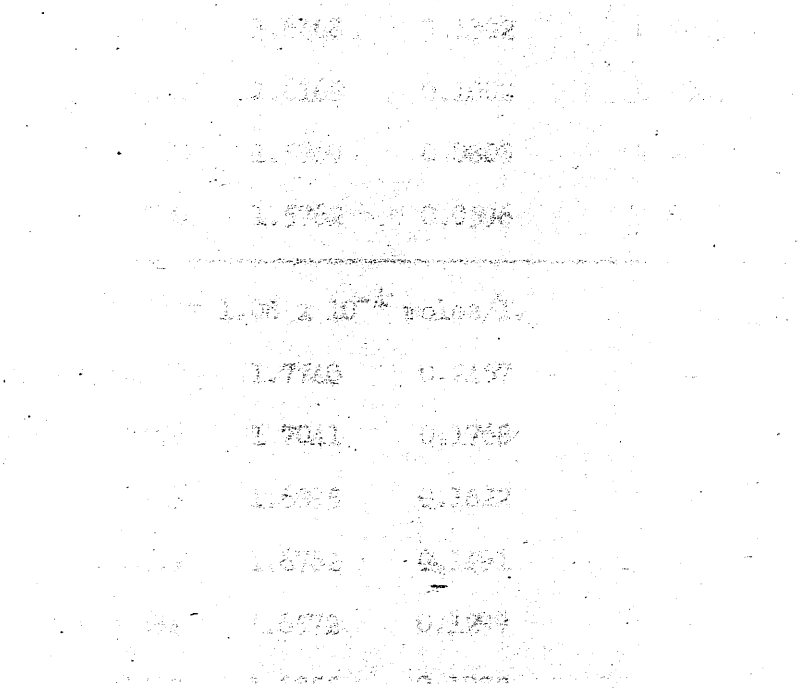

TABLE. 21. Lead Sulphate Crystallisation in Presence of Cetyl Trimethyl Ammonium Bromide.

Time	$10^3 / R$ ohms^{-1}	10^4 m moles/l.	$10^4 (m-m_o)$ moles/l.	$10^{-4} / (m-m_o)$ l./mole.	I* l./mole.
Run 116.	[CTB] = 9.75×10^{-7} moles/l.			Cell E.	
0 min.	1.25780	1.7740	0.2574	0.3885	-
6	1.23482	1.7139	0.1973	0.5068	11.83
15	1.23088	1.7036	0.1870	0.5348	14.63
30	1.22740	1.6945	0.1779	0.5621	17.36
1 hr.	1.22190	1.6801	0.1635	0.6116	22.31
3	1.20918	1.6468	0.1302	0.7680	37.95
7	1.19771	1.6168	0.1002	0.9980	60.95
12	1.19010	1.5969	0.0803	1.2453	85.68
36	1.18216	1.5762	0.0596	1.6779	128.94
Run 119.	[CTB] = 1.08×10^{-4} moles/l.			Cell E.	
0 min.	1.40150	1.7740	0.2467	-	-
6	1.37476	1.7041	0.1768	-	-
15	1.36919	1.6895	0.1622	-	-
30	1.36409	1.6762	0.1491	-	-
1 hr.	1.35684	1.6572	0.1299	-	-
2	1.34853	1.6355	0.1082	-	-
4	1.33979	1.6126	0.0853	-	-
6	1.33590	1.6024	0.0751	-	-
11	1.33100	1.5896	0.0623	-	-

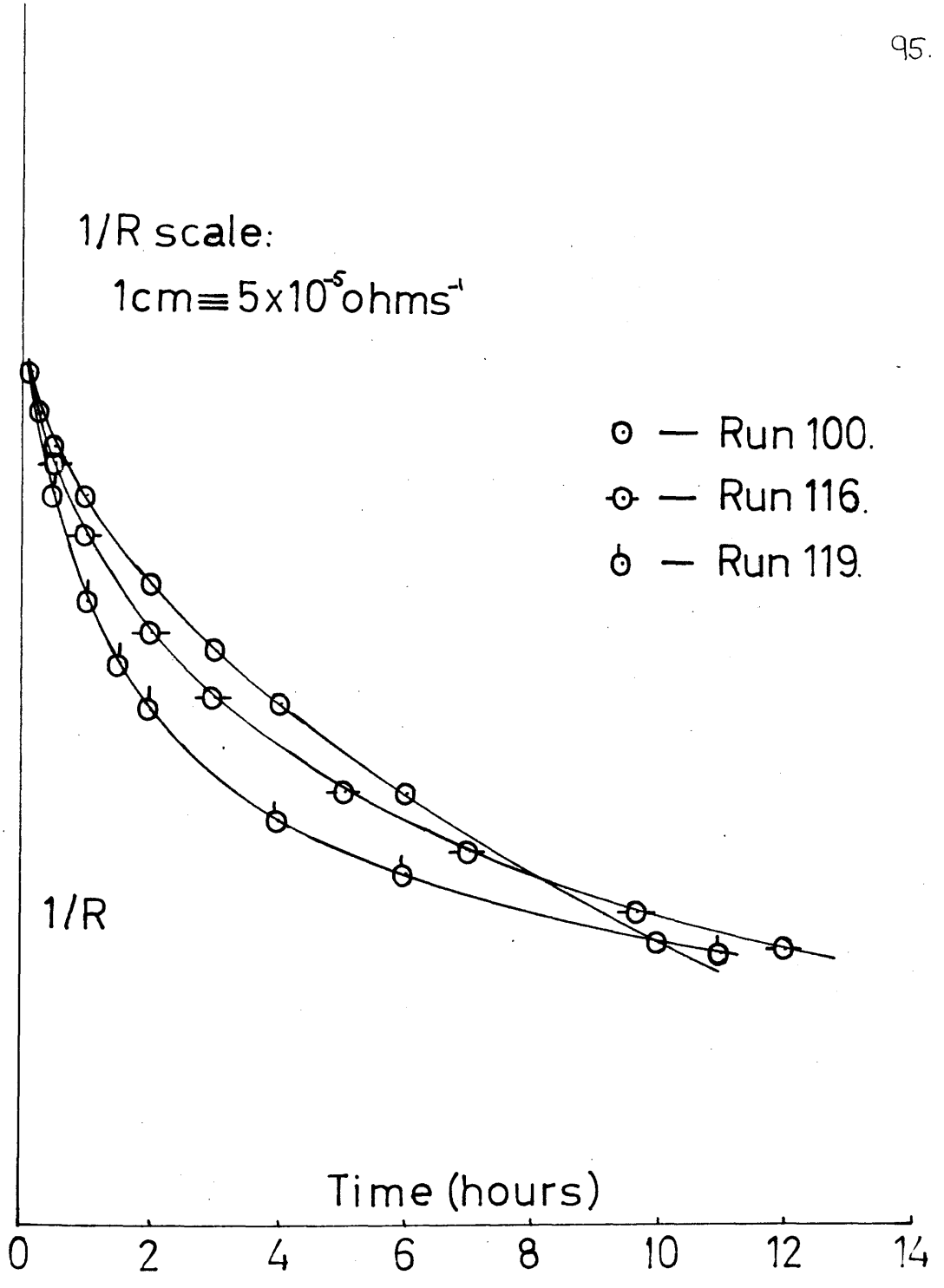
1/R scale:
1cm≡5x10⁻⁵ohms⁻¹
⊙ — Run 100.
⊙ — Run 116.
⊙ — Run 119.
1/R
Time (hours)
0
2
4
6
8
10
12
14

Figure 16.

Lead Sulphate Crystallisation at Non-equivalent Ionic Concentrations.

Time	$10^3 / R$ ohms^{-1}	$\Delta \times 10^4$ moles/l.	Time	$10^3 / R$ ohms^{-1}	$\Delta \times 10^4$ moles/l.
Run 121.	Pb/SO_4 = 1/2.		Run 122.	Pb/SO_4 = 2/1.	
0 min.	1.31730	0.4291	0 min.	1.37440	0.4291
6	1.30073	0.3858	6	1.35884	0.3884
15	1.29503	0.3709	15	1.35190	0.3703
30	1.29019	0.3577	30	1.34467	0.3513
1 hr.	1.28255	0.3377	1 hr.	1.33552	0.3274
2	1.27341	0.3142	3	1.31797	0.2815
3.5	1.26542	0.2934	5.5	1.30919	0.2586
7	1.25744	0.2726	7	1.30801	0.2555
12	1.25113	0.2560	8	1.30673	0.2521
Run 123.	Pb/SO_4 = 4/1		Run 126.	Pb/SO_4 = 1/4	
0 min.	1.62625	0.3503	0 min.	1.53445	0.3503
6	1.61864	0.3304	6	1.52355	0.3218
15	1.61597	0.3234	15	1.51871	0.3091
30	1.61276	0.3150	30	1.51478	0.2989
1 hr.	1.60866	0.3043	1 hr.	1.50916	0.2842
2	1.60295	0.2894	2	1.50288	0.2677
4.25	1.59619	0.2717	4	1.49656	0.2512
7.5	1.59188	0.2604	6	1.49407	0.2447
23.5	1.58555	0.2439	22.25	1.48613	0.2239

Cell E.

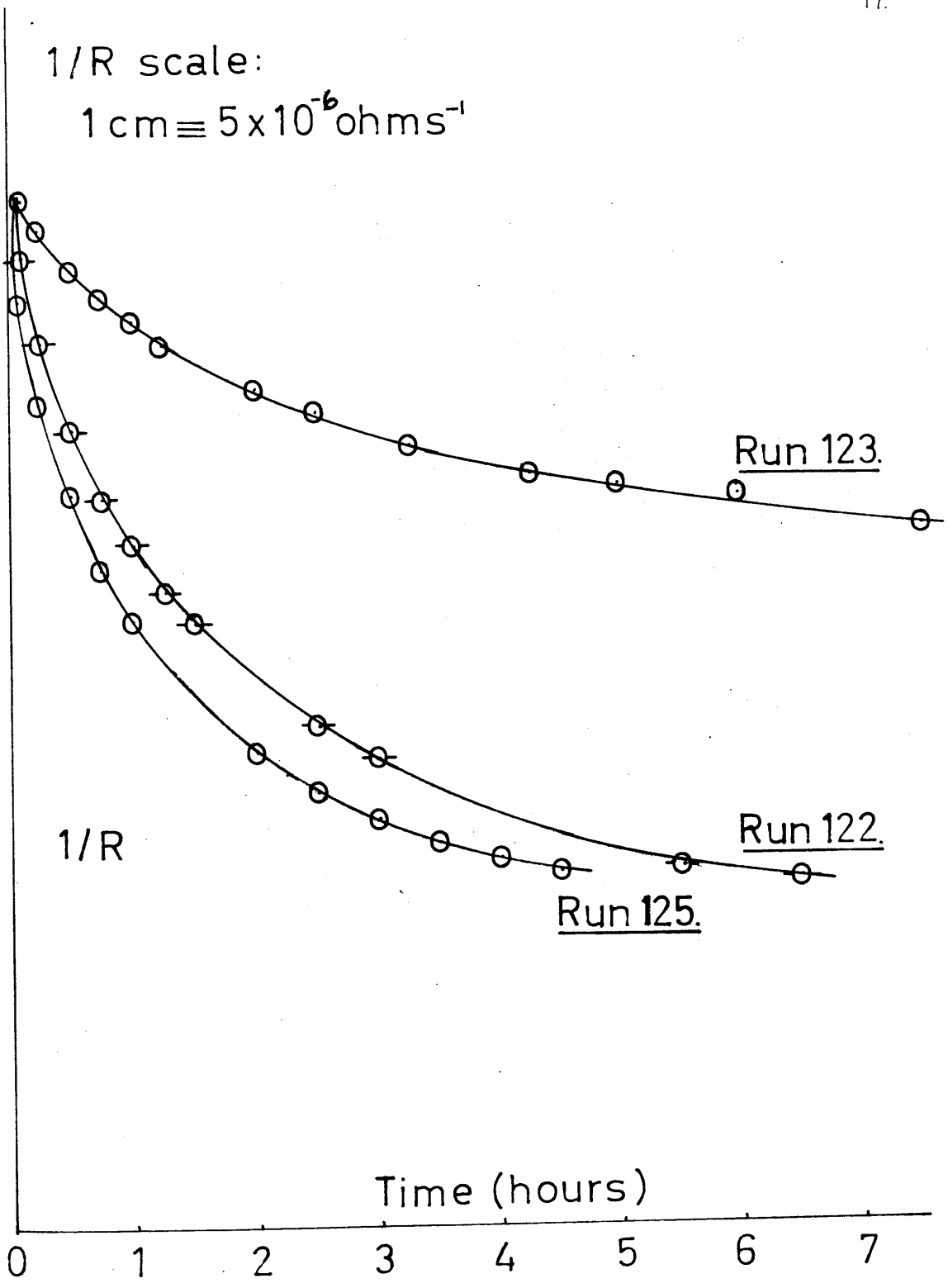
1/R scale:
1 cm ≡ 5 x 10⁻⁶ ohms⁻¹
Run 123.
Run 122.
Run 125.
1/R
Time (hours)
0
1
2
3
4
5
6
7

Figure 17.

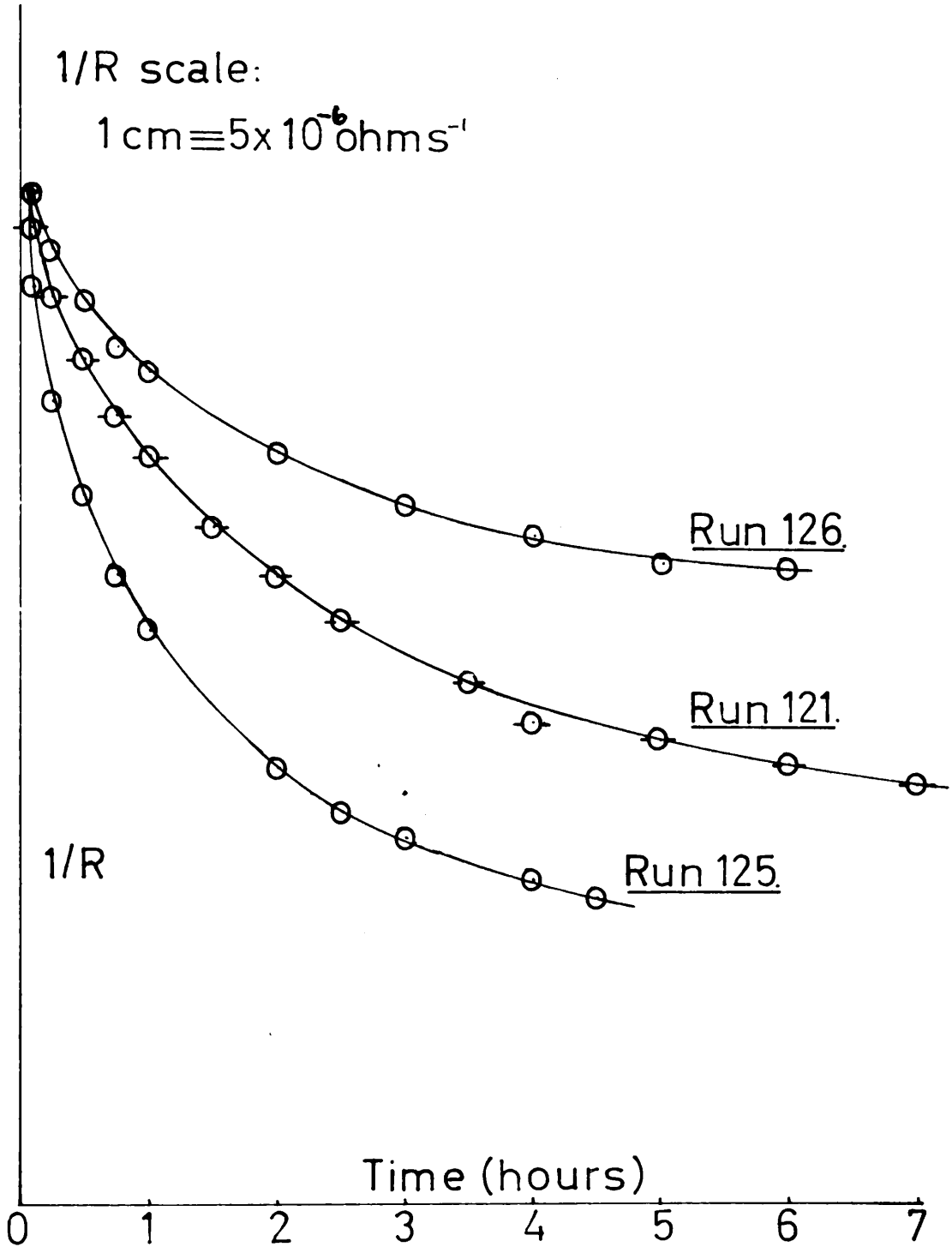
1/R scale:
1 cm ≡ 5 x 10⁻⁶ ohms⁻¹
Run 126.
Run 121.
Run 125.
1/R
Time (hours)
0
1
2
3
4
5
6
7

Figure 18.

PART 1b.

Crystallisation of Barium Sulphate from Supersaturated Aqueous Solutions at Various Temperatures.

PART 1b.

INTRODUCTION.

The precipitation of barium sulphate, because of its importance in gravimetric analysis, has been studied extensively, and many mechanisms of nucleation and growth have been advanced (9 -12, 26, 29, 30, 32, 35, 36) An account of the main theories has been given on pages 1 - 10.

Electron microscope studies of barium sulphate crystals by Otani (86) revealed that there are two types of crystal shapes formed above and below a concentration of 5×10^{-4} moles/l. In the more dilute solutions regular orthorhombic platelets were produced, while dendritic crystals resulted in the more concentrated region. Suito and Takiyama (87) have also shown that the aging of barium sulphate takes place by Ostwald ripening, with the larger particles growing at the expense of the smaller ones.

Fischer and Rheinehammer (88) observed that the size and number of barium sulphate crystals produced depended on the age of the barium chloride solution used in their preparation. An old solution of barium chloride gave fewer and larger crystals than a fresh solution. If a fresh solution was filtered, however, it behaved as an old one, suggesting that the number of nuclei decreased on aging.

Walton and Walden (89) found that barium sulphate crystals

occluded many cations, including NH_4^+, K^+, Na^+, Li^+ in the crystal lattice, and established that the co-precipitated ions formed a substitutional solid solution. An electron microscopical study of colloidal barium sulphate by Dawson and McCaffney (90) revealed pores of diameter 15 - 70 Å in the crystal surface, in which occlusions could be made.

Part 1b is a report on the crystallisation of barium sulphate from its supersaturated solution. Nancollas and Purdie (58) have established that the growth follows a second order rate law, from solutions of equivalent and non-equivalent ionic concentrations at 25°C., and the study has now been extended to temperatures between 15 and 45°C. In a similar study of silver chloride crystallisation between 15 and 35°C., Davies and Nancollas (38) reported that the rate constant was unaltered by the change in temperature, indicating an activation energy of zero for the process. In the present work, however, barium sulphate has been found to have a positive energy of activation for growth.

EXPERIMENTAL.

Preparation of Solutions.

Supersaturated solutions were prepared by mixing dilute solutions of barium chloride and sodium sulphate in situ. The apparatus and experimental technique used have already been described in detail in Part Ia. With barium sulphate, the cell was washed between experiments with 1% hydrochloric acid, in addition to the normal washing procedure. In experiments at 35° and 45°C., the cap of the cell was brought to the same temperature to minimise condensation.

Preparation of Seed Crystals.

Due to the low temperature coefficient of solubility, it was not possible to prepare barium sulphate crystals by recrystallisation. Accordingly, the crystals were prepared by simultaneous dropwise addition of equimolar portions of barium chloride and sulphuric acid, to water at 90°C. A typical preparation involved addition of 100 ml. portions of 0.1 Molar solutions, to 200 ml of water in an asbestos-lagged beaker, on a hotplate. A magnetic stirring device was employed, and the solution was agitated throughout the addition, and for about 24 hours thereafter. The crystals were maintained at 90°C. for about six hours after the additions were complete, since it has been observed that crystals aged at the higher temperature were more perfectly formed (88). The crystals were

washed by decantation twenty times with distilled and conductivity water, and stored in pyrex bottles at 25°C. The seed crystals were uniform rhombohedra, and the suspensions prepared were

Seed suspension A, average size 9.5 μ.

Seed suspension B, average size 5.0 μ.

Determination of Solubility.

Solubility at 25°C.

Literature values for the solubility of barium sulphate at 25°C. range from 0.955×10^{-5} moles/l. (91) to 1.403×10^{-5} moles/l. (92). The value found in this work, by allowing dissolution experiments to proceed to equilibrium was 1.024×10^{-5} moles/l., which agrees with the value of Rosseinsky (93), (1.039×10^{-5} moles/l.) and that of Nancollas and Purdie (57), (1.040×10^{-5} moles/l.). The thermodynamic solubility product was

$$K = [Ba^{2+}][SO_4^{2-}]\, f_2^2 = 0.9880 \times 10^{-10} \text{ moles}^2/\text{l}^2.,$$

f_2 being evaluated using the Davies equation (page 41).

Solubility at Other Temperatures.

No values at 15°, 35°, or 45°C. are quoted in the literature, but these could be interpolated from data reported for temperatures from 0° - 100°C. (80). A plot of solubility against temperature resulted in a fairly good straight line, which enabled an estimate

to be made of the solubility at intermediate temperatures. In addition, measurements were made at each temperature, by allowing dissolution experiments to proceed to equilibrium. Agreement with the interpolated values at 15°, 35°, and 45°C. was good, as can be seen from Table 23.

TABLE 23.

Solubility of Barium Sulphate at Various Temperatures.

Temperature (°C.)	Interpolated S_o (moles/l.)	Experimental S_o (moles/l.)
15°	0.93×10^{-5}	0.904×10^{-5}
35°	1.22×10^{-5}	1.196×10^{-5}
45°	1.38×10^{-5}	1.389×10^{-5}

The corresponding thermodynamic solubility products were

at 15°C., $K = 0.7725 \times 10^{-10}$ moles^2/l^2.,

at 35°C., $K = 1.3401 \times 10^{-10}$ moles^2/l^2.,

at 45°C., $K = 1.7948 \times 10^{-10}$ moles^2/l^2.,

where f_2 was again evaluated using the Davies equation, with the appropriate Debye-Huckel constants, A = 0.5002 at 15°C., 0.5190 at 35°C., and 0.5296 at 45°C. (94).

RESULTS.

Following on the work of Nancollas and Purdie (57) who established that barium sulphate crystallised from its supersaturated solution according to a second order rate law at 25°C., the study has now been extended to determine the kinetics of growth at other temperatures. Experiments have been carried out at 15°, 25°, 35°, and 45°C., and an estimate of the heat of reaction made.

Ionic Mobilities and Equivalent Conductance.

Mobilities of sulphate and barium ions at 15°, 35°, and 45°C., were obtained by interpolation of existing data (94). Values used are given in Table 24.

TABLE 24.

Mobilities of Barium and Sulphate Ions.

Temperature (°C.)	Sulphate	Barium
15	63.0	52.0
25	80.00	63.63
35	95.0	75.0
45	113.5	95.0

The Onsager equations at these temperatures were (95)

$\Lambda = \Lambda^\circ - (1.7896\Lambda^\circ + 186.12)\sqrt{2m}$ at 15°C., ($\Lambda^\circ = 115.0$)

$\Lambda = \Lambda^\circ - (1.8216\Lambda^\circ + 239.44)\sqrt{2m}$ at 25°C., ($\Lambda^\circ = 143.63$)

$\Lambda = \Lambda^\circ - (1.8576\Lambda^\circ + 299.24)\sqrt{2m}$ at 35°C., ($\Lambda^\circ = 170.0$)

$\Lambda = \Lambda^\circ - (1.8992\Lambda^\circ + 363.96)\sqrt{2m}$ at 45°C., ($\Lambda^\circ = 208.5$)

where m is expressed in g. mols./l.

Experimental and calculated conductivities of the solutions agreed to within 0.5% (page 43).

With the small concentrations involved in crystallisation, the value of Λ was taken to be constant, 112.61 at 15°C.; 140.45 at 25°C.; 165.62 at 35°C.; and 202.79 at 45°C. Activity coefficients were assumed to be unity at the low ionic strengths involved. The concentration change during growth was calculated as described on page 44.

Cell Constant.

Variation of the cell constant was considered to be negligible, since the coefficients of expansion of platinum and pyrex glass are so small. This has been illustrated by Gunning and Gordon (96), who showed that the total error involved between 15° and 35°C. was only 0.005%.

Crystallisation Experiments at 15°, 25°, 35°, and 45°C.

The results are summarised in Table 25 and plots of 1/R against time are shown in Fig. 19. The data are plotted according to a second order integrated equation in Fig. 20 (Tables 26 - 29). It is seen that the growth follows a second order rate law and the rate constants at each temperature are given in Table 25.

The integrated form of the Arrhenius equation is

$$\ln k = \ln A - E/RT,$$

and $\log_{10}k$ is plotted against $(\text{Temperature})^{-1}$ in Fig. 21. The best straight line through the points was drawn by the method of least squares, giving an energy of activation of 8 K.Cals./mole.

TABLE. 25.

Crystallisation of Barium Sulphate.

Experiment Number	Temperature (°C.)	Seed conc. (mg/ml.)	$m_i \times 10^5$ (moles/l.)	Rate Const. (l./mole./min.)
7	15	0.06	1.860	125
8	15	0.02	1.860	113
1	25	2.01	2.0505	167
5	35	0.73	2.460	267
3	45	2.59	2.760	450
4	45	2.10	2.760	450

TABLE. 26. Crystallisation of Barium Sulphate at 15°C.

Time	10^3 / R ohms^{-1}	10^4 m moles/l.	10^4 ($m-m_o$) moles/l.	10^{-4} /($m-m_o$) l./mole.	I* l./mole.
Run 7.					
0 min.	1.22925	1.8600	0.9377	1.0664	-
5	1.22669	1.8516	0.9293	1.0761	0.97
15	1.22349	1.8411	0.9188	1.0884	2.20
30	1.21570	1.8156	0.8933	1.1194	5.30
1 hr.	1.20698	1.7871	0.8648	1.1563	8.99
2.5	1.18305	1.7087	0.7864	1.2716	20.52
5.5	1.14985	1.5999	0.6776	1.4758	40.94
10.25	1.10461	1.4517	0.5294	1.8889	82.25
24	1.02155	1.1797	0.2574	3.8850	281.86
Run 8.					
0 min.	1.05140	1.8600	0.9377	1.0664	-
5	1.04999	1.8554	0.9331	1.0717	0.53
15	1.04703	1.8457	0.9234	1.0830	1.66
30	1.04155	1.8277	0.9054	1.1045	3.81
1 hr.	1.03318	1.8003	0.8780	1.1390	7.26
2	1.02073	1.7595	0.8372	1.1945	12.81
4	1.00028	1.6837	0.7614	1.3134	24.70
7	0.96751	1.5852	0.6629	1.5085	44.21
24	0.92504	1.4461	0.4538	2.2036	113.72

TABLE. 27.

Crystallisation of Barium Sulphate at 25°C.

Time	10^3 / R ohms^{-1}	10^4 m moles/l.	10^4 ($m-m_o$) moles/l.	10^{-4} /($m-m_o$) l./mole.	I* l./mole.
Run 1.					
0 min.	1.60975	2.0505	0.9405	1.0633	-
1.5	1.60458	2.0370	0.9270	1.0787	1.54
6	1.60200	2.0303	0.9203	1.0866	2.33
15	1.60153	2.0291	0.9191	1.0880	2.47
30	1.59950	2.0238	0.9138	1.0943	3.10
1 hr.	1.59121	2.0022	0.8922	1.1208	5.75
2.5	1.55543	1.9091	0.7991	1.2514	18.81
4	1.52196	1.8220	0.7120	1.4044	34.41
5.5	1.49569	1.7536	0.6436	1.5538	49.05
7	1.47388	1.6969	0.5869	1.7039	64.06
23.75	1.37793	1.4470	0.3370	2.9674	190.41

Cell E. $$I^* = \left\{(m - m_o)^{-1} - (m_i - m_o)^{-1}\right\} \times 10^{-3}$$

TABLE. 28. Crystallisation of Barium Sulphate at 35°C.

Time	10^3 / R ohms^{-1}	10^4 m moles/l.	10^4 (m-m_o) moles/l.	10^{-4} /(m-m_o) l./mole.	I* l./mole.
Run 5.					
0 min.	2.31700	2.4600	1.2408	0.8059	-
1	2.31034	2.4457	1.2265	0.8153	0.94
9	2.30264	2.4292	1.2100	0.8264	2.05
15	2.29396	2.4106	1.1914	0.8393	3.34
30	2.27350	2.3668	1.1476	0.8714	6.55
1.5 hr.	2.19772	2.2044	0.9852	1.0150	20.91
3	2.11522	2.0277	0.8085	1.2369	43.10
5	2.03886	1.8641	0.6449	1.5506	74.47
7	1.98406	1.7466	0.5274	1.8961	109.02

Cell E. F = 0.2143.

$$I^* = \left\{(m - m_o)^{-1} - (m_i - m_d)^{-1}\right\} \times 10^{-3}$$

TABLE. 29. Crystallisation of Barium Sulphate at 45°C.

Time	10^3 / R ohms^{-1}	10^4 m moles/l.	10^4 (m-m_o) moles/l.	10^{-4} /(m-m_o) l./mole	I^* l./mole.
Run 3.					
0 min.	3.11750	2.7600	1.3374	0.7477	-
3	3.09516	2.7197	1.2971	0.7710	1.76
10	3.05996	2.6563	1.2337	0.8106	5.72
15	3.03778	2.6163	1.1937	0.8377	8.43
30	2.99450	2.5383	1.1157	0.8963	14.29
1 hr.	2.93828	2.4369	1.0143	0.9859	23.25
2	2.80654	2.1994	0.7768	1.2873	53.39
4.5	2.66200	1.9389	0.5163	1.9369	118.35
6	2.61052	1.8461	0.4235	2.3613	160.79
Run 4.					
0 min.	3.13750	2.7600	1.3374	0.7477	-
3	3.10974	2.7100	1.2874	0.7768	2.34
10	3.08220	2.6603	1.2377	0.8080	5.46
15	3.06496	2.6292	1.2066	0.8288	7.54
30	3.02310	2.5538	1.1312	0.8840	13.06
1 hr.	2.95050	2.4229	1.0003	0.9997	24.63
2	2.83700	2.2183	0.7957	1.2568	50.34
4.5	2.70798	1.9857	0.5631	1.7759	102.25
7.5	2.59126	1.7753	0.3527	2.8353	208.19

Cell B. $F = 0.1803$. $I^* = \left\{(m - m_o)^{-1} - (m_1 - m_o)^{-1}\right\} =$

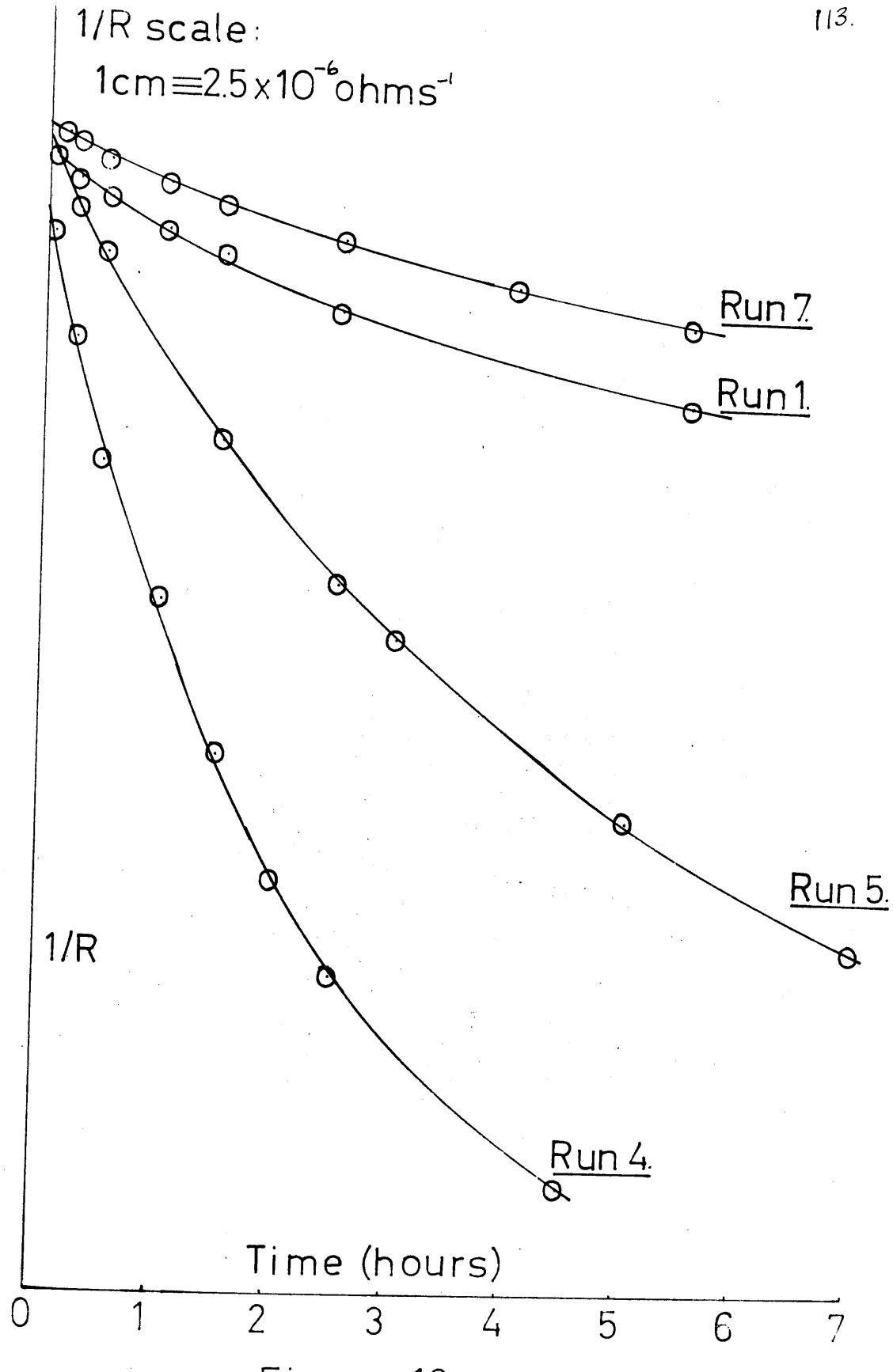
1/R scale:
1cm≡2.5x10⁻⁶ohms⁻¹
Run 7.
Run 1.
Run 5.
Run 4.
1/R
Time (hours)
0
1
2
3
4
5
6
7

Figure 19.

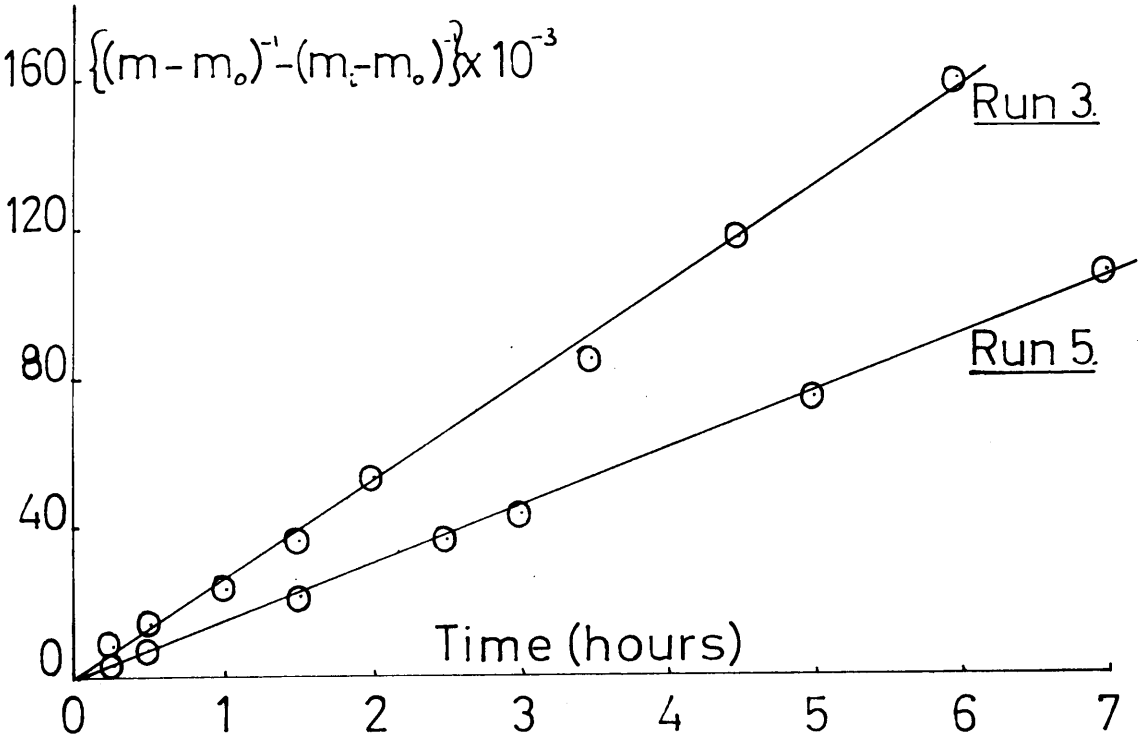
160
120
80
40
0
$\{(m-m_o)^{-1}-(m_i-m_o)^{-1}\}\times 10^{-3}$
Run 3.
Run 5.
Time (hours)
0
1
2
3
4
5
6
7

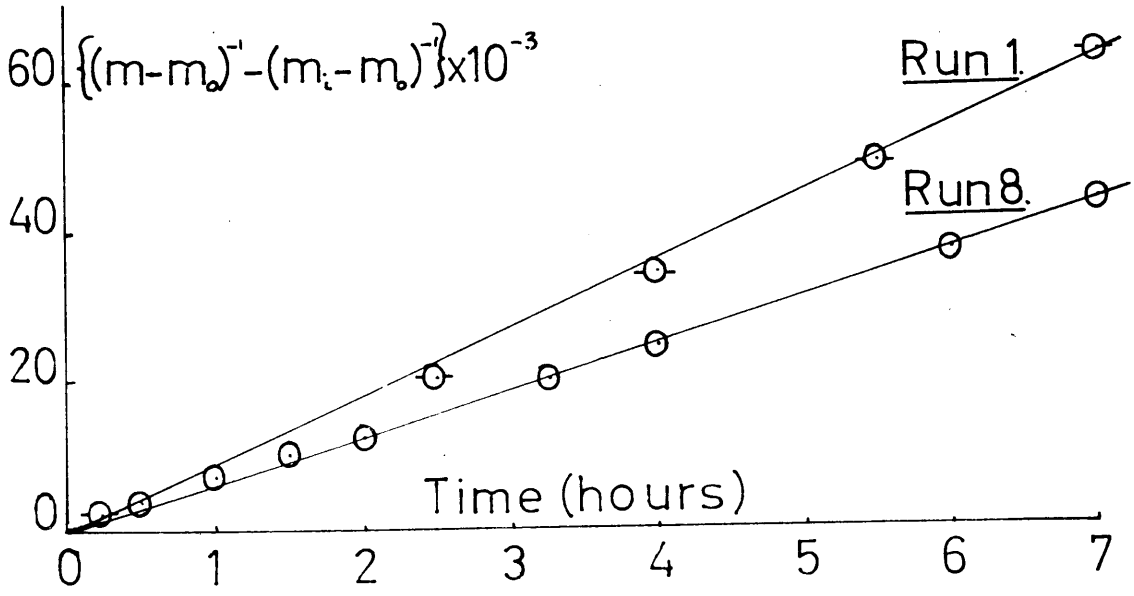
60
40
20
0
$\{(m-m_o)^{-1}-(m_i-m_o)^{-1}\}\times 10^{-3}$
Run 1.
Run 8.
Time (hours)
0
1
2
3
4
5
6
7

Figure 20.

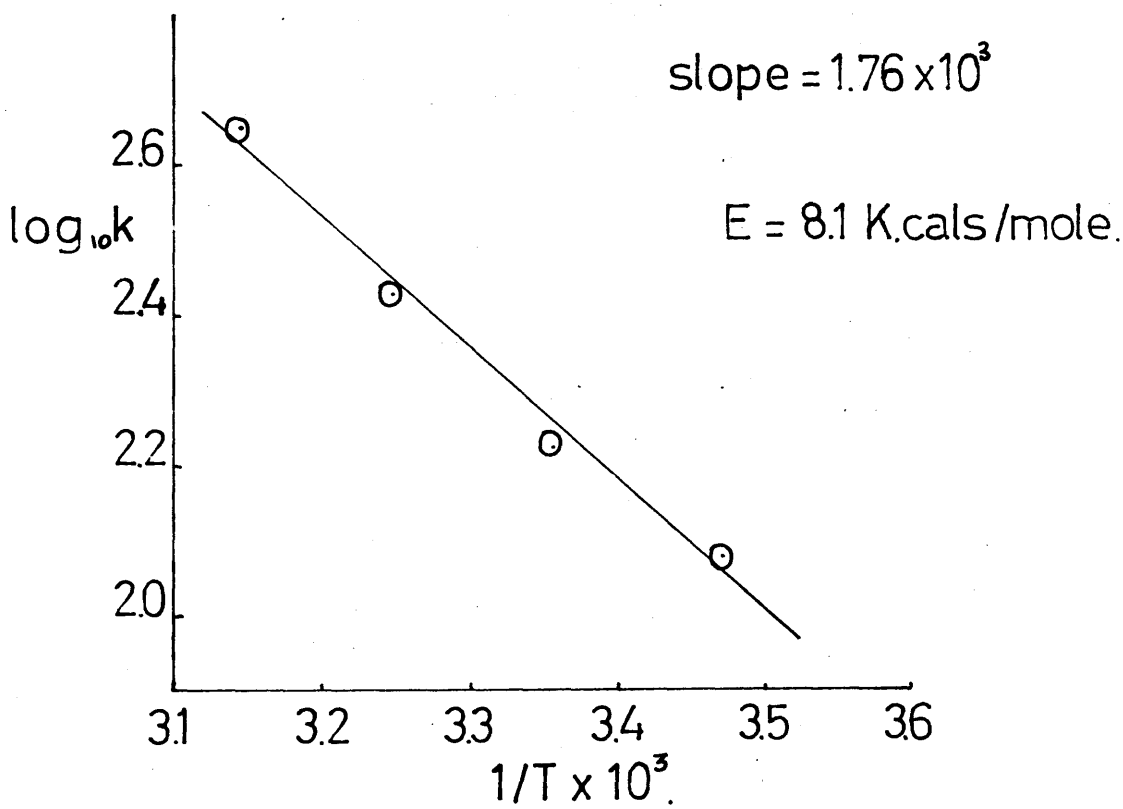
slope = 1.76 x10³
E = 8.1 K.cals/mole.
log₁₀k
2.6
2.4
2.2
2.0
3.1
3.2
3.3
3.4
3.5
3.6
1/T x 10³.

Figure 21.

DISCUSSION.

The crystallisation of lead sulphate has been shown to follow a second order rate law, with the exception of an initial, very fast growth surge. Similar results were obtained with barium sulphate (57), and it has been suggested that the initial fast period might be due to two-dimensional nucleation on the surface of the added seed crystals. If insufficient sites for growth are provided initially, nucleation will take place at active sites on the crystals, and this will continue until the supersaturation at the crystal surface is reduced to a value at which there are sufficient sites available to accommodate the growth. Nancollas and Purdie postulated that normal second order growth then sets in, and is the controlling factor. Bulk nucleation could not be the explanation of the growth surge, since this is characteristically associated with an induction period or slow stage, which was never observed.

Results obtained in the present work support the suggestion of surface nucleation. Addition of a larger amount of seed crystals substantially reduced the duration of the fast part (Table 2), and in Run 13 (Fig. 3) it was eliminated completely. Lowering the initial supersaturation had a similar effect.

In experiments in which the less regular needle-shaped crystals (Plate 2, B, C, D) were used, it was noticed that the duration of the initial growth surge was longer, suggesting that enhanced two-dimensional

was taking place. The particular faces which are developed in these crystals may contain fewer suitable sites for normal second order growth than the faces which are present in the rhombic type.

The rate of growth of lead sulphate was retarded by the presence of anionic adsorbates, a result similar to that described by Otani (66, 97). In a study of strontium sulphate precipitation he found that both spontaneous crystallisation, and growth on added seed crystals were inhibited almost completely by sodium triphosphate, at a concentration of 5×10^{-5} moles/l. He attributed this observation to adsorption on to the nuclei or growing crystals, and postulated that the triphosphate ion may be preferentially adsorbed at active sites on the crystals, thus retarding layer growth. Since the mole ratio of strontium to triphosphate was 670/1, the inhibition of growth could not be explained by complex formation. Similar results have been obtained with a variety of other phosphates (74

The effectiveness of the various adsorbates can be explained by considering the size of the ions. The larger, more highly charged additives will be attached more firmly to the crystal surface, and will cover a larger area (19).

Dodecylsulphate, the least effective of the additives studied, is composed of a long hydrocarbon chain, terminating in a univalent ionic group. When this ion is attached to the surface, the hydrocarbon part of the molecule would not be very efficient in blocking other growth sites.

The pyrophosphate ion is composed of two phosphate tetrahedra, linked through an oxygen atom, the O - O distance being 2.50 Å, which compares with an O - O distance of 2.47 Å in the sulphate ion. With its four negative charges, electrostatic forces would result in the strong attachment of this ion to the positive surface of lead sulphate (98, 99), but since it is fairly compact it would not cover a very large area. The trimetaphosphate and tetrametaphosphate ions are also composed of phosphate tetrahedra (100, 101) linked through oxygen atoms, with an O - O distance of 2.51 Å. (100). Tetrametaphosphate, being larger, and having one more negative charge would be slightly more effective in retarding the crystallisation of lead sulphate. These ideas are in agreement with the suggestion of Cabrera and Vermilyea (19) that the size of the impurity is the most important factor in retarding growth.

Cuming and Schulmann (102) have estimated the surface area of the dodecylsulphate ion from surface tension and surface potential measurements (103, 104) made on adsorbed and spread films of long chain sulphates at the air-water interface. They concluded that the limiting area per ion is about 20 $Å^2$, under conditions where the charge on the sulphate group is effectively neutralised.

Mulra and his co-workers (74) have determined the surface area of the triphosphate ion, by considering its adsorption on strontium sulphate crystals of known surface area. They arrived at a value of 37 $Å^2$ for the area occupied per triphosphate molecule, and concluded

that the area covered per phosphate tetrahedron was 12 $Å^2$.

In the present study the concentration of impurity and the amount of seed added in each experiment were known. Hence it was possible to calculate for each run the available surface area of the crystals, and the surface area which would be covered by impurity, assuming a monomolecular adsorbed layer. Such a comparison can only be, at the best, very qualitative, since estimations of crystal surface area are based on the average size of the crystals, assumed cubic, and having atomically smooth surfaces. However, when this calculation was made, it was established that in Run 103, in which the concentration of sodium tetrametaphosphate was 1.64×10^{-6} moles/l., and growth was very slow, the ratio of crystal to adsorbate surface area was 0.8/1. In Runs 110 and 111, with sodium pyrophosphate and sodium dodecylsulphate respectively, values of this ratio were 3/1 and 230/1, the corresponding concentrations of impurity being 9.41×10^{-6} moles/l. for pyrophosphate, and 2.19×10^{-4} moles/l. for dodecylsulphate.

The results obtained in the presence of adsorbates are consistent with the idea proposed by Sears (77) that the impurity reduces the critical free energy for two-dimensional nucleation, causing an increase in surface nucleation. As the concentration of additive was increased, the duration and n - value of the initial growth surge, which has been attributed to two-dimensional nucleation, also increased. The trend in the values of n_1, and the

time for which the fast part lasted, can be seen in Tables 10 and 15. It seems probable that the adsorbate molecules occupy suitable growth sites, and that when fewer of these sites are available, more surface nucleation is needed to accommodate the growth.

Whereas the crystallisation of magnesium oxalate (43) and silver chloride (39) has been shown to follow a second order rate equation in the presence of adsorbates, this was not the case with lead sulphate. With this salt, the value of n_2 was found to increase with increasing concentration of impurity, this being especially marked when deionised water was used. It is possible that two-dimensional nucleation never stopped completely, although it became less than its initial value of n_1 (Tables 10 and 15). It seems reasonable to assume that as new sites are created by surface nucleation, some are immediately occupied by the impurity molecules. Further, less extensive nucleation may still be necessary, and this may continue throughout the entire growth period. With increasing concentration of adsorbate, the value of n_2 rose from three to as much as 36 (Table 10), but in all cases these values were substantially less than n_1. Little significance can be attached to values as large as 36, since they refer to growth experiments in which the rates were very slow and gradients correspondingly difficult to obtain.

Although the method of preparation of conductivity water did

not affect the kinetics of crystallisation of silver chloride (45), this has not been found to be true for lead sulphate, strontium sulphate (105) or silver iodate (44). Deionised water has been shown to have a marked effect on the kinetics of growth of strontium sulphate and silver iodate, and of lead sulphate in the presence of low concentrations of additives. It has been suggested (33, 105-107) that this is due to the presence of small amounts of organic matrix, which has been leached off the ion-exchange resin. Although such organic impurity does not increase the conductivity of the water, it appears to behave in a similar manner to the inorganic adsorbates studied, by occupying some of the active growth sites, and so enhancing the need for surface nucleation.

The crystallisation of lead sulphate in the presence of adsorbates was affected by deionised water. In particular, the values of n_1 and n_2 were found to increase with increasing concentration of additive. When distilled water was used, the value of n_1 was lower than that in deionised water, at a similar concentration of adsorbate, as can be seen from Table 30 below.

This would be the expected result if organic impurities from the resin block some of the existing growth sites. In the absence of such additional impurities, more active sites will be available, and surface nucleation will be reduced.

TABLE. 30.

Comparison of the Effect of Deionised and Distilled Water on Lead Sulphate Crystallisation.

[Adsorbate] (moles/l.)	Deionised Water		Distilled Water	
	n_1	n_2	n_1	n_2
Dodecylsulphate.				
3.4×10^{-5}	21	3	8	2
4.0×10^{-4}	100	36	13	6
Pyrophosphate.				
3×10^{-6}	35	6	29	2
1×10^{-5}	73	8	14	2
Tetrametaphosphate.				
7×10^{-8}	14	4	-	2
2×10^{-7}	40	19	7	2

With distilled water and low concentrations of adsorbate, the value of n_2 did not deviate from two, as can be seen from Tables 15 and 30. This is in agreement with the suggestion made above, that when organic impurities are present, they occupy some of the active sites created by surface nucleation. Hence, there

are never sufficient sites for growth to occur purely by the dislocation mechanism, which would give rise to a second order rate law.

At high concentrations of adsorbate, however, values of n_2 greater than two were observed, but the growth rate in these experiments was extremely slow. It was possible to use higher concentrations of additive before growth stopped completely when distilled water was used in the preparation of the solutions, and this would also be expected if there are more growth sites available.

When a cationic additive, cetyl trimethyl ammonium bromide, was used, the rate of crystallisation was not reduced, even at concentrations as high as 10^{-4} moles/l. This contrasts with the results of Davies and Nancollas (39), who found the rate of crystallisation of silver chloride to be reduced in the presence of the nitrate of this cation.

Crystallisation of lead sulphate from distilled water solutions containing non-equivalent concentrations of lead and sulphate ions showed deviations from second order kinetics, in contrast to results obtained by Nancollas and Purdie (57) with barium sulphate. Lead sulphate growth was slower with the cation in excess rather than the anion, and a similar result was obtained with barium sulphate (57) and silver chloride (7). Buchanan and Heyman (98) have found that the surface of lead sulphate crystals carries

a positive charge and it therefore seems reasonable that the rate of adsorption of the anion should be greater than that of the cation. No explanation of the change in kinetic order at non-equivalent ionic concentrations can be advanced at present. This positive charge carried by lead sulphate may be the reason for the ineffectiveness of the cationic additive in affecting the rate of growth.

When crystallisation begins with an initial surge of varying extent it is not possible to compare absolute values for the rate of the subsequent growth. The concentration at which the transition to second order growth takes place must depend on the amount of seed crystals added, and the number of growth sites provided by them. A large amount of seed crystals was added to the solution (500 - 1500 mg.) and it was not possible to ensure that the same quantity was used in each experiment.

Barium sulphate has also been found to crystallise from supersaturated solution according to a second order rate law at 15°, 25°, 35°, and 45°C., indicating that the slow step at the crystal-solution interface is controlling, but, in contrast to the results of Nancollas and Purdie (57), no initial growth surge was observed. In general, a larger weight of crystals was added to each experiment than in the previous study, and the seed suspension was composed of slightly smaller crystals. The increased surface area must therefore have provided sufficient active sites for normal

growth, making two-dimensional surface nucleation unnecessary. Indeed, this was observed by Nancollas and Purdie, who succeeded in eliminating the initial growth surge by increasing the amount of seed crystals added to their experiments.

Davies and Nancollas (38), in a study of silver chloride crystallisation, found the rate constants to be invariant with temperature, indicating an activation energy of zero for the process. In the present work, the rate constants for barium sulphate growth have been shown to increase with increasing temperature, corresponding to an activation energy of 8 K.Cals./mole.

Little work on temperature coefficients of growth has been reported, but Lichstein and Brescia (108), who studied the spontaneous precipitation of magnesium oxalate, also found that the rate was temperature dependent, with a heat of activation of ~3 K.Cals. They found (109) the kinetics to be first order, however, and concluded that diffusion was the rate-controlling mechanism, with

$$(MgC_2O_4)_2 + MgC_2O_4 \longrightarrow (MgC_2O_4)_3$$

being the slow step, where $(MgC_2O_4)_2$ is the critical nucleus.

One disadvantage of the conductimetric technique for studying the growth of crystals is that no information about the slow step can be obtained, other than that it takes place at the crystal-solution interface. The slow step may be due to the presence of only a limited number of suitable growth sites, to the dehydration of the ions, or to the time taken for a cation and an anion to reach

an active site in a favourable orientation for incorporation into the lattice. Of these possibilities, the first is unlikely to be affected by temperature, hence, if this step were rate controlling, the rate of growth should be independent of temperature. On the other hand, both the second and third alternatives are likely to be temperature dependent. The greater mobility of ions in the adsorbed layer as the temperature is raised should result in a greater number of collisions with growth sites, and thus an increase in the rate of growth.

It would seem, therefore, that in the case of barium sulphate, the rate determining process is not the availability of growth sites, but rather some mechanism such as the dehydration of ions before entering the crystal lattice, or the frequency with which ions in the mobile adsorbed layer collide with growth sites. With silver chloride, for which an energy of activation for growth of zero has been reported, the slow step may have been due to a limitation in the number of growth sites available on the crystals.

In conclusion, therefore, it has been shown that in the crystallisation of both lead sulphate and barium sulphate, the general theory of growth proposed by Davies and Jones was followed for most of the reaction. Deviations from this theory occurred, however, in the presence of adsorbates, and at non-equivalent ionic concentrations with the lead salt. Organic contaminants present in water prepared by ion-exchange techniques also had a profound effect on the growth

PART 2. Dissolution of Sparingly Soluble Salts in Aqueous Solution.

2a. Lead Sulphate.

2b. Barium Sulphate.

INTRODUCTION.

One of the earliest theories proposed to explain the phenomenon of dissolution was that of Noyes and Whitney (110), who found that the rate of solution of rods of benzoic acid and lead chloride could be represented by the equation

$$\frac{dm}{dt} = k_d s (m_o - m) \quad . \quad . \quad . \quad . \quad . \quad . \quad . \quad (1)$$

where m is the concentration of the solution at time t, m_o is the solubility, and s the surface of crystal exposed. This was modified by Nernst (111) to include the growth process, so that

$$\frac{dm}{dt} = \frac{Ds}{\delta} (m_o - m) \quad . \quad . \quad . \quad . \quad . \quad . \quad . \quad (2)$$

where D is the coefficient of diffusion and δ is the thickness of the layer through which diffusion is taking place. Thus, since $s (m - m_o)$ could be made equal, but of opposite sign, and $\frac{D}{\delta}$ should be equal for growth and solution, in any system the two processes should occur at the same rate.

Marc (5), however, established that the velocity of growth is usually much less than that of solution, indicating that the two processes cannot be regarded as reciprocal. Indeed, Marc showed that growth followed, in general, a second order rate equation. Many workers , however, have found that dissolution can be represented

quite satisfactorily by a first order rate law such as that proposed by Nernst, although many valid criticisms (8) have been made of the assumptions involved.

Nernst assumed that the reaction at the surface was very fast compared with the transport process, and that, in a well-stirred system, the concentration gradient was confined to a thin layer of thickness δ , adhering to the solid surface. The concentration would vary linearly with the perpendicular distance from the solid surface in this layer, and its thickness would be a function of the rate and type of stirring employed.

Van Name and Hill (112) disagreed with such a sharp delineation in the relative rates of the diffusion and interface processes. They suggested that heterogeneous processes controlled by diffusion, or by the chemical reaction at the interface are the extreme cases, and that there are many reactions in which these two rates are comparable. Hence, heterogeneous reactions would be expected to show a gradation in order between one and two. Despite this, many widely different reactions such as the dissolution of salts into their subsaturated solutions (113), of metals into acids (114, 115), liquid ammonia (116) and aqueous iodine (117) have all been shown to follow first order kinetics, although higher orders have been reported for the dissolution of silver chloride into water (38).

Many workers have established that the rate of solution increases with the rate of stirring up to very high speeds of agitation, as would be expected for systems in which diffusion is important. From a study of the solution of calcium carbonate in acetic and hydrochloric acids, however, although the rate of solution increased with the speed of stirring up to 7000 r.p.m., King and Ling Liu (118) were of the opinion that the rate would tend to reach a maximum at even higher rates of agitation.

Further evidence in support of a diffusion controlled process has been supplied by Riddiford and Bircumshaw (117) who found that several metals dissolved at the same rate in aqueous iodine. From a similar study King and Braverman (115) have established that the rate of solution of various metals in hydrochloric acid was the same, suggesting that the rate controlling step was the diffusion of solvent up to the solid surface. On the other hand, Johnson and Macdonald (116) investigated the dissolution of sodium in liquid ammonia, and concluded that the probable rate determining step was the diffusion of products away from the solid surface.

King and his co-workers (115, 118) have also shown that the rate of solution is inversely proportional to the viscosity, and that most of the dissolution reactions studied have a temperature coefficient in the region of 1.1 - 1.5 per 10° rise, which is of the order of that expected for diffusion control.

Nernst assumed that the thickness, δ , of the stationary layer

was approximately the same for all reactions, under the same conditions of stirring, and Brunner (119) has estimated a value of 0.03 mm. at 20°C. for δ . On the other hand, Fage and Townend (120) have shown from ultramicroscope studies that fluid motion persists up to points in the region of 6×10^{-5} cm. from the solid surface. In view of this, King (121) modified the picture of Nernst's film, in terms of a layer next to the solid surface which was still in turbulent flow, and in which the velocity component of turbulence normal to the interface was negligible compared with diffusion for transporting the reagent. In a study of the dissolution of zinc and magnesium in acid, he found that δ was proportional to the diffusion coefficient, but that it changed little with viscosity or temperature.

It seems therefore, that a slightly modified Nernst diffusion theory provides a satisfactory explanation for most dissolution processes. In those reactions for which a kinetic order greater than one is obeyed, it must be assumed that the chemical reaction at the interface is of comparable rate, or faster than the rate of transport by diffusion, and hence a different mechanism is controlling.

In the present study, Part 2a deals with the dissolution of lead sulphate into subsaturated solution, and in the presence of sodium tetrametaphosphate. Part 2b deals with the solution of barium sulphate into water at temperatures ranging from 15°-45°C.

and into subsaturated solution at 25°C. A radiochemical technique has also been used, with ^{35}Sulphur as tracer, to follow the dissolution of labelled barium sulphate seed crystals into water at 15° - 35°C.

PART 2a. Lead Sulphate.

The dissolution of lead sulphate seed crystals into subsaturated solutions, and the effect of added impurities has been studied.

Marc (122) studied the growth and dissolution of potassium chlorate crystals in the presence of the dye Ponceau 2R, and found that the same concentration of dye was much more effective in retarding crystallisation than solution. Herzfeld (123), who considered that the breaking loose of an ion from a crystal should not be affected by the presence of an adsorbed molecule, conceded, however, that if such an impurity was attached simultaneously to more than one surface ion, or was sufficiently large, the rate of solution could be retarded.

The study of etch pit formation has led to further advances in the theory of dissolution. Burton, Cabrera and Frank (17) suggested that dissolution should take place by the retreat of monomolecular steps across the crystal surface, individual molecules being removed from kinks in the surface. Gilman, Johnston and Sears (79) have proposed that dissolution begins with the creation of unit pits, one molecule deep. These pits grow as steps retreat across

the crystal through the action of kinks. On a real crystal, dislocations, due to the energy that is localised at them, may be preferred sites for the initiation of unit pits.

In a study of the dissolution of lithium fluoride crystals (124), it was established that the formation of etch pits was due to traces of ferric ion present. When this was complexed by the addition of ammonium hydroxide, even dissolution, with few etch pits was obtained. From a similar investigation (79) it was established that the presence of ferric ions or other cations which adsorb at kinks protect the surface from dissolution, and cause etch pits to form at dislocations.

Sears (78) considers that severe hindrance of solution at a step is associated with complete coverage of adsorption sites on the step. He proposed (124) that the formation of an etch pit at a dislocation occurred by the generation of loops of step concentric with the dislocation, and that the most important effect of the poison depended on the inhibition of general dissolution. Etch pits therefore cannot be formed unless an impurity is present, but, as in the case of lithium fluoride, this may be supplied by the dissolving crystal itself (79).

The solution of lead sulphate into subsaturated solution has been shown to follow a second order rate law, but the apparent kinetic order was found to be extremely sensitive to minute traces of

impurity. Sodium tetrametaphosphate has been found to cause a considerable reduction in the rate of dissolution, and also to cause an increase in the value of n in the expression

$$\frac{dm}{dt} = k_d\, s\, (m_o - m)^n.$$

EXPERIMENTAL.

Preparation of Seed Crystals.

Seed crystals were prepared by the method described in Part 1a of this work. Only those rhombic in form (Plate 2A) were used in the dissolution experiments. The amount added to the cell in each experiment was determined by filtration as before.

Preparation of Cell Solution.

Subsaturated solutions were prepared by the slow mixing of dilute solutions of sodium sulphate and lead nitrate, and after inoculation with seed crystals, the rate of dissolution was measured by following the increase in conductivity with time. Adsorbate solutions were added in the same way as in the crystallisation work.

RESULTS.

Experiments on the rate of dissolution of lead sulphate into subsaturated solution at 25°C. have been made. The effect of adding sodium tetrametaphosphate has also been studied, and experiments with this adsorbate were made using both deionised and distilled water. The initial ionic product used in all the experiments was 1.4982×10^{-8} moles^2/l^2.

Dissolution Experiments at Equivalent Ionic Concentrations.

The results are summarised in Table 31. Some typical smooth curves obtained by plotting the reciprocal of resistance against time are given in Fig. 22 and show the low degree of scatter of the points.

The rate of increase of conductivity at any instant was determined by measuring slopes of the 1/R against time curve, and hence dm/dt could be calculated. Instantaneous values of ionic concentration were obtained as described on page 44. The solubility of lead sulphate (page 41) was corrected for ionic strength effects using activity coefficients calculated from the Davies equation (p. 41) and a value of 1.476×10^{-4} moles/l. was used for m_o.

To determine the order of the dissolution, plots were made of log dm/dt against log $(m_o - m)$, and these are shown in Fig. 23. Two distinct straight lines were obtained, of slopes n_1 and n_2, corresponding to an initial fast part and the subsequent dissolution process. The value of n_2 was found to be two, while n_1 was always greater than two. Thus, for the main part of the reaction, after the initial surge, the dissolution follows the equation

$$\frac{dm}{dt} = k_d \, s \, (m_o - m)^2 \quad . \quad . \quad . \quad . \quad . \quad . \quad (1)$$

Graphs of dm/dt against $(m_o - m)^2$ are given in Fig. 24, using data from Table 32.

In equation (1), s will be some function of the surface area of the seed crystals, which decreases as dissolution proceeds. Assuming that s varies linearly with surface area, a more precise form of the rate equation

$$\frac{dm}{dt}\left(\frac{w_1}{w_2}\right)^{\frac{2}{3}} = k'(m_o - m)^2$$

should be used, where w_1 is the initial weight of seed crystals, and w_2 is their weight at time t. For lead sulphate experiments, relatively large amounts of seed crystals were used (70 - 900 mg.) and the decrease in weight was less than 0.01% of the total, making the correction unnecessary.

A number of experiments were made using solutions prepared from deionised water, and n_2 was also found to be two. Second order plots are shown in Fig. 25, and the data are recorded in Table 33.

Dissolution of Lead Sulphate in Presence of Sodium Tetrametaphosphate.

Concentrations of sodium tetrametaphosphate ranging from 7.40×10^{-8} moles/l. to 3.26×10^{-5} moles/l. were studied, and the results are summarised in Table 31. Plots of 1/R against time for data in Tables 34 and 35 are shown in Figs. 26 and 27. Although different amounts of seed crystals were used for each experiment, it can be seen quite clearly that the additive decreases the rate of solution even at concentrations as low as 7×10^{-8} moles/l.

The effect is rather marked, since the seed concentrations were generally greater in the experiments with adsorbate (Table 31).

Values of n were obtained as before, and were found to increase with increasing concentration of tetrametaphosphate ions; in all cases n was greater than two. Using deionised water for the adsorbate experiments produced an even larger effect, as can be seen from Table 31. Little significance can be attached, however, to the high values of n, which are difficult to justify as reaction orders. They correspond to extremely slow rates of solution.

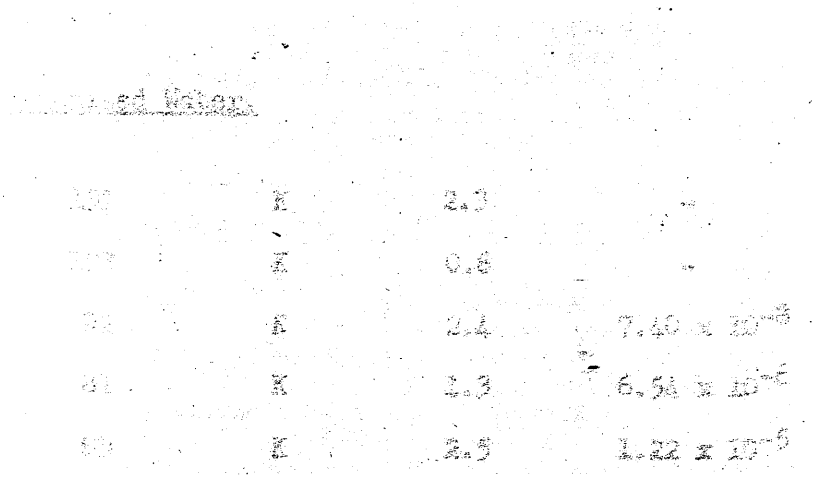

TABLE. 31.

Dissolution of Lead Sulphate.

Experiment Number	Seed Suspension	Seed Conc. (mg/ml.)	[TMP] (moles/l.)	Cell	n_2
Distilled Water.					
97	L	0.2	-	E	2
99	K	0.2	-	E	2
101	M	0.2	-	E	2
115	M	2.8	6.36×10^{-8}	E	3
114	M	0.6	1.15×10^{-7}	E	8
130	M	1.0	4.99×10^{-5}	A	11
Deionised Water.					
131	K	2.3	-	A	2
128	K	0.8	-	A	2
92	K	2.4	7.40×10^{-8}	E	3
81	K	1.3	6.54×10^{-6}	E	11
83	K	2.5	1.22×10^{-5}	E	(47)
90	K	2.5	3.24×10^{-5}	E	(135)

TABLE. 32. Dissolution of Lead Sulphate.

Distilled Water.

Time	$10^3 / R$ ohms^{-1}	10^4 m moles/l.	$10^4 (m_o-m)$ moles/l.	dm/dt x 10^8	$10^9 (m_o-m)^2$ moles^2/l^2.
Run 97.					
0 min	0.86999	1.2240	0.2523	-	0.6366
6	0.87100	1.2266	0.2497	9.05	0.6235
15	0.87310	1.2320	0.2443	5.28	0.5968
30	0.87662	1.2411	0.2352	4.83	0.5532
1 hr.	0.88245	1.2562	0.2201	4.52	0.4844
3	0.90017	1.3020	0.1743	2.95	0.3038
5	0.91330	1.3360	0.1403	2.26	0.1968
7.25	0.92603	1.3689	0.1074	1.51	0.1153
10.5	0.93460	1.3910	0.0853	1.08	0.0728
23.5	0.95504	1.4439	0.0324	0.21	0.0105
Run 99.					
0 min.	0.77380	1.0868	0.3895	-	1.5171
6	0.78233	1.1089	0.3674	10.0	1.3498
15	0.78603	1.1184	0.3579	7.52	1.2809
30	0.79089	1.1310	0.3453	6.68	1.1923
1 hr.	0.79895	1.1518	0.3245	6.14	1.0530
2	0.81292	1.1879	0.2884	4.83	0.8317
4	0.83476	1.2444	0.2319	4.20	0.5378
7	0.85833	1.3053	0.1710	2.80	0.2924
10	0.87447	1.3471	0.1292	1.05	0.1669
23.5	0.90299	1.4208	0.0555	-	0.0308

TABLE. 32. (cont.)

Time	10^3 / R $ohms^{-1}$	10^4 m moles/l.	10^4 (m_o-m) moles/l.	dm/dt x 10^8	10^9 (m_o-m)^2 $moles^2/l^2$.
Run 101.					
0 min.	0.87850	1.2240	0.2523	-	0.6366
1.5	0.88316	1.2360	0.2403	18.7	0.5774
6	0.88800	1.2486	0.2277	15.25	0.5185
15	0.89157	1.2578	0.2185	9.48	0.4774
30	0.89577	1.2686	0.2077	6.68	0.4314
1 hr.	0.90245	1.2859	0.1904	5.34	0.3625
2	0.91272	1.3125	0.1638	3.88	0.2683
3	0.92121	1.3344	0.1419	3.02	0.2014
5	0.93419	1.3680	0.1083	2.11	0.1173
7	0.94371	1.3926	0.0837	0.77	0.0701

TABLE. 33. Dissolution of Lead Sulphate.

Deionised Water.

Time	10^3 / R ohms^{-1}	10^4 m moles/l.	10^4 (m_o-m) moles/l.	dm/dt x 10^8	10^9 (m_o-m)^2 moles^2/ l^2.
Run 128.					
0 min.	0.91120	1.2240	0.2523	-	
1.5	0.91657	1.2373	0.2390	39.10	0.5712
6	0.92321	1.2537	0.2226	23.64	0.4955
15	0.92952	1.2693	0.2070	17.60	0.4285
30	0.93869	1.2920	0.1843	13.10	0.3397
1 hr.	0.95176	1.3244	0.1519	9.61	0.2307
3	0.97999	1.3943	0.0820	3.14	0.0672
5	0.99064	1.4206	0.0557	1.29	0.0310
7	0.99541	1.4324	0.0439	0.87	0.0193
Run 131.					
0 min.	0.90360	1.2240	0.2523	-	
1.5	0.90706	1.2326	0.2401	20.04	0.5765
6	0.91071	1.2416	0.2347	12.42	0.5508
15	0.91473	1.2515	0.2248	10.64	0.5054
30	0.92099	1.2670	0.2093	9.48	0.4381
1 hr.	0.93101	1.2918	0.1845	8.00	0.3404
3	0.95711	1.3564	0.1199	3.79	0.1438
5.5	0.97373	1.3976	0.0787	1.90	0.0619
7	0.97960	1.4121	0.0642	1.24	0.0412.

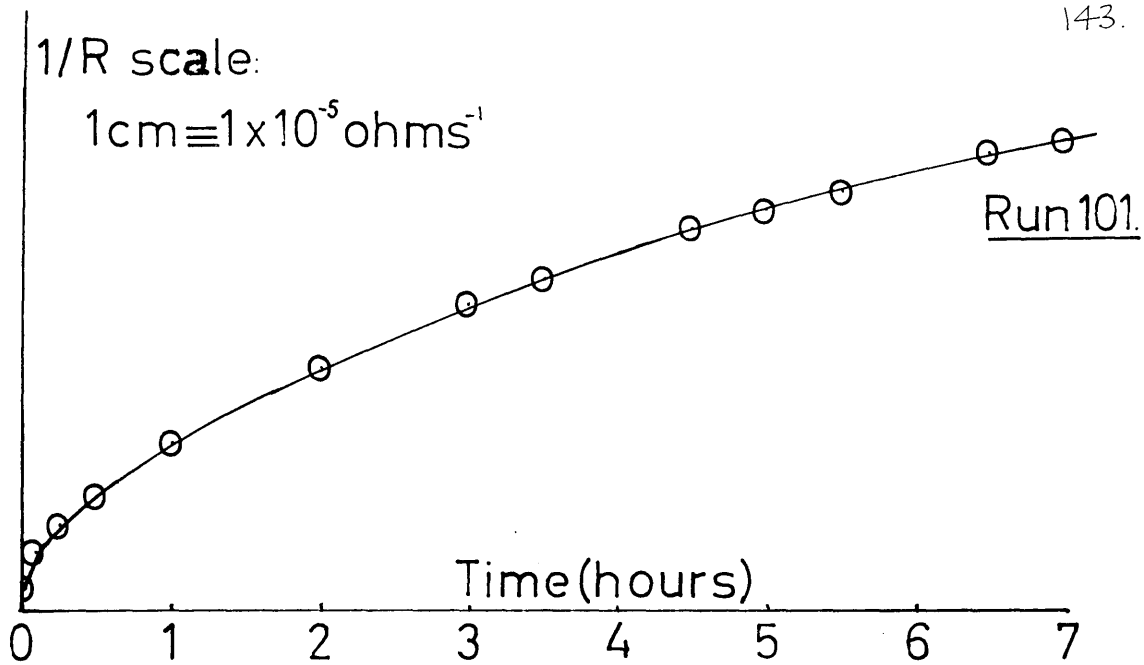
1/R scale:
1cm≡1x10⁻⁵ohms⁻¹
Run 101.
Time (hours)
0
1
2
3
4
5
6
7

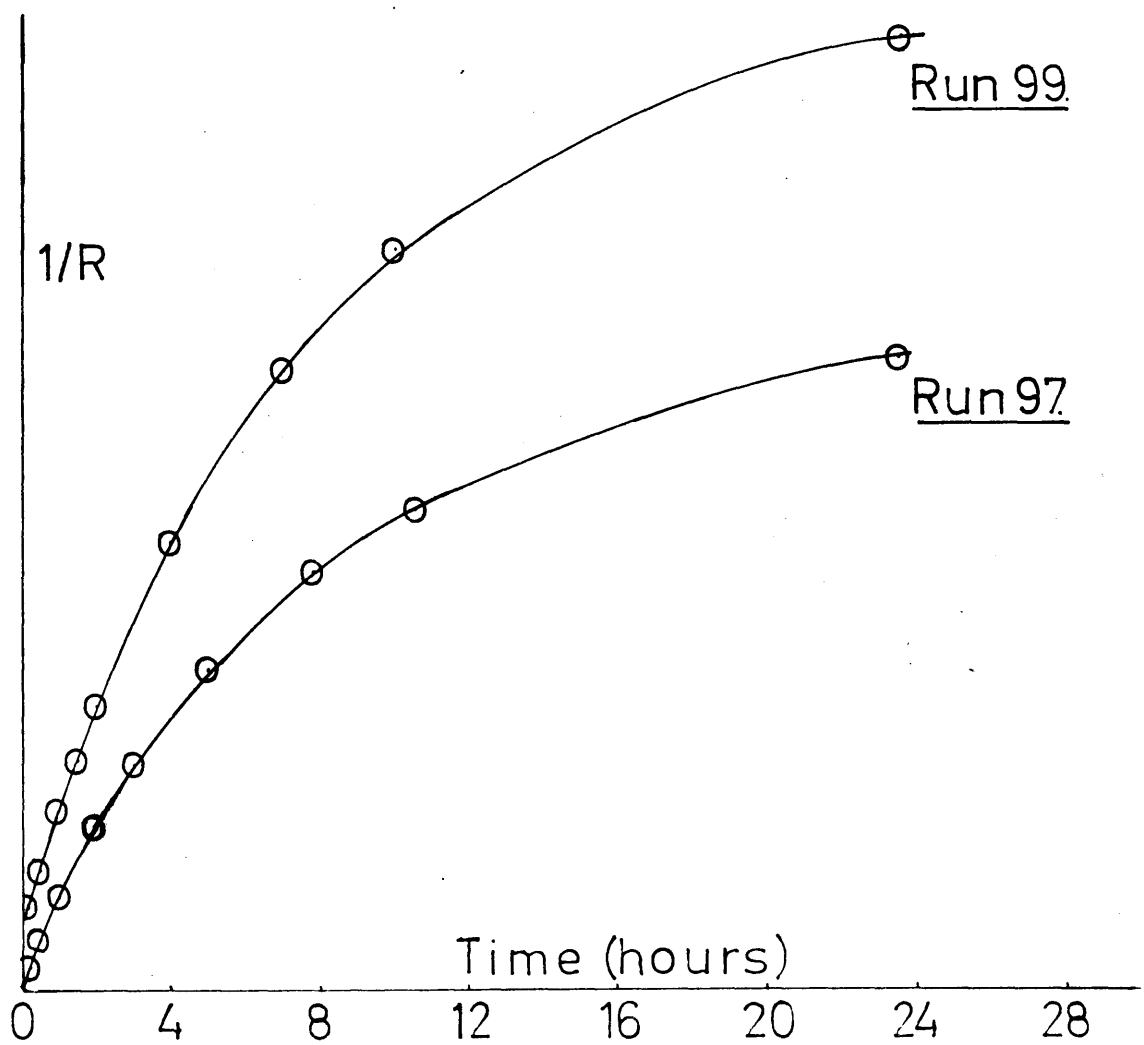
Run 99.
1/R
Run 97.
Time (hours)
0
4
8
12
16
20
24
28

Figure 22.

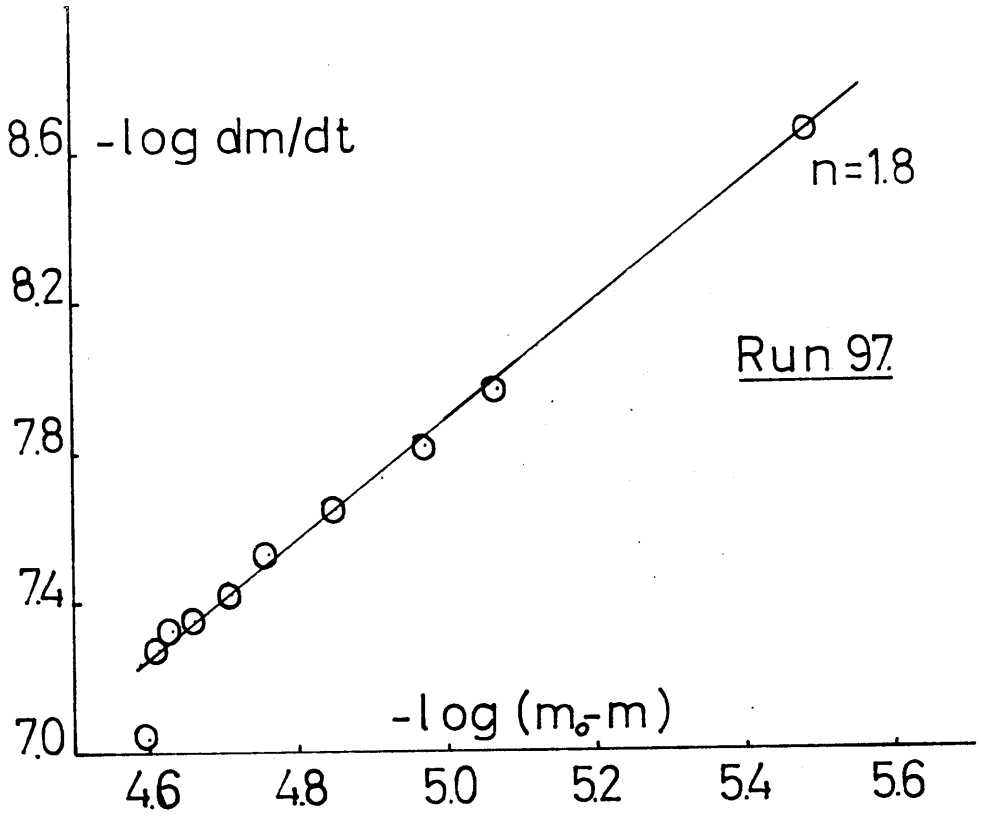
8.6
8.2
7.8
7.4
7.0
-log dm/dt
n=1.8
Run 97.
-log (m₀-m)
4.6
4.8
5.0
5.2
5.4
5.6

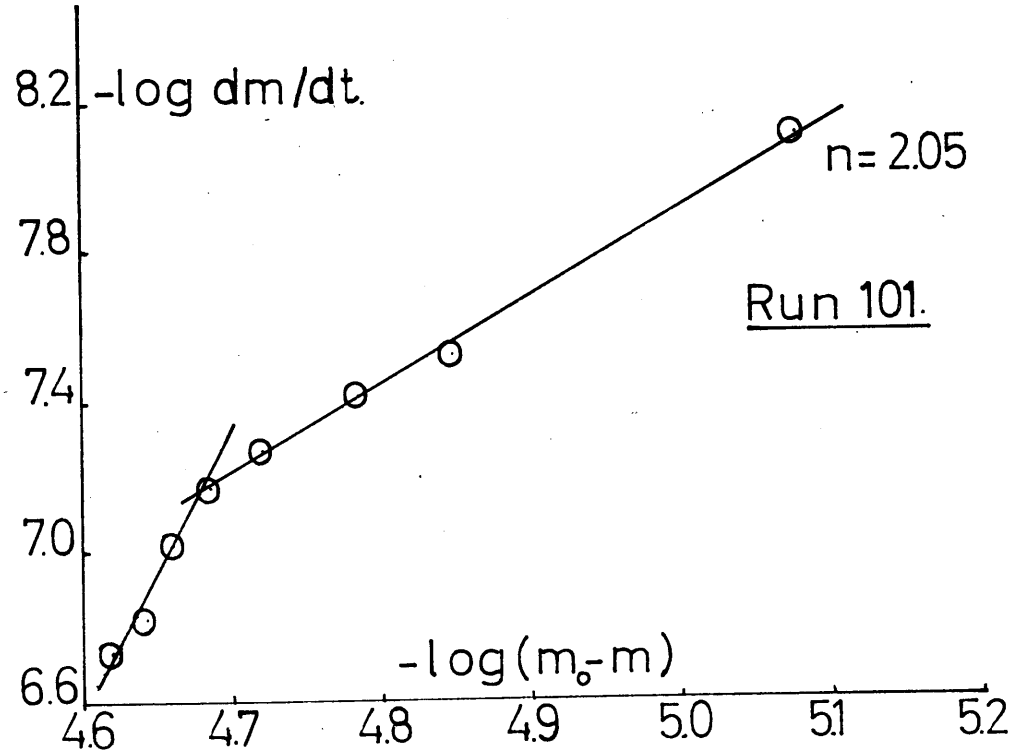
8.2
7.8
7.4
7.0
6.6
-log dm/dt.
n= 2.05
Run 101.
-log(m₀-m)
4.6
4.7
4.8
4.9
5.0
5.1
5.2

Figure 23.

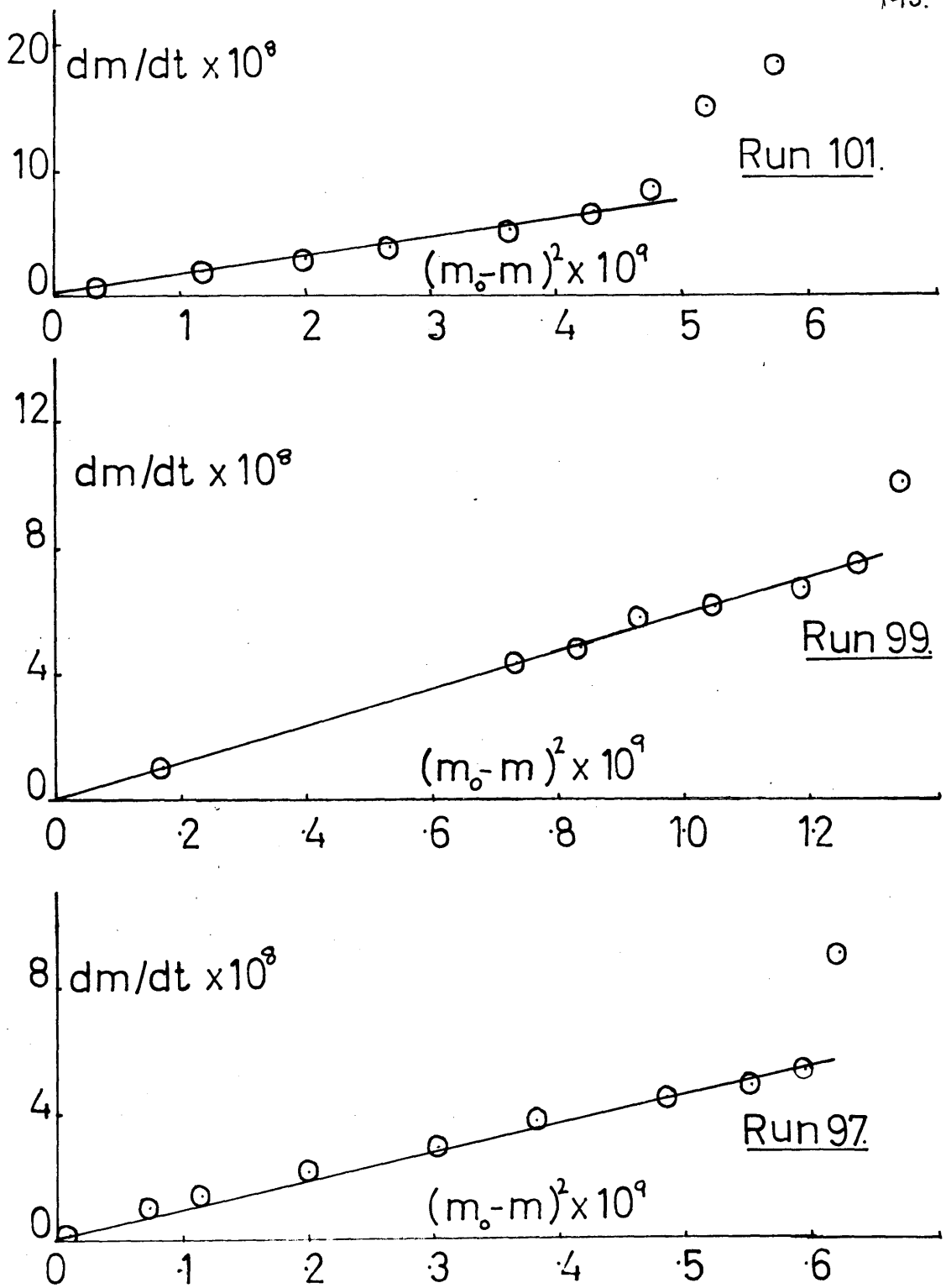
20
dm/dt x 10⁸
10
0
Run 101.
(m₀-m)² x 10⁹
0
1
2
3
4
5
6
12
dm/dt x 10⁸
8
4
0
Run 99.
(m₀-m)² x 10⁹
0
·2
·4
·6
·8
1·0
1·2
8
dm/dt x 10⁸
4
0
Run 97.
(m₀-m)² x 10⁹
0
·1
·2
·3
·4
·5
·6

Figure 24.

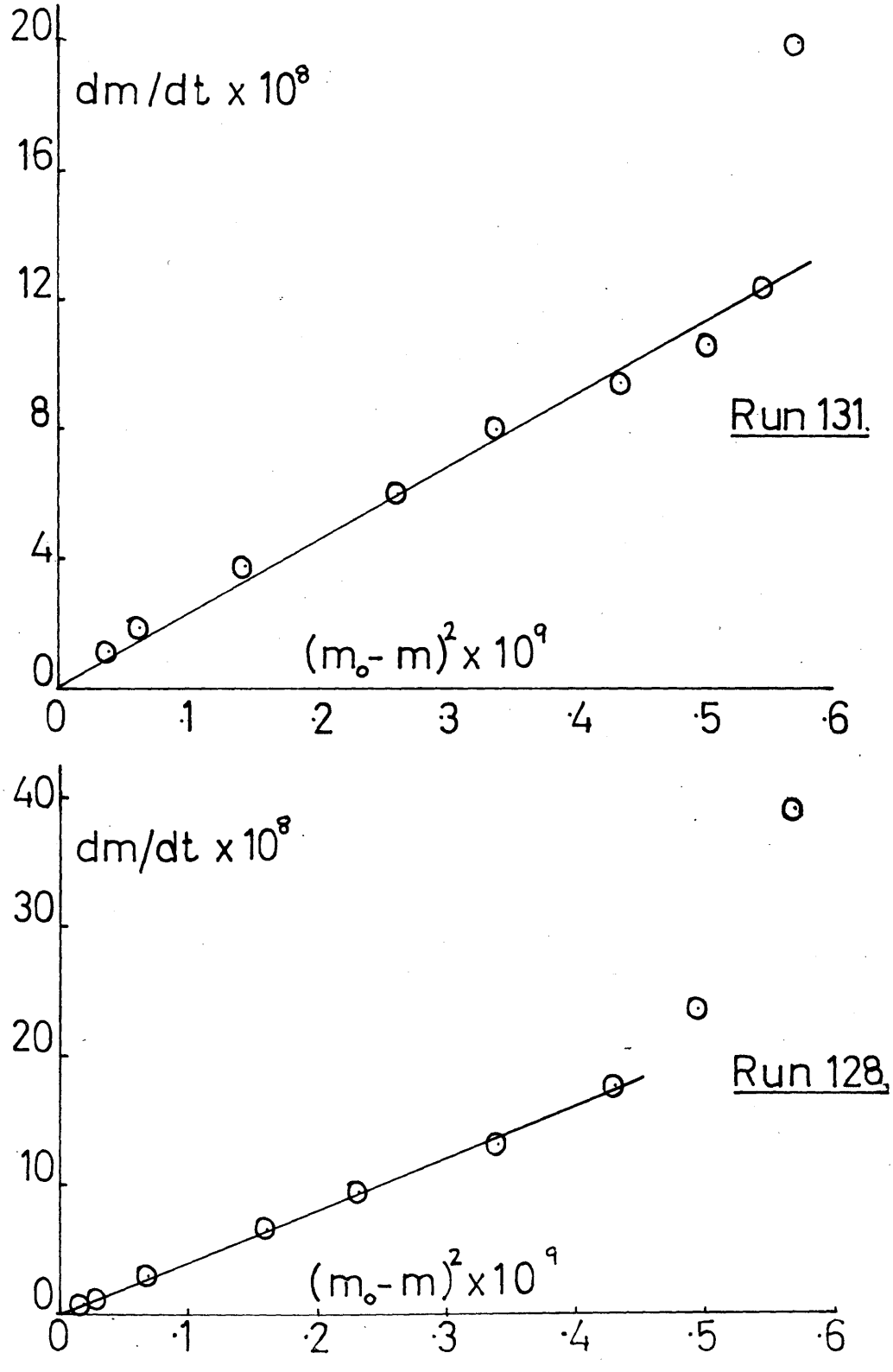
dm/dt x 10^8
20
16
12
8
4
0
Run 131.
(m_o - m)^2 x 10^9
0
·1
·2
3
·4
·5
·6
dm/dt x 10^8
40
30
20
10
0
Run 128.
(m_o - m)^2 x 10^9
0
·1
·2
·3
·4
·5
·6

Figure 25.

TABLE. 34. Deionised Water.

Dissolution of Lead Sulphate in Presence of Tetrametaphosphate.

Time	$10^3 / R$ ohms^{-1}	m x 10^4 moles/l.	$(m_o - m)$ x 10^4 moles/l.
Run 92. [TMP] = 7.40 x 10^{-8} moles/l.			
0 min.	0.87650	1.2240	0.2523
3	0.88210	1.2385	0.2378
6	0.88455	1.2448	0.2315
15	0.88954	1.2577	0.2186
30	0.89656	1.2757	0.2004
1.5 hrs.	0.91569	1.3253	0.1510
3	0.93232	1.3683	0.1080
5.5	0.94751	1.4077	0.0686
26	0.96558	1.4543	0.0220
Run 81. [TMP] = 6.54 x 10^{-6} moles/l.			
0 min.	0.89706	1.2240	0.2523
1	0.89757	1.2253	0.2510
6	0.89851	1.2277	0.2486
15	0.89927	1.2297	0.2466
30	0.90003	1.2317	0.2446
1 hr.	0.90126	1.2348	0.2415
2	0.90408	1.2421	0.2342
3	0.90601	1.2471	0.2292

TABLE. 34. (cont.)

Time	$10^3 / R$ ohms^{-1}	$m \times 10^4$ moles/l.	$(m_o-m) \times 10^4$ moles/l.
Run 83. [TMP] = 1.22×10^{-5} moles/l.			
0 min.	0.91350	1.2240	0.2523
1.5	0.91448	1.2265	0.2498
6	0.91547	1.2291	0.2472
15	0.91657	1.2319	0.2444
30	0.91749	1.2343	0.2420
1 hr.	0.91911	1.2385	0.2378
3	0.92084	1.2430	0.2330
6.25	0.92129	1.2441	0.2322
21	0.92451	1.2525	0.2238
Run 90. [TMP] = 3.24×10^{-5} moles/l.			
0 min.	0.97545	1.2240	0.2523
1	0.97564	1.2245	0.2518
6	0.97639	1.2264	0.2499
15	0.97685	1.2276	0.2487
30	0.97717	1.2284	0.2479
1 hr.	0.97748	1.2292	0.2471
2.5	0.97826	1.2313	0.2450
3.5	0.97877	1.2326	0.2437

TABLE. 35. Distilled Water.

Dissolution of Lead Sulphate in Presence of Tetrametaphosphate.

Time	$10^3 / R$ ohms^{-1}	m x 10^4 moles/l.	(m_o-m) x 10^4 moles/l.
Run 115. [TMP] = 6.36 x 10^{-8} moles/l.			
0 min.	0.89790	1.2240	0.2523
6	0.90626	1.2456	0.2307
15	0.90917	1.2531	0.2232
45	0.91631	1.2716	0.2047
1.25 hrs.	0.92206	1.2865	0.1898
4	0.94110	1.3357	0.1406
9.5	0.95922	1.3825	0.0938
12.25	0.96423	1.3955	0.0808
23.25	0.97416	1.4211	0.0552
Run 114. [TMP] = 1.15 x 10^{-7} moles/l.			
0 min.	0.89090	1.2240	0.2523
6	0.89437	1.2330	0.2433
15	0.89567	1.2363	0.2400
30	0.89721	1.2403	0.2360
1 hr.	0.89908	1.2451	0.2312
3	0.90303	1.2554	0.2209
8	0.90888	1.2705	0.2058
15.25	0.91327	1.2818	0.1945
23.5	0.91712	1.2918	0.1845

TABLE. 35 (cont.)

Time	$10^3 / R$ ohms^{-1}	m x 10^4 moles/l.	(m_o-m) x 10^4 moles/l.
Run 130. [TMP] = 4.99 x 10^{-5} moles/l.			
0 min.	1.03735	1.2240	0.2523
1.5	1.03772	1.2249	0.2514
6	1.03814	1.2260	0.2503
15	1.03856	1.2270	0.2493
30	1.03897	1.2280	0.2483
1 hr.	1.04001	1.2306	0.2457
2	1.04105	1.2332	0.2431
3.5	1.04231	1.2363	0.2400
7.75	1.04398	1.2404	0.2359
9.25	1.04481	1.2429	0.2334

Cell E.

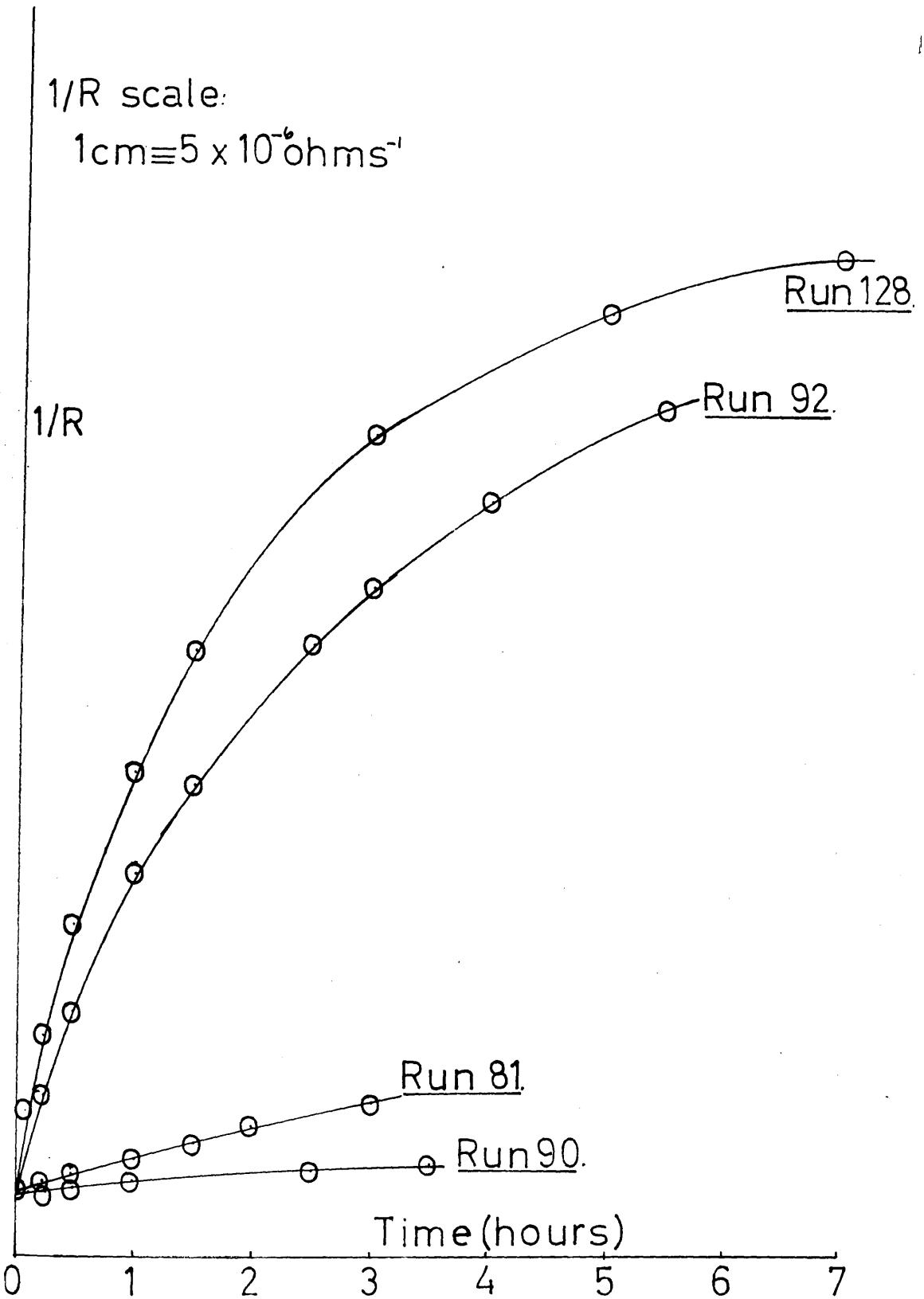
1/R scale:
1cm≡5 x 10⁻⁶ ohms⁻¹
1/R
Run 128.
Run 92.
Run 81.
Run 90.
Time (hours)
0
1
2
3
4
5
6
7

Figure 26.

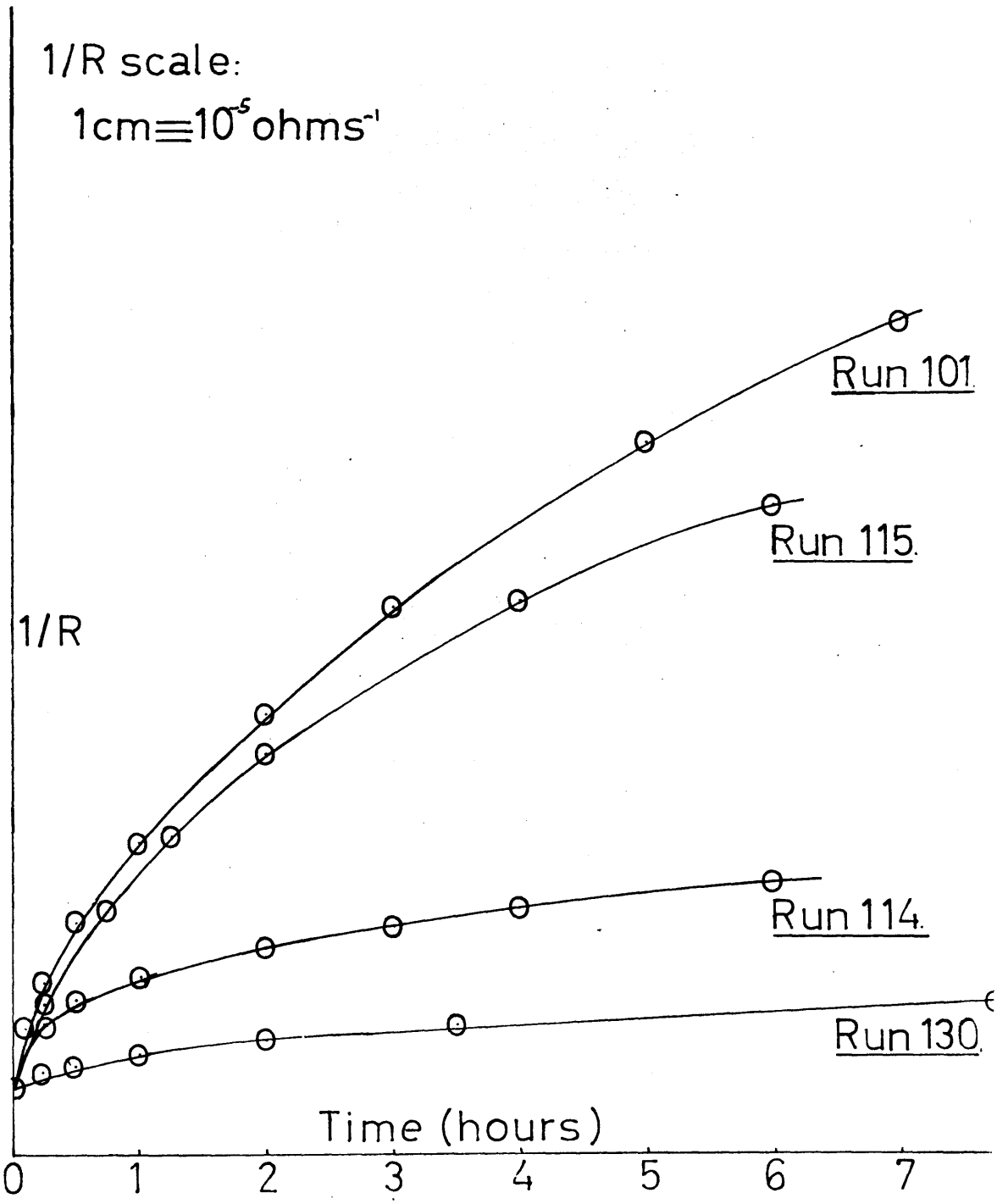
1/R scale:
1cm≡10⁻⁵ohms⁻¹
Run 101.
Run 115.
Run 114.
Run 130.
1/R
Time (hours)
0
1
2
3
4
5
6
7

Figure 27.

PART 2b.

Dissolution of Barium Sulphate into Water and Subsaturated Solutions at Various Temperatures.

PART. 2b.

INTRODUCTION.

Although a large amount of work has been done on the precipitation of barium sulphate, little attention has been paid to its dissolution. The present study was carried out to determine the effect of temperature on the rate of solution.

Johnson and MacDonald (116) studied the rate of solution of sodium in liquid ammonia at various temperatures, and by applying the Arrhenius equation,

$$\ln k = \ln A - E/RT,$$

obtained a value of 4.2 K.Cals. / mole for E, the apparent energy of activation for diffusion. Howard, Nancollas and Purdie (113) investigated the dissolution of silver chloride seed crystals into subsaturated solutions, and found a value of 4.5 K.Cals./mole for the energy of activation. Van Name (126), who studied the dissolution of cadmium in an aqueous solution of iodine in potassium iodide at temperatures between 0° and 65°C., found the energy of activation to be 4.4K.Cals./mole. Moelwyn-Hughes (127), who considered the temperature variation of diffusion ceefficients, and assumed the thickness of the interfacial layer to be independent of temperature, calculated the energy of activation for diffusion to be about 4.5 K.Cals. / mole.

Davies and Nancollas (38), who observed the rate of

dissolution of silver chloride into water to be proportional to (subsaturation)$^{3/2}$ at 15° and 25°C., and the second power at 35°C., found an activation energy of 15.4 K.Cals./ mole. It seems unlikely that such a high value would be observed for a process in which diffusion was important, and this is confirmed by the higher orders obtained for the kinetics of the process.

In the present work, the dissolution of barium sulphate seed crystals into subsaturated solutions at 25°C., and into water at 15° - 45°C. has been studied conductimetrically. An independent study of the dissolution into water has also been made at 15° - 35°C., using a radioactive tracer technique. Barium sulphate seed crystals labelled with ^{35}sulphate were allowed to dissolve in water, and the rate of the reaction was followed by measuring the increase in activity of the solution with time. A similar method has been employed by Jones (128), who found first order kinetics for the dissolution of a silver-silver chloride electrode into water.

Dissolution of barium sulphate into water and subsaturated solution has been found to follow a second order rate law, which suggests that for this sparingly soluble salt, as for lead sulphate, diffusion is less important than some chemical reaction at the crystal-solution interface.

EXPERIMENTAL.

1. Conductimetric Studies.

Preparation of Seed Crystals.

The seed crystals used were prepared by the method described on page 102. Suspension B contained crystals of average size 5μ. The weight of crystals added to each experiment was determined by filtration of the final cell solution as described previously.

Procedure.

Dissolution into water was studied at 15°, 25°, 35°, and 45°C., and into subsaturated solutions at 25°C. The cell was filled with a known weight of conductivity water, and once carbon dioxide and temperature equilibrium had been attained, carbon dioxide free seed suspensions were added. Subsaturated solutions were prepared in situ as described in Part 2a, and the change in conductivity with time after inoculation with seed crystals was followed.

2. Radiochemical Studies.

Isotopic Tracers.

The isotope used in this study was ^{35}Sulphur, which is supplied by the Radiochemical centre as $Na_2{}^{35}SO_4$ in aqueous solution. It is

a weak β-emitter, of energy 0.167 MeV., with a half life of 87.1 days.

Preliminary experiments were also made using ^{133}barium, which emits weak γ-rays (0.36 MeV.) and has a half life of 7.5 years. With the counting techniques available, however, the barium isotope gave no improvement in statistics over the sulphur one, and its use was discontinued.

Counting Technique.

A thin end-window Geiger-Muller counter, type EHM 2/S, with window thickness 1.7-2.1 mg./cm^2, and operating voltage 1500 volts was used in conjunction with an Ekco Electronics probe unit type N558B, and an Ekco scalar, type N 529B. The counter was mounted in a lead castle type 1065D, with 4 cm. thick walls, and the resulting background count was never in excess of nine counts per minute.

Preparation of Labelled Seed Crystals.

5 mC. of $Na_2{}^{35}SO_4$ were added to the sulphuric acid used in the precipitation of the crystals, which were then prepared as described on page 102. The crystals were washed thoroughly and set aside to age as before. Seed suspension D consisted of regular rhombohedra, of average size 10μ.

Experimental Technique.

The cell used in these experiments was a 500 ml. three-necked round-bottomed Quickfit flask, and rotary stirring was supplied by a Citenco motor. An efficient water thermostat, the temperature of which was controlled to ± 0.1°C., was used.

Samples of solution to be counted were withdrawn by suction through a Number 4 sinter, thus ensuring that the seed crystals remained in the cell (Fig. 28). Approximately 0.5 ml. samples were then removed with a graduated pipette, transferred to a nickel-plated mild steel planchet (2.2 cm. diameter, 1 mm. deep) and weighed. Due to the low energy of the β radiation, it was not possible to count the solution, since self-absorption was appreciable. Hence, two drops of ethanol (129) were added to each sample, which was then allowed to evaporate to dryness under a radiant lamp. The addition of ethanol assisted the even evaporation of the samples, and the planchets were thoroughly cleaned before use by boiling in detergent. The maximum amount of solid per planchet was about 5×10^{-6} g., and reproducibility to ± 1.5% was obtainable using this technique (over 10,000 counts).

A typical experiment involved filling the cell with about 450 ml. of conductivity water, and allowing it to come to temperature equilibrium in the thermostat. Four ml. of seed suspension was then added using a rapid delivery pipette, and samples of solution were

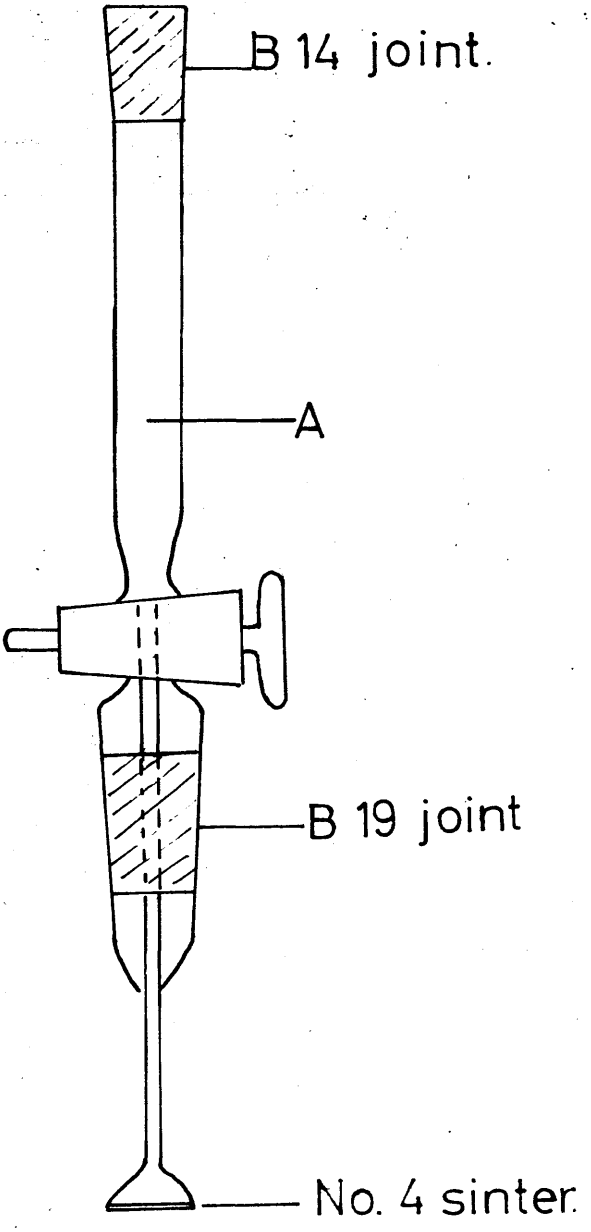

Figure 28.

withdrawn at frequent time intervals, weighed, evaporated to dryness and counted. Solution remaining in A (Fig. 28) after removal of the sample was blown back into the cell. Counting was generally continued until 10,000 counts had been registered - this usually took about 30 minutes at the start of an experiment. The volume of cell solution was not depleted by more than 1.5% in any experiment.

RESULTS.

The experiments described in this section were made to investigate the kinetics of dissolution of barium sulphate at various temperatures, and to determine whether there is a change of reaction order such as that observed by Davies and Nancollas (38). Distilled water only was used in the experiments with barium sulphate.

1. Conductimetric Studies.

Since there was a considerable concentration change in dissolution experiments into water, it was not possible to consider Δ constant, as in the crystallisation experiments. Values of Δ were therefore evaluated for each concentration using the appropriate Onsager equations.

Dissolution Experiments at 15°, 25°, 35°, and 45°C.

The results are summarised in Table 36 and some typical time plots of 1/R at 15°, 25°, 35°, and 45°C. are shown in Fig. 29, the corresponding data being given in Tables 37 - 40. To obtain the order of the dissolution reaction, log dm/dt was plotted against log (m_o-m), and this was found to consist of two intersecting straight lines, gradients n_1 and n_2, the value of n_2 being two. These plots are shown in Fig. 30. Thus, the equation

$$\frac{dm}{dt} = k_d\, s\, (m_o - m)^2$$

holds after an initial dissolution surge, and plots of dm/dt against $(m_o - m)^2$ are given in Fig. 31.

Dissolution into solutions of 30%, 60% and 90% subsaturation was also found to follow a second order rate law, and the results are given in Fig. 32, and Table 41.

2. Radiochemical Studies.

The results are summarised in Table 42, and plots of count rate against time are shown in Fig. 33. The initial count rate was obtained by applying a short extrapolation to zero time, and background corrections were made. All counts were then converted

to counts per minute per gram of solution, and the statistical accuracy expressed in terms of the standard deviation, given by $\sqrt{N}$, where N is the total number of counts.

All dissolution experiments were allowed to go to equilibrium, and the final count rate was determined and corrected for decay. The final concentration was measured conductimetrically, and was found to be close to the solubility value of barium sulphate. Independent conductimetric determinations, in which carbon dioxide was rigorously excluded from the cell led to the same solubility value. Since the count rates of these final solutions were known, intermediate count rates during a run could be converted to molar concentrations.

The kinetics of dissolution were found to obey a second order rate law,

$$\frac{dm}{dt} = k_d \, s \, (m_o - m)^2$$

and dm/dt is plotted against $(m_o - m)^2$ in Fig. 34, from data presented in Tables 43 - 45.

TABLE. 36.

Dissolution of Barium Sulphate.

Experiment Number	Temperature (°C.)	$m_i \times 10^5$ moles/l.	Seed Suspension	Seed Conc. (mg/ml.)	$k_{d_2} \times 10^{-2}$ moles^2/l.^{2}/min.
16	15	-	B	0.037	2.95
17	15	-	B	0.035	2.75
20	25	-	B	0.017	5.25
22	25	-	B	0.016	5.20
37	35	-	B	0.026	7.50
26	45	-	B	0.066	17.50
28	45	-	B	0.032	12.50
34	25	0.8567	B	0.094	2.90
35	25	0.6476	B	0.086	18.00
36	25	0.3263	B	0.065	20.00

TABLE. 37.

Dissolution of Barium Sulphate at 15°C.

Time	10^4 / R ohms^{-1}	10^5 m moles/l.	10^5 (m_o-m) moles/l.	10^{10} (m_o-m)^2 moles^2/l.^{2}	dm/dt x 10^8
Run 16. Cell E.					
0 min.	0.12353	-	0.9036	-	-
3	0.13116	0.0242	0.8794	0.7733	4.78
15	0.14580	0.0711	0.8325	0.6931	2.68
30	0.15552	0.1022	0.8014	0.6422	2.36
1 hr.	0.17121	0.1525	0.7511	0.5642	1.77
3	0.22363	0.3210	0.5826	0.3394	1.08
4	0.24159	0.3789	0.5247	0.2753	0.92
6	0.26909	0.4676	0.4360	0.1901	0.65
28	0.32072	0.6346	0.2690	0.0724	-
Run 17. Cell E.					
0 min.	0.06164	-	0.9036	-	-
3	0.06809	0.0206	0.8830	0.7797	4.06
15	0.08166	0.0639	0.8397	0.7051	2.52
30	0.09146	0.0883	0.8153	0.6647	1.83
1 hr.	0.10379	0.1347	0.7689	0.5912	1.45
3.5	0.15250	0.2912	0.6124	0.3750	0.86
5	0.17286	0.3568	0.5468	0.2990	0.62
7	0.19482	0.4276	0.4760	0.2266	0.43
24.5	0.26856	0.6661	0.2375	0.0564	-

TABLE. 36.

Dissolution of Barium Sulphate at 25°C.

Time	10^4 / R ohms^{-1}	10^5 m moles/l.	10^5 (m_o-m) moles/l.	10^{10} (m_o-m)^2 moles^2/l^2	dm/dt x 10^8
Run 20.					
0 min.	0.11269	-	1.0246	-	-
3	0.12753	0.0379	0.9861	0.9724	9.36
15	0.16369	0.1305	0.8935	0.7983	5.20
30	0.18665	0.1895	0.8345	0.6964	4.28
1 hr.	0.22042	0.2764	0.7476	0.5589	2.91
3.5	0.32233	0.5400	0.4840	0.2343	1.24
7	0.38838	0.7109	0.3131	0.0980	0.62
11	0.42667	0.8104	0.2136	0.0456	0.30
30.25	0.47842	0.9450	0.0790	0.0062	-
Run 22.					
0 min.	0.05912	-	1.0246	-	-
3	0.07388	0.0377	0.9863	0.9728	6.96
15	0.10401	0.1148	0.9092	0.8266	4.35
30	0.12617	0.1717	0.8523	0.7264	3.63
1 hr.	0.15785	0.2532	0.7708	0.5941	2.89
2	0.20889	0.3849	0.6391	0.4084	1.71
5	0.30094	0.6231	0.4009	0.1607	0.99
7	0.33672	0.7159	0.3081	0.0949	0.76
24	0.38440	0.8397	0.1843	0.0340	-

Cell E.

TABLE. 39.

Dissolution of Barium Sulphate at 35°C.

Time	10^4 / R ohms^{-1}	10^5 m moles/l.	10^5 (m_o-m) moles/l.	10^{10} (m_o-m)^2 moles^2/l^2	dm/dt x 10^8
Run 37.					
0 min.	0.16850	-	1.1960	-	-
1.5	0.18857	0.0433	1.1527	1.3287	21.58
6	0.22512	0.1225	1.0735	1.1524	10.88
15	0.26291	0.2045	0.9915	0.9831	7.58
30	0.30360	0.2931	0.9029	0.8152	5.23
1 hr.	0.36353	0.4239	0.7721	0.5961	3.67
1.5	0.41202	0.5300	0.6660	0.4436	2.87
2.5	0.47597	0.6702	0.5258	0.2765	2.33
3	0.51840	0.7634	0.4326	0.1871	1.91
7	0.63112	1.1565	0.0395	0.0156	0.31

Cell E.

TABLE. 40.

Dissolution of Barium Sulphate.

Time	10^4 / R ohms^{-1}	10^5 m moles/l.	10^5 (m_o-m) moles/l.	10^{10} (m_o-m)^2 moles^2/l^2	dm/dt x 10^8
Run 26.					
0 min.	0.14531	-	1.3890	-	-
3	0.29040	0.2565	1.1325	1.2826	53.92
15	0.46376	0.5653	0.8237	0.6785	12.35
30	0.54081	0.7031	0.6859	0.4705	7.56
1 hr.	0.68991	0.9705	0.4185	0.1751	4.09
3.5	0.80466	1.1721	0.2169	0.0470	1.16
7.5	0.87320	1.3004	0.0886	0.0078	0.30
24	0.91937	1.3838	0.0052	0.0003	-
Run 28.					
0 min.	0.14402	-	1.3890	-	-
3	0.23507	0.1607	1.2283	1.5087	39.13
15	0.38326	0.4241	0.9649	0.9310	11.78
30	0.45830	0.5579	0.8311	0.6907	7.37
1 hr.	0.56034	0.7403	0.6487	0.4208	4.85
4	0.78202	1.1384	0.2506	0.0628	1.10
7.5	0.84539	1.2526	0.1364	0.0186	0.33
24.75	0.89904	1.3493	0.0397	0.0016	-

Cell. E.

TABLE. 41.

Dissolution of Barium Sulphate into Subsaturated Solution.

Time	10^4 / R ohms^{-1}	10^5 m moles/l.	10^5 (m_o-m) moles/l.	10^{10} (m_o-m)^2 moles^2/l^2	dm/dt x 10^8
Run 36. 90% Subsaturated.					
0 min.	0.28570	0.3263	0.6977	-	-
1.5	0.29936	0.3616	0.6624	0.4388	14.90
6	0.32639	0.4315	0.5925	0.3511	8.56
15	0.35517	0.5057	0.5183	0.2686	5.47
30	0.37815	0.5650	0.4590	0.2107	4.41
1 hr.	0.41610	0.6630	0.3610	0.1303	2.72
3.5	0.49825	0.8751	0.1489	0.0222	0.37
5	0.51080	0.9075	0.1165	0.0136	0.30
6	0.51840	0.9272	0.0968	0.0094	0.21
Run 35. 60% Subsaturated.					
0 min.	0.54590	0.6474	0.3766	-	-
3	0.56461	0.6959	0.3281	0.1076	8.06
9	0.57518	0.7232	0.3008	0.0905	2.15
15	0.58084	0.7378	0.2862	0.0819	1.51
30	0.59020	0.7620	0.2620	0.0686	1.14
1 hr.	0.60099	0.7898	0.2342	0.0548	0.95
2.5	0.62490	0.8516	0.1724	0.0297	0.55
4.5	0.64435	0.9018	0.1222	0.0149	0.21

Cell E.

TABLE. 41 (cont.)

Time	$10^4 / R$ ohms^{-1}	10^5 m moles/l.	$10^5 (m_o-m)$ moles/l.	$10^{11} (m_o-m)^2$ moles^2/l^2	dm/dt x 10^9
Run 34.	30% Subsaturation.				
0 min.	0.69090	0.8567	0.1673	-	-
1.5	0.69281	0.8616	0.1624	0.2638	16.01
6	0.69644	0.8710	0.1530	0.2341	8.69
15	0.70045	0.8814	0.1426	0.2033	6.15
30	0.70300	0.8879	0.1361	0.1852	4.65
1 hr.	0.70850	0.9022	0.1218	0.1484	4.39
2	0.71660	0.9231	0.1009	0.1018	2.97
4	0.72735	0.9508	0.0732	0.0536	1.89
6	0.73481	0.9701	0.0539	0.0291	0.56

Cell E.

$$\% \text{ Subsaturation} = \frac{\text{Solubility product} - \text{initial conc. product}}{\text{Solubility Product}}$$

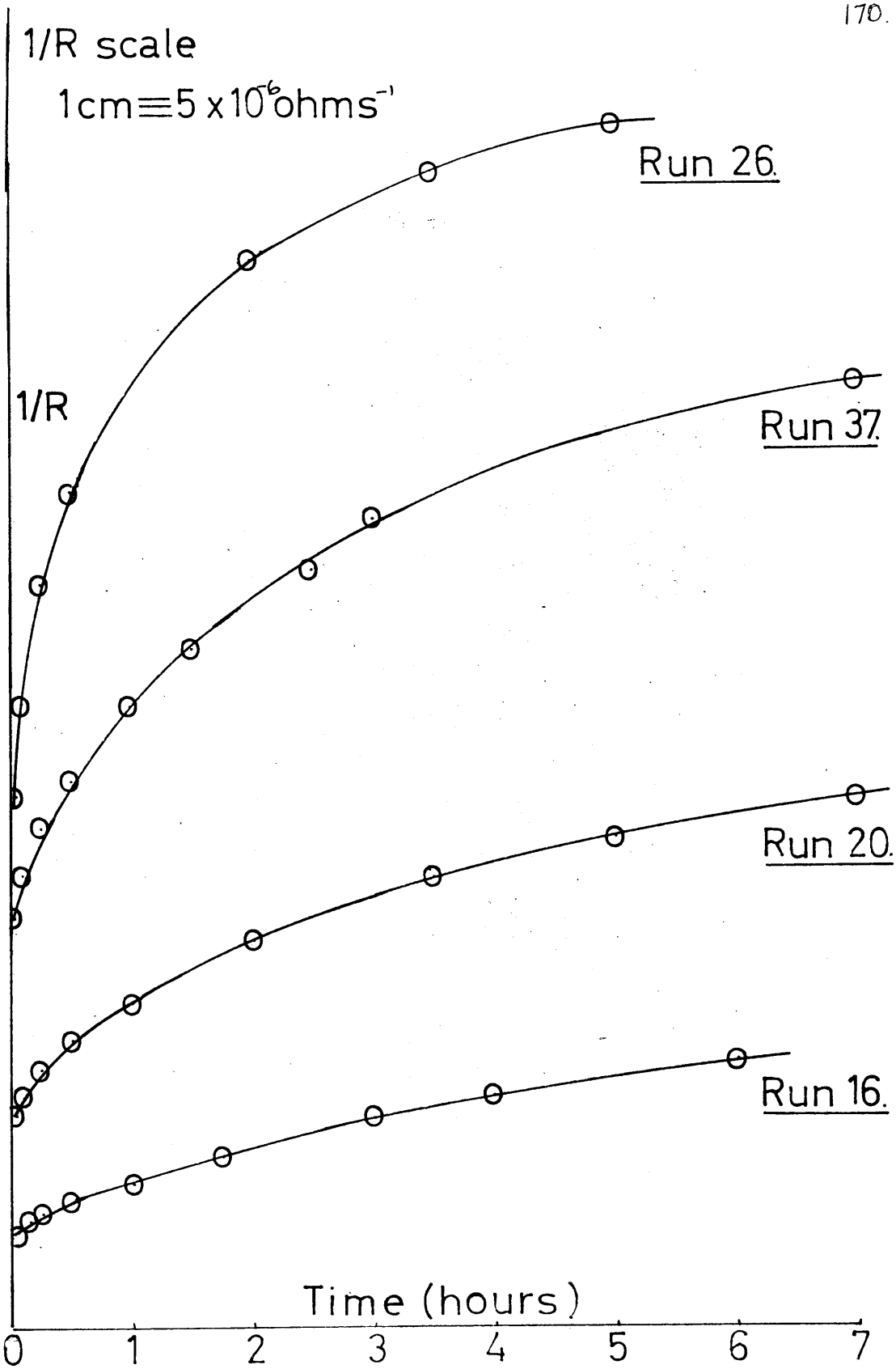
1/R scale
1cm≡5 x 10⁻⁶ ohms⁻¹
1/R
Run 26.
Run 37.
Run 20.
Run 16.
Time (hours)
0
1
2
3
4
5
6
7

Figure 29.

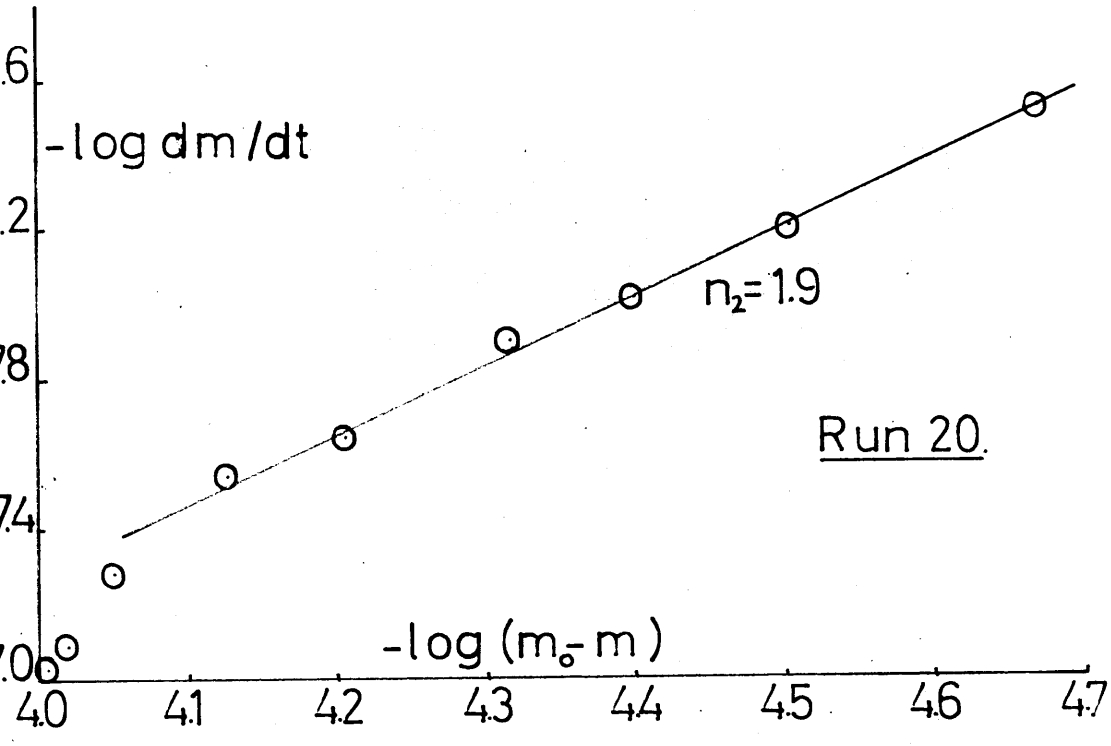
-log dm/dt
n_2=1.9
Run 20.
-log (m_o-m)
4.0
4.1
4.2
4.3
4.4
4.5
4.6
4.7

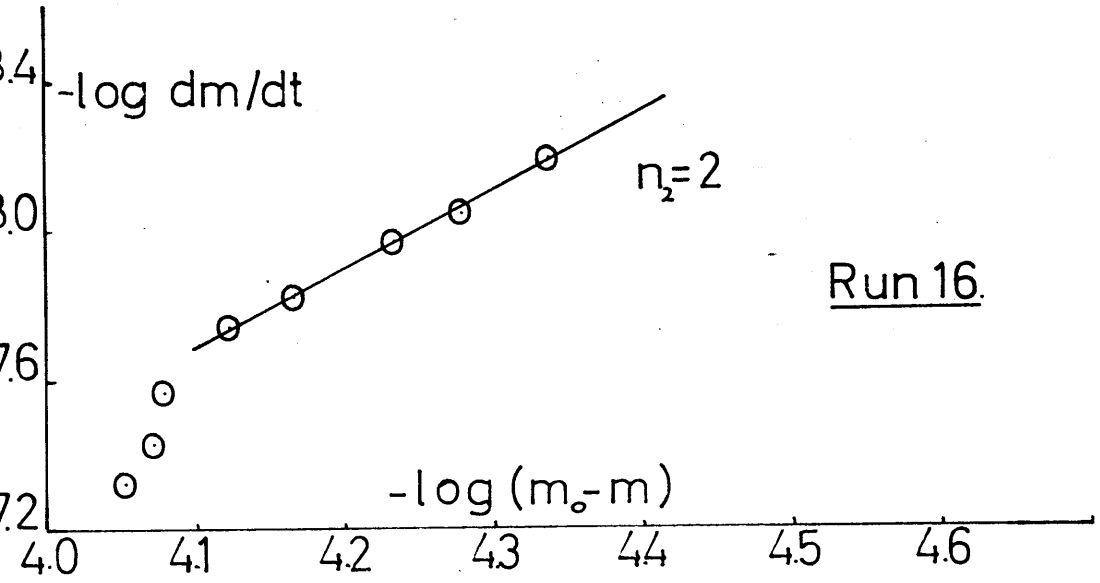
-log dm/dt
n_2=2
Run 16.
-log (m_o-m)
4.0
4.1
4.2
4.3
4.4
4.5
4.6

Figure 30.

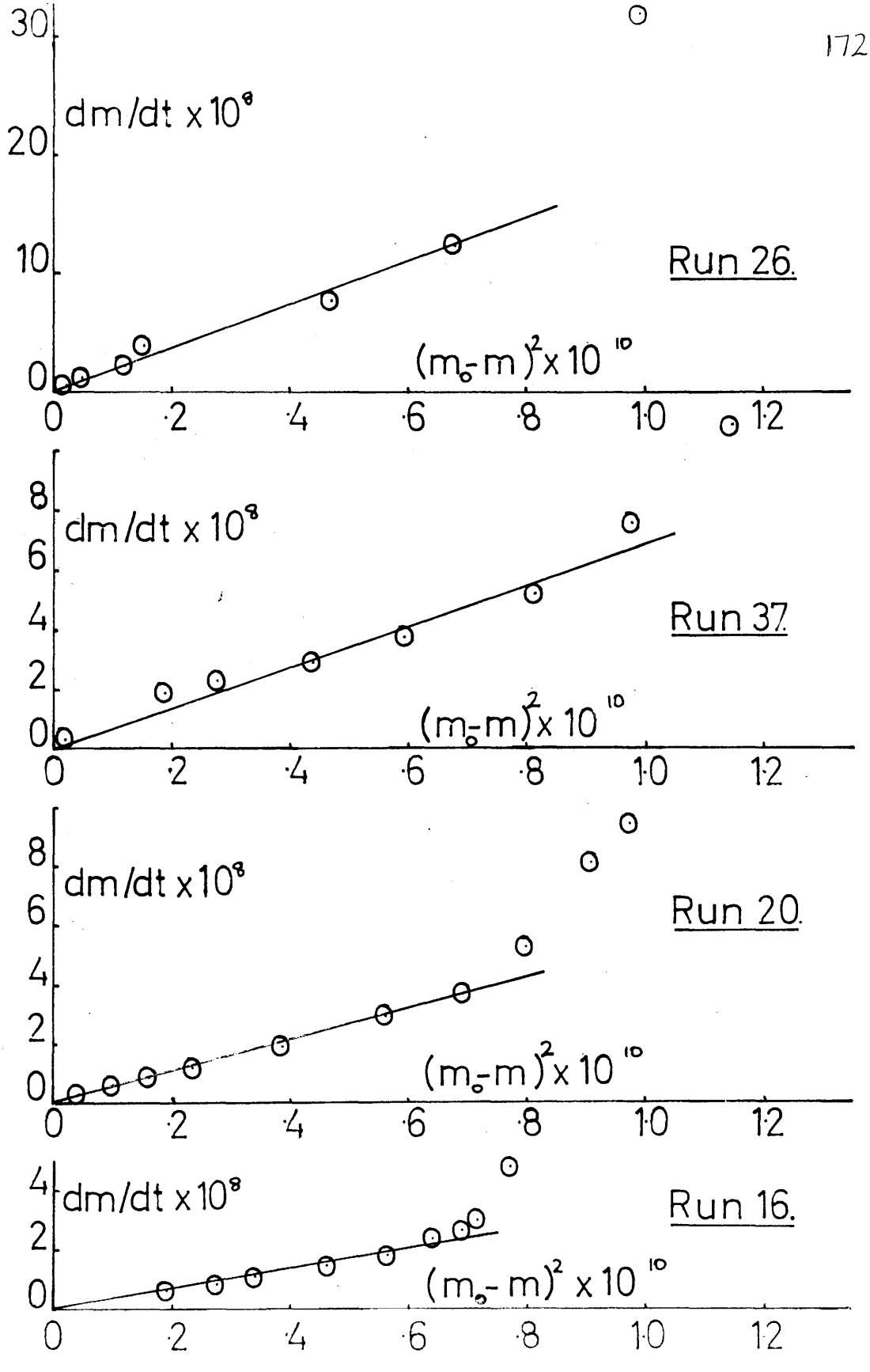
dm/dt x 10⁸
30
20
10
0
Run 26.
(m₀-m)² x 10¹⁰
0
·2
·4
·6
·8
1·0
1·2
dm/dt x 10⁸
8
6
4
2
0
Run 37.
(m₀-m)² x 10¹⁰
dm/dt x 10⁸
Run 20.
(m₀-m)² x 10¹⁰
dm/dt x 10⁸
4
2
0
Run 16.
(m₀-m)² x 10¹⁰

Figure 31.

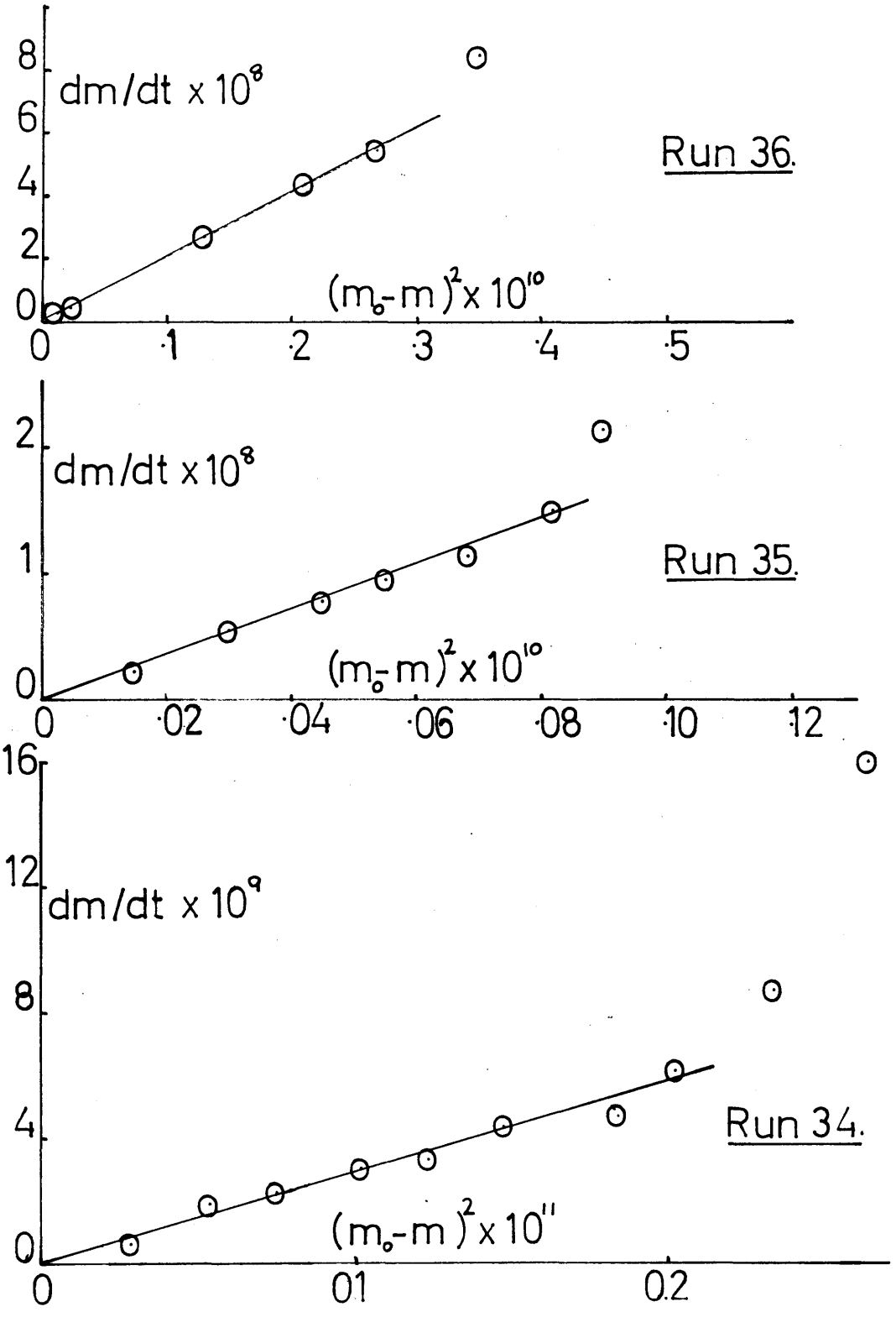
8
6
4
2
0
dm/dt x 10^8
Run 36.
(m_o-m)^2 x 10^10
0
·1
·2
·3
·4
·5
2
1
0
dm/dt x 10^8
Run 35.
(m_o-m)^2 x 10^10
0
·02
·04
·06
·08
·10
·12
16
12
8
4
0
dm/dt x 10^9
Run 34.
(m_o-m)^2 x 10^11
0
01
0.2

Figure 32.

TABLE. 42.

Dissolution of Barium Sulphate into Water.

Radiochemical Study.

Experiment Number	Temperature (°C.)	Seed Suspension	k_d moles^2/l^2./min.
50	15	D	1100
42	25	D	1600
43	25	D	1400
45	35	D	4400

TABLE. 43.

Dissolution of Barium Sulphate at 15°C.

Time	Weight of Solution	c.p.m./gm.	10^5 m moles/l.	$10^{10}(m_o-m)^2$ moles^2/l^2.	dm/dt x 10^8
Run 50.					
15 min.	0.515	54.4 ± 2.8	0.082	0.675	8.04
30	0.505	129.5 ± 3.5	0.195	0.502	4.82
1 hr.	0.508	176.6 ± 4.0	0.266	0.407	3.34
2	0.508	290.6 ± 4.4	0.438	0.217	1.99
4.25	0.499	419.7 ± 5.7	0.632	0.074	0.87
5.5	0.501	443.9 ± 5.0	0.669	0.055	0.63
7.5	0.510	503.4 ± 6.1	0.758	0.021	0.42
10	0.511	519.0 ± 5.7	0.782	0.015	-
24.25	0.509	582.7 ± 6.3	0.878	0.007	-

TABLE. 44. Dissolution of Barium Sulphate at 25°C.

Time	Weight of Solution (gm.)	c.p.m./gm.	10^5 m moles/l.	10^{10} $(m_o-m)^2$ $moles^2/l^2$.	$dm/dt \times 10^8$
Run 42.					
2 min.	0.987	30.0 ± 1.6	0.025	0.998	16.23
15	0.989	217.5 ± 4.6	0.181	0.711	13.32
30	0.987	422.6 ± 5.8	0.352	0.452	6.70
1 hr.	0.986	618.5 ± 7.5	0.515	0.259	3.71
1.5	0.987	717.0 ± 3.3	0.597	0.182	2.46
4	0.986	924.9 ± 7.0	0.770	0.065	0.69
6	0.989	1010.5 ± 7.3	0.841	0.033	0.22
24	0.983	1200.1 ± 6.3	0.999	-	-
72	0.990	1230.0 ± 7.5	-	-	-
Run 43.					
1.5 min	0.512	90.0 ± 3.1	0.099	0.856	13.59
15	0.513	218.9 ± 5.5	0.218	0.650	8.45
30	0.509	346.4 ± 6.7	0.344	0.462	5.47
1 hr.	0.513	464.8 ± 7.4	0.462	0.316	3.43
2	0.514	576.2 ± 8.2	0.573	0.204	1.67
3	0.506	672.8 ± 5.5	0.669	0.126	1.07
6	0.510	838.0 ± 9.6	0.833	0.036	0.68
7.5	0.502	875.2 ±10.4	0.870	0.024	0.61
12	0.517	1000.2 ±19.9	0.994	0.009	0.20
26	0.510	1017.4 ± 9.9	1.012	0.002	..

TABLE. 45.

Dissolution of Barium Sulphate at 35°C.

Time	Weight of Solution (gm.)	c.p.m./gm.	10^5 m moles/l.	10^{10} $(m_o-m)^2$ $moles^2/l^2$	dm/dt x 10^8
Run 45.					
1.5 min.	0.507	298.7 ± 5.4	0.317	0.773	33.22
15	0.507	568.5 ± 7.1	0.603	0.551	23.80
30	0.506	748.2 ± 9.0	0.794	0.162	7.69
1 hr.	0.511	927.2 ±10.5	0.984	0.045	3.35
2	0.510	1003.1 ± 8.7	1.064	0.017	0.92
3	0.509	1054.4 ±11.8	1.119	0.006	0.44
5	0.505	1096.6 ± 9.8	1.164	0.001	0.19
28.25	0.513	1100.5 ±12.3	1.168	-	-
72	0.509	1127.0 ± 9.9	1.196	-	-

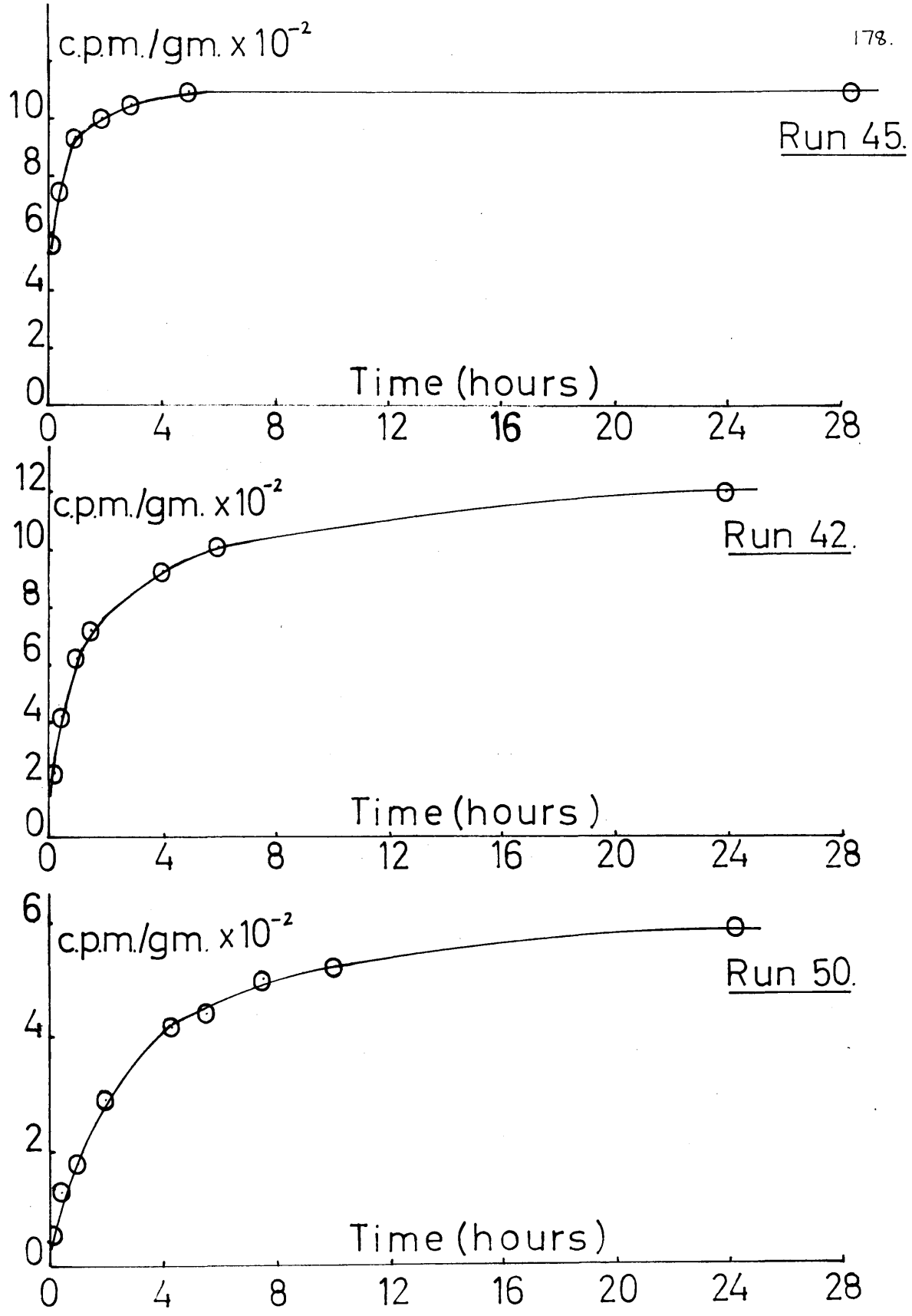
c.p.m./gm. x 10⁻²
Run 45.
Time (hours)
0 4 8 12 16 20 24 28
0 2 4 6 8 10
c.p.m./gm. x 10⁻²
Run 42.
Time (hours)
0 4 8 12 16 20 24 28
0 2 4 6 8 10 12
c.p.m./gm. x 10⁻²
Run 50.
Time (hours)
0 4 8 12 16 20 24 28
0 2 4 6

Figure 33.

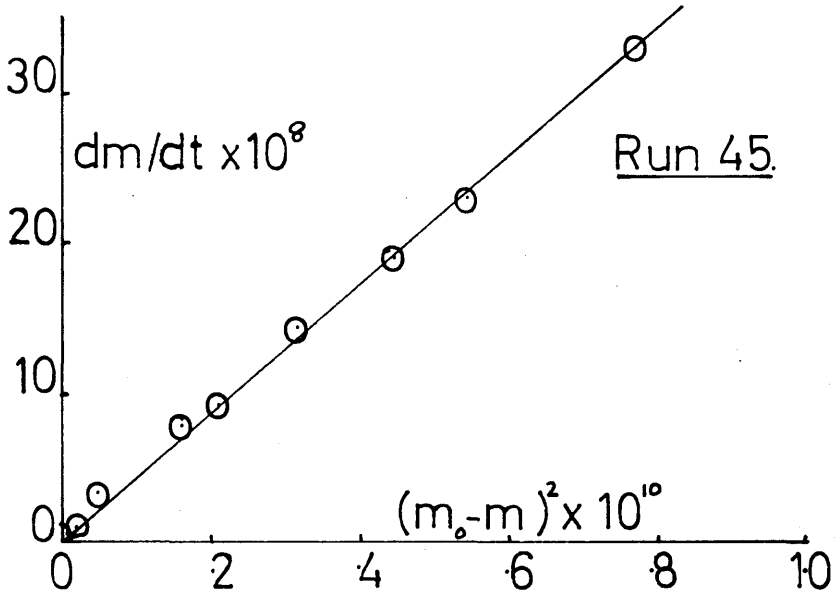
30
20
10
0
dm/dt x10⁸
Run 45.
(m₀-m)²x 10¹⁰
0
·2
·4
·6
·8
1·0

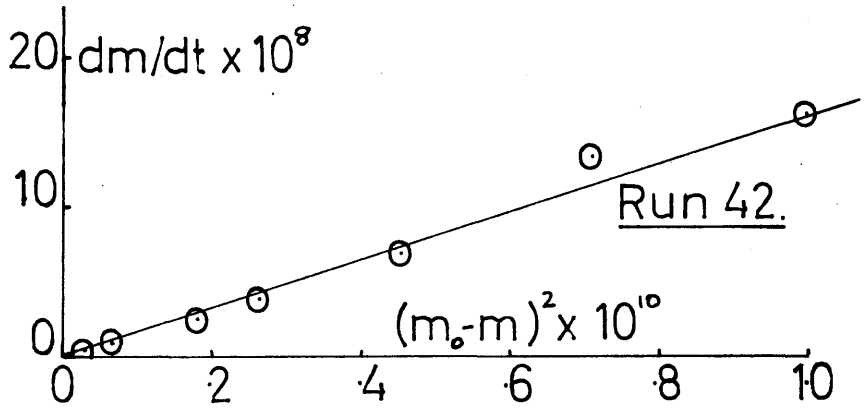
20
10
0
dm/dt x 10⁸
Run 42.
(m₀-m)²x 10¹⁰
0
·2
·4
·6
·8
1·0

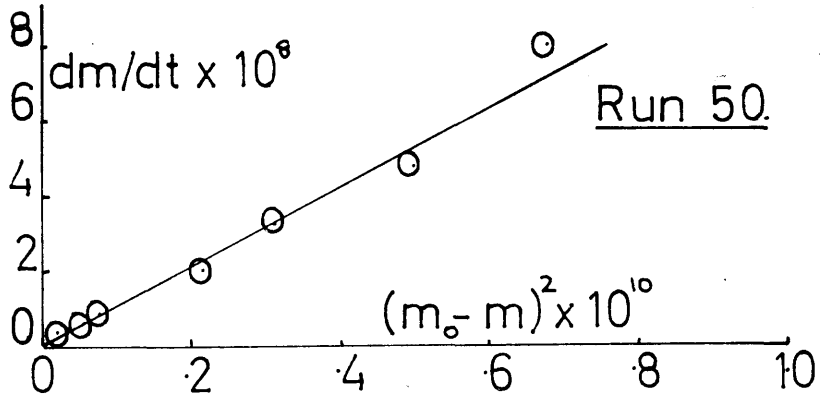
8
6
4
2
0
dm/dt x 10⁸
Run 50.
(m₀- m)²x 10¹⁰
0
·2
·4
·6
·8
1·0

Figure 34.

DISCUSSION.

After a short initial fast part, the dissolution of both lead sulphate and barium sulphate into subsaturated solutions at 25°C. has been found to follow a second order rate law,

$$\frac{dm}{dt} = k_d \, s \, (m_o - m)^2 \, .$$

This was also observed for barium sulphate dissolution into water at temperatures between 15° and 45°C. Under similar experimental conditions, Howard, Nancollas and Purdie (113) found first order kinetics for the dissolution of both silver chloride and silver chromate into subsaturated solutions, while Davies and Nancollas (38) showed that the dissolution of silver chloride into water was proportional to (subsaturation)$^{3/2}$. Jones mentioned (128) that lead sulphate dissolution followed a second order rate law, but did not state whether this was into water or subsaturated solution. It would seem , therefore, that the solution of sparingly soluble salts is not always a straightforward diffusion-controlled process, and that for some 2:2 electrolytes some other step, possibly occurring at the crystal surface, is rate determining.

Dissolution must involve the following simple steps:

1) Removal of a pair of ions from the crystal lattice
2) Separation of the ions
3) Hydration of the ions
4) Diffusion away from the surface.

If 1, 2, and 3 are sufficiently rapid, the rate controlling mechanism will be one of diffusion of ions away from the surface (4), and dissolution will follow a first order rate law, as has been found for silver chloride. The slow step could, however, involve the removal of a pair of positive and negative ions from the crystal lattice, and their separation against mutual attraction, and subsequent hydration - i.e., steps 1, 2 and 3. In this case we might expect a kinetic order greater than unity. It is interesting that second order kinetics have been observed for the dissolution of 2:2 electrolytes, since electrostatic forces of attraction between the ions in the crystal lattices, and between the ions themselves will be much stronger than for a 1:1 salt. The work required to separate the ions will therefore be greater than for a 1:1 salt, and this is reflected in the differences in lattice energy.

The lattice energy of barium sulphate was estimated by the method of Kapustinskii (130), using the expression

$$U = 287.2 \sum n \frac{z_1 z_2}{r_c + r_a} \left(1 - \frac{0.345}{r_c + r_a} \right),$$

where U is the lattice energy, z_1 and z_2 are the ionic charges, r_c and r_a are radius of cation and anion respectively, and $\sum n$ is the number of ions in the molecule. The lattice energy was found to be approximately 540 K.Cals., and the value for lead sulphate will be similar. This can be compared with 207 K.Cals.

for silver chloride.

The lower lattice energy associated with the 1:1 electrolyte will mean that less energy is required to remove the ions from the crystal, and since a first order rate equation was usually followed, the subsequent diffusion of hydrated ions away from the surface must be slower than the separation of ions from the crystal lattice. For 2:2 electrolytes the reaction at the surface may be slower than the rate of diffusion, resulting in the observed second order kinetics. In support of this, the rate of solution of barium sulphate was much less than that of silver chloride, although the two salts have similar solubilities.

Unfortunately, the heat of hydration of the sulphate ion has not been reported in the literature, and so it is not useful to attempt a comparison of the relative heats of hydration of 1:1 and 2:2 salts. It is interesting to note, however, that the values (131) for Pb^{2+} and Ba^{2+} (168 and 210 K.Cals.) are not much greater than Ag^{+} (147 K.Cals.), Cl^{-} being 89 K.Cals.

The rate of dissolution of barium sulphate seed crystals was found to be greater when followed by the radiochemical technique, as can be seen from Tables 36 and 42. There are two possible explanations for this, firstly the different fluid dynamics in operation in the two techniques, due to changes in the shape of the cells and the method of stirring. Secondly, the

greater efficiency of stirring by the rotary method, in comparison with the vibratory stirring, necessarily used in the conductivity experiments (113). With the large weights of seed crystals used in these experiments, a fair proportion may have been resting on the bottom of the cell, causing a reduction in the effective surface area available.

The lack of correlation in barium sulphate crystallisation experiments (Table 25) between the weight of seed crystals supplied and the resulting rate constant could also be explained if a proportion of these crystals was inactive at the bottom of the cell, instead of participating fully in the growth process. Previous studies (132) have shown a direct relationship to hold between rate constant and surface area of seeds used for inoculation. Because of the initial fast start of varying extent in both lead sulphate and barium sulphate dissolution experiments, it is not worthwhile to compare the subsequent rate constants with the weight of seed crystals used.

The initial dissolution surge may be due to rapid solution occurring at sites of high localised energy, such as the centres of dislocations, which, in the case of a divalent salt, will carry a fairly high charge. This would result in rapid dissolution from inner regions of the crystal, rather than uniform dissolution over the crystal surface, and would cease when the energy at the centre

became equal to that at the edge of the dislocation at the surface. Dissolution would then proceed by the second order mechanism, the removal of ions from the lattice being the slow step. The method of preparation of the seed crystals of lead sulphate and barium sulphate, by precipitation rather than the slow recrystallisation method used for silver chloride, will favour the formation of many dislocations.

Although this initial surge was observed without exception in the conductivity experiments, it was not found in the radiochemical study. It is possible that the sampling technique used in the tracer experiments was not sufficiently accurate, and that the surge was in fact present, although undetected, since its duration was rarely more than 15 minutes. The initial part of the radiochemical experiments was usually the least accurate, since the length of time required to remove a sample for counting was such that a maximum of three readings was possible in the first 15 minutes. Also, the count rate was lower at the start of a run, and the time taken to remove a sample, which could be as much as half a minute, had the greatest effect on the accuracy. Adsorption of activity on the walls of the sinter tube into which the solution was drawn, and on the pipette with which the sample was removed, would also have the greatest effect during the early stages of the experiment. With so many possible sources of error in the initial points, therefore,

little significance can be attached to the apparent lack of an initial surge in the tracer experiments.

When the logarithms of the rate constants at the three temperatures studied were plotted against the reciprocal of the temperature in degrees Absolute, the slope of the line corresponded to an energy of activation of 12 K.Cals. /mole. Writing the solution process

$$Ba^{2+}SO_4^{2-}\,(s) \xrightarrow{E_s} Ba^{2+}SO_4^{2-}\,(aq.) \xrightarrow{-E_c} Ba^{2+}\,(aq.) + SO_4^{2-}\,(aq.)$$

where $Ba^{2+}SO_4^{2-}$ (aq.) represents the activated intermediate in the hydrated monolayer, the heat of solution, $\Delta H = E_s - E_c = 4$ K.Cals. In view of the uncertainties in the determination of E_c, and particularly in the radiochemical calculation of E_s, this agrees fairly well with the heat of solution of 5 K.Cals./mole calculated from the solubility of barium sulphate at various temperatures.

The rate of dissolution of lead sulphate crystals was greatly retarded in the presence of tetrametaphosphate ions. A concentration of 7×10^{-8} moles/l. was sufficient to cause a small reduction in the rate of solution, and this is comparable with the concentration required to produce a similar effect in growth experiments. Slow rates of dissolution could just be detected at adsorbate concentrations as high as 5×10^{-5} moles/l., and this contrasts with crystallisation, which was stopped by a concentration of 7×10^{-7} moles/l. These

observations are similar to those of Marc (5) who studied the growth and dissolution of potassium chlorate crystals and found that the dye Ponceau 2R had a much greater effect on crystallisation than solution.

The adsorption of tetrametaphosphate ions on a crystal surface has been discussed on page 119. Assuming a monomolecular layer of adsorbate molecules, the effective area which they would cover in Run 130 is 300 times greater than the available crystal surface area, which illustrates the inefficiency of such impurities for inhibiting dissolution. The presence of the adsorbate also led to an increase in the values of n, an effect which was observed with both distilled and deionised water, although more pronounced with the latter. This can be seen from Table 31.

Gilman, Johnston and Sears (79) have postulated that dissolution of a perfect crystal surface in a solvent begins by the creation of unit pits, one molecule deep, and that these pits grow as steps retreat across the surface by the action of kinks. On a real crystal dislocations are likely to be preferential sites for the initiation of such unit pits, and it may be assumed that dissolution proceeds from these sites of localised high energy on the crystal faces. The energy of the dislocation will, however, be lowered by the presence of impurity molecules, since these will adsorb at the active sites. Thus, the rate of formation of unit

pits, and hence the rate of solution, will be reduced.

Gilman, Johnston and Sears, who made a photomicroscopic study of etch pit formation in lithium fluoride crystals, observed the rate of solution to be reduced by a factor of 10 in the presence of ferric ions. They found that the etch pits became deeper as the concentration of impurity was increased, because the poison retarded the movement of monomolecular steps so that dissolution proceeded more rapidly into the crystal than over its surface.

In the lead sulphate experiments it is probable that the tetrametaphosphate ions lowered the energy at the dislocations, causing a decrease in the rate of solution. When a large concentration of impurity is present, it seems reasonable to assume that the energy of the dislocation will be reduced to such an extent that it is the same as, or even less than, the remainder of the crystal surface. In such a situation, with adsorbate ions occupying active sites on the surface, there will be no preferential sites for the creation of unit pits, and the rate of dissolution will be greatly reduced. Unit pits would have to be initiated in energetically unfavourable conditions, and this will proceed slowly all over the surface, causing the observed increase in the value of n. Even when a pit is formed, it is likely to be quickly covered by impurity molecules which will inhibit any further dissolution. The presence of organic contaminant from deionised water would enhance

this effect, leading to the larger n values for experiments in which this water was used. These can be seen from Table 31.

The presence of tetrametaphosphate ions only had a small effect on the duration of the initial surge, and this may be due to the size of the ions preventing them from entering the dislocation centres. Thus, the initial surge was able to take place, but once the energy differences were equalised, the rate of the subsequent second order dissolution was greatly reduced by the presence of the additive.

In two interesting papers Spitsyn and his co-workers (133,134) stated that the solubility in water of barium sulphate crystals labelled with radioactive tracers changed with the specific activity of the salt. Using ^{35} sulphur, they observed a maximum solubility at an activity of 2 mC./gm. of barium sulphate, although this maximum was less pronounced when sulphuric acid was used in the precipitation instead of sodium sulphate. Ramette and Anderson (135) attempted to reproduce these results and found a constant solubility for barium sulphate at activities of 5, 20, and 50 mC./gm sulphur, corresponding to 0.75, 3.0, and 7.5 mC./gm barium sulphate. In the present work, the specific activity was approximately 1mC./gm. barium sulphate, and although sulphuric acid was used in the preparation of the crystals, no variation in solubility was observed. This is in agreement with the results of Ramette and Anderson.

BIBLIOGRAPHY.

(1). VAN HOOK, "Crystallisation, in Theory and Practice", Reinhold Publ. Corp., 1961.

(2). OSTWALD, Z. Physik. Chem., 1897, 22, 289.
ibid., 1897, 23, 365.
ibid., 1900, 24, 444.

(3). FISCHER, Anal. Chim. Acta, 1960, 22, 501.

(4). MARC, Z. Physik. Chem., 1908, 61, 385

(5). MARC, Z. Physik. Chem., 1909, 67, 470.

(6). LEBLANC & SCHMANDT, Z. Physik. Chem., 1911, 77, 614

(7). DAVIES & JONES, Trans. Far. Soc., 1955, 51, 812.

(8). BIRCUMSHAW & RIDDIFORD, Quart. Rev., 1952, 6, 157.

(9). TURNBULL, Acta. Met., 1953, 1, 684.

(10). DOREMUS, J. Amer. Chem. Soc., 1958, 80, 1068.

(11). O'ROURKE & JOHNSON, Anal. Chem., 1955, 27, 1699.

(12). COLLINS & LEINEWEBER, J. Phys. Chem., 1956, 60, 389.

(13). BECKER & DORING, Ann. Physik., 1935, 24, 719.

(14). GIBBS, "Collected Works", Longmans, London, 1928.

(15). VOLMER & SCHULTZE, Z. Phys. Chem., 1931, 156A, 1.

(16). FRANK, Disc. Far. Soc., 1949, 5, 48.

(17). BURTON, CABRERA & FRANK, Phil. Trans. Roy. Soc., 1951, A243, 299.

(18). FRANK, Advanc. Phys., 1952, 1, 91.

(19). CABRERA & VERMILYEA, "Growth and Perfection of Crystals", ed. Doremus, Roberts and Turnbull, p. 393

(20). ALBON, Phil. Mag., 1963, 8, 1335.

(21). NEWKIRK, Acta. Met., 1955, 3, 121.

(22). NEWKIRK, Acta. Met., 1957, 5, 52.

(23). SEARS, J.Chem. Phys., 1958, 29, 979.

(24). SEARS, Acta. Met., 1955, 3, 361.

(25). REYNOLDS & GREENE, J. Appl. Phys., 1958, 29, 559.

(26). NIELSEN, Acta. Chem. Scand., 1959, 13, 784.

(27). SEARS, Acta. Met., 1953, 1, 457.

(28). SEARS, Acta. Met., 1955, 3, 367.

(29). CHRISTIANSEN, Acta Chem. Scand., 1954, 8, 909.

(30). COLLINS, Z. Elektrochem., 1955, 59, 404.

(31). VON WEIMARN, Chem. Rev., 1925, 2, 217.

(32). CHRISTIANSEN & NIELSEN, Acta Chem. Scand., 1951, 5, 673.

(33). KLEIN, GORDON & WALNUT, Talanta, 1959, 3, 187.

(34). DUKE & BROWN, J. Amer. Chem. Soc., 1954, 76, 1443.

(35). LA MER & DINEGAR, J. Amer. Chem. Soc., 1951, 73, 380.

(36). JOHNSON & O'ROURKE, J. Amer. Chem. Soc., 1954, 76, 2124.

(37). NIELSEN, Acta Chem. Scand., 1957, 11, 1512.

(38). DAVIES & NANCOLLAS, Trans. Far. Soc., 1955, 51, 818.

(39). DAVIES & NANCOLLAS, ibid, 1955, 51, 823.

(40). DAVIES, JONES & NANCOLLAS, ibid, 1955, 51, 1232.

(41). TING & McCABE, Ind. & Eng. Chem., 1934, 26, 1201.

(42). HOWARD & NANCOLLAS, Trans. Far. Soc., 1957, 53, 1449.

(43). NANCOLLAS & PURDIE, ibid, 1961, 57, 2272.

(44). CAMPBELL & NANCOLLAS, unpublished results.

(45). NANCOLLAS, Ph. D. Thesis, Wales, 1951.

(46). JONES & JOSEPH, J. Amer. Chem. Soc., 1928, 50, 1049.

(47). SHEDLOVSKY, J. Amer. Chem. Soc., 1930, 52, 1793.

(48). NAIR & NANCOLLAS, J. Chem. Soc., 1958, 4144.

(49). DAVIES & NANCOLLAS, Chem. & Ind., 1950, 7, 129.

(50). HARTLEY & BARRATT, J. Chem. Soc., 1913, 786.

(51). KOHLRAUSCH, "Textbook of Analytical Chemistry", Treadwell & Hall, 5th ed., New York, 1924.

(52). FRAZER & HARTLEY, Proc. Roy. Soc., 1925, A109, 351.

(53). SHEDLOVSKY, J. Amer. Chem. Soc., 1932, 35, 1411.

(54). DAVIES, Trans. Far. Soc., 1929, 25, 129.

(55). WALTON, J. Phys. Chem., 1963, 67, 1920.

(56). VAN HOOK, J. Amer. Chem. Soc., 1940, 44, 751.

(57). NANCOLLAS & PURDIE, Trans. Far. Soc., 1963, 59, 735.

(58). HAHNERT, Kolloid Z., 1959, 162, 36.

(59). KOLTHOFF & VAN'T RIET, J. Phys. Chem., 1959, 63, 817.

(60). KOLTHOFF & ROSENBLUM, J. Amer. Chem. Soc., 1935, 57, 2577.

(61). KOLTHOFF & VAN'T RIET, J. Phys. Chem., 1960, 64, 1045.

(62). KOLTHOFF & ROSENBLUM, J. Amer. Chem. Soc., 1936, 58, 121.

(63). KOLTHOFF & ROSENBLUM, J. Amer. Chem. Soc., 1933, 55, 2656.

(64). KOLTHOFF & ROSENBLUM, J. Amer. Chem. Soc., 1934, 56, 832.

(65). BUCKLEY, "Crystal Growth", Wiley, New York, 1951, p. 330.

(66). OTANI Bull. Chem. Soc. Japan, 1960, 33, 1543.

(67). MIURA, OTANI ET AL., Bull. Chem. Soc. Japan, 1963, 36, 1091.

(68). COLEMAN & SEARS, Acta Met., 1957, 5, 131.

(69). RIGTERINK & FRANCE, J. Phys. Chem., 1938, 42, 1079.

(70). REITEMEIR & BUEHRER, J. Phys. Chem., 1940, 44, 535.

(71). PACKTER, J. Phys. Chem., 1955, 59, 1140.

(72). MICHAELS & COLVILLE, J. Phys. Chem., 1960, 64, 13.

(73). MICHAELS & TAUSCH, J. Phys. Chem., 1961, 65, 1730.

(74). MIURA ET AL., J. Phys. Chem., 1962, 66, 252.

(75). RAISTRICK, Disc. Far. Soc., 1949, 5, 234.

(76) SEARS, J. Chem. Phys., 1956, 25, 154.

(77) SEARS, "Growth and Perfection of Crystals", ed. Roberts, Doremus and Turnbull, p. 441.

(78). SEARS, J. Chem. Phys., 1958, 29, 1045.

(79). GILMAN, JOHNSTON & SEARS, J. Appl. Phys., 1958, 29, 747.

(80). SEIDELL, "Solubilities of Inorganic and Metal Organic Compounds", 3rd edition, Vol. 1, New York.

(81). DAVIES, J. Chem. Soc., 1938, 2093.

(82). JENKINS & MONK, J. Amer Chem. Soc., 1950, 72, 2695.

(83). NAIR & NANCOLLAS, J. Chem. Soc., 1955, 1458.

(84). HARNED & OWEN, "Physical Chemistry of Electrolyte Solutions", Reinhold Publ. Corp., New York, 1943, p. 127.

(85). GODDARD, HARVA & JONES, Trans. Far. Soc., 1953, 49, 980.

(86). OTANI ET AL., Bull. Chem. Soc. Japan, 1959, 32, 68.

(87). SUITO & TAKIYAMA, Bull. Chem. Soc. Japan, 1954, 27, 123.

(88). FISCHER & REINEHAMMER, Anal. Chem., 1953, 25, 1544.

(89). WALTON & WALDEN, J. Amer. Chem. Soc., 1946, 68, 1742.

(90). DAWSON & McGAFFNEY, 4th International Conference on Electron Microscopy, Berlin, 1958.

(91). NEUMANN, J. Amer. Chem. Soc., 1933, 55, 879.

(92). NORBERG & CLEMENDSON, Arkiv. Kemi., Mineral Geol., 1942, A16,

(93). ROSSEINSKY, Trans. Far. Soc., 1958, 54, 116.

(94). ROBINSON & STOKES, "Electrolyte Solutions", Butterworth's Scientific Publications, 1955.

(95). HARNED & OWEN, "Physical Chemistry of Electrolyte Solutions", Reinhold Publ. Corp., 1943, p.127. (2nd ed.)

(96). GUNNING & GORDON, J. Chem. Phys., 1942, 10, 126.

(97). OTANI ET AL., Bull. Chem. Soc. Japan, 1962, 33, 1549.

(98). BUCHANAN & HEYMANN, J. Colloid Sci., 1949, 4, 137.

(99). BUCHANAN & HEYMANN, Proc. Roy. Soc., 1948, A195, 150.

(100). VAN WAZER, "Phosphorus and its Compounds", Vol. 1, Interscience, New York, 1958, p.p. 686, 698.

(101). AUDRIETH & HILL, J. Chem. Ed., 1948, 25, 80.

(102). CUMING & SCHULMANN, Aust. J. Chem., 1959, 12, 413.

(103). PETHICA & FEW, Disc. Far. Soc., 1954, 18, 258.

(104). MATIJEVIC & PETHICA, Trans. Far. Soc., 1958, 54, 1382.

(105). CAMPBELL & NANCOLLAS, unpublished results.

(106). VINCENT, Ph. D. Thesis, Glasgow, 1963.

(107). IVES & JANZ, "Reference Electrodes", Academic Press, 1961, p. 62.

(108). LICHSTEIN & BRESCIA, J. Amer. Chem. Soc., 1957, 79, 1591.

(109). PEISACH & BRESCIA, ibid, 1954, 76, 5946.

(110). NOYES & WHITNEY, Z. Physik. Chem., 1897, 23, 689.

(111). NERNST, ibid, 1904, 47, 52.

(112). VAN NAME & HILL, Amer. J. Sci., 1916, 42, 301.

(113). HOWARD, NANCOLLAS & PURDIE, Trans. Far. Soc., 1960, 56, 278.

(114). KING & SCHACK J.Amer. Chem. Soc., 1935, 57, 1212.

(115). KING & BRAVERMANN, ibid, 1932, 54, 1744

(116). JOHNSON & MACDONALD, ibid, 1950, 72, 666.

(117). RIDDIFORD & BIRCUMSHAW, J. Chem. Soc., 1952, 698.

(118). KING & LING LIU, J. Amer. Chem. Soc., 1933, 55, 1928

(119). BRUNNER, Z. Physik. Chem., 1904, 47, 56.

(120). FAGE & TOWNEND, Proc. Roy. Soc., 1932, A135, 656.

(121). KING, J. Amer. Chem. Soc., 1935, 57, 828.

(122). MARC, Z. Physik. Chem., 1912, 79, 71.

(123). HERZFELD, Colloid Symposium Monograph, 1930, p. 51 - 57.

(124). SEARS, J. Chem. Phys., 1960, 32, 1317.

(126). VAN NAME, Amer. J. Sci., 1917, 43, 449.

(127). MOELWYN-HUGHES, "Kinetics of Reactions in Solutions", 2nd. Ed., Cambridge, 1947, p. 370.

(128). JONES, Trans. Far. Soc., 1963, 59, 2355.

(129). FRANCIS, MULLIGAN & WORMALL, "Isotopic Tracers", Athlone Press, 1954.

(130). KAPUSTINSKII, Quart. Rev., 1956, 10, 283.

(131). BENJAMIN & GOLD, Trans. Far. Soc., 1954, 50, 797.

(132). HOWARD, Ph. D.. Thesis, Glasgow, 1958.

(133). SPIYSYN, TORCHENKOVA & GLAZKOVA, Dokl. Akad. Nauk. S. S. S. I 1960, 132, 449 (Eng. Tr.)

(134). SPITSYN, TORCHENKOVA & GLAZKOVA, ibid, 1960, 133, 929. (Eng. Tr.)

(135). RAMETTE & ANDERSON, J. Inorg. and Nucl. Chem., 1963, 25, 7